WARWICK MOBILE ROBOTICS
URBAN SEARCH AND RESCUE

NEXT GENERATION URBAN SEARCH AND RESCUE ROBOTICS

2015/16
TECHNICAL REPORT



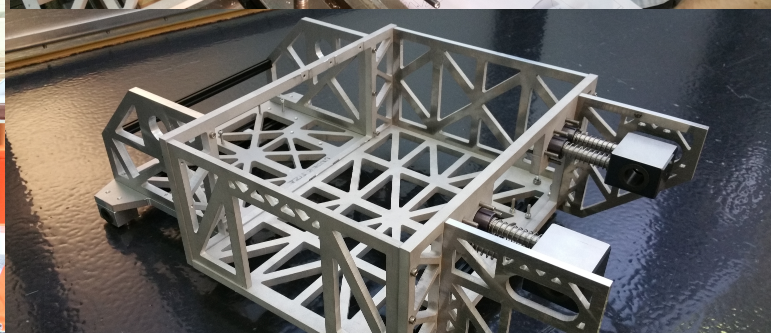

JOSEPH **FLANNERY** | HARVEY **FRANCIS** | MAXIMILLIAN **GLOGER**
ALEX **LAMM** |YUNG-YU **LAU** | DANIEL **RILEY**

PROUDLY SPONSORED BY

WMG Innovative Solutions
School of Engineering
maxon motor driven by precision
HARWiN INTERCONNECT DESIGN & MANUFACTURE

Abstract

It is inevitable that disasters will occur, both natural and man-made. It is in such environments that the deployment of Urban Search and Rescue (USAR) robots can mitigate the dangers faced by first responders, as well as aiding the rescue of those whose lives may be at risk. Cyclone, a new modular robot, has been designed and developed by a multidisciplinary team of engineers, incorporating the lessons learnt from the 2014/15 team, significantly improving upon their robot, Orion.

This report documents the 2015/16 Warwick Mobile Robotics (WMR) project, which includes the design and manufacture of a miniature urban search and rescue robot with the intention of competing in the *2017 RoboCup*. The project aims for this year's WMR team were to:

- Further develop the capabilities of the 2014/15 robot.
- Engage with the community and businesses, to promote the work carried out by WMR and as an educational platform.
- Ensure the longevity of the design so that future teams can expand upon it.

The team's design work was based on the requirements for the *RoboCup*. A critical analysis of last year's robot, Orion, concluded that the design of an entirely new robot, Cyclone, was needed to perform competitively at the competition. The results of the team's efforts have lead to a new mechatronic design, with areas of significant innovation including a modular chassis, the inclusion of a battery monitoring board and an integrated torsion blade suspension and dynamic tensioning system.

Lessons learnt from previous WMR teams formed the basis of a development process streamlined over multiple design iterations, detailed throughout the report. A scrutinous analysis of Cyclone demonstrated significant improvements, including an overall weight reduction of 21 %, an improvement in assembly time of 85 % and the near-doubling of its battery life. However, Cyclone requires further work before full system testing can commence, where potential weaknesses may be exposed and can be addressed by the 2016/17 team.

The team took part in multiple outreach events, stimulating interest in the work carried out by WMR and the application of USAR robots. These had a positive impact on the community and young engineers alike, observed through the increased web page traffic and local news publications; this is expanded upon in the cost-benefit analysis.

Cyclone is on track to meet the goals set out in the four year plan. Upon completion of minor modifications, and the implementation of the sensor array and robotic arm, it can be entered into the *2017 RoboCup* as a field testing exercise.

Declaration

We, the authors, hereby declare that the work presented in this document, relating to ”Next Generation Urban Search & Rescue Robotics,” is entirely our own, in partial fulfilment of Academic Deliverable ES410 Group Project.

Joseph Flannery - 1118446	Date
Harvey Francis - 1123969	Date
Maximillian Gloger - 1214240	Date
Alex Lamm - 1218958	Date
Yung-Yu Lau - 1112233	Date
Daniel Riley - 1213097	Date

Acknowledgements

The Warwick Mobile Robotics team would like to take this opportunity to acknowledge the contributions and assistance of the following people without whom this project could not have been completed.

Dr. Emma Rushforth	For her constant guidance throughout the project.
Carl Lobjoit	For his assistance with component design and manufacture.
Stefan Winkvist **Edgar Zauls**	For sharing their technical knowledge, advice and experience.
Technicians **Research Assistants**	At both WMG and the School of Engineering for sharing their technical knowledge and assisting with manufacture.
Margaret Low	Who gave us the opportunity to inspire the next generation of engineers and programmers.
Scott Flower **Ben Green** **Mark Gibbons** **Chris Partridge**	For their assistance in the selection of critical components of the robot build.
Sponsors	WMG, the School of Engineering, Harwin and Maxon Motor for their continuous support.

Contents

List of Figures

List of Tables

Acronyms

ADC Analogue-to-Digital Converter.

AWG American Wire Gauge.

CAD Computer Aided Design.

COTS Commercial Off The Shelf.

DDR3 Double Data Rate Type 3.

E-Stop Emergency Stop.

GUI Graphical User Interface.

HCI Human Controllable Interface.

HTTP Hypertext Transfer Protocol.

IC Integrated Circuit.

IDE Integrated Development Environment.

IMU Inertial Measurement Unit.

IR Infrared.

LAN Local Area Network.

LED Light Emitting Diode.

LiDAR Light Detection and Ranging.

LiPo Lithium Polymer.

M-USAR Miniature Urban Search and Rescue.

OS Operating System.

PCB Printed Circuit Board.

PS3 Play Station 3.

PWM Pulse Width Modulation.

RAM Random Access Memory.

ROS Robot Operating System.

RP Rapid Prototyping.

SMART Specific, Measurable, Achievable, Realistic, Time-related..

SSH Secure Socket Shell.

TCP/IP Transmission Control Protocol/Internet Protocol.

UART Universal Asynchronous Receiver/Transmitter.

UDP User Datagram Protocol.

USAR Urban Search and Rescue.

USB Universal Serial Bus.

WMR Warwick Mobile Robotics.

XMLRPC Extensible Mark up Language - Remote Procedure Call Protocol.

1 Introduction

Disasters happen all over the globe, they can be natural such as earthquakes, tsunamis and volcanic eruptions, or they can be man-made including terrorist attacks, nuclear meltdowns and industrial accidents. These disasters could have victims that need to be rescued and therefore emergency personnel put their own lives at risk to save those in need. This risk can be mitigated by the development and deployment of an Urban Search and Rescue (USAR) robots [1].

Warwick Mobile Robotics (WMR), a research group at the University of Warwick, conducts a number of projects in the field of mobile robotics. The robots designed and manufactured by the WMR teams serve as valuable platforms for research, innovation and education. The team has a large USAR robot, developed by previous years, that competed at an international level. The team also has two Miniature Urban Search and Rescue (M-USAR) robots that are not operational. Orion, the M-USAR robot designed by the 2014/15 team, whilst an improvement over previous designs, was identified to have fundamental flaws that meant it could not function as intended.

For 2015/16, the team took the principles and development strategy developed by the previous year to re-design and build upon Orion, to be more capable and versatile in a rescue situation. The strategy implemented was guided by the specification, scheduling and objectives set out by the team. The following technical report presents the projects technical aspects, whilst the accompanying cost-benefit analysis details project administration, budgeting and outcomes.

2 Strategy

The strategy for the 2015/16 Warwick Mobile Robotics team was based around the following points;

- Reviewing Orion, the robot from the 2014/15 WMR team and deciding which aspects require redesign and improvement and which can be carried on.
- Basing the designs for Cyclone on Orion as much as possible in order to reuse components to save on design and manufacturing time.
- Building bridges between suppliers and society by means of meetings and outreach events to raise awareness of WMR projects and create relationships between suppliers useful for this project and for any future WMR projects.

- Completing the project with a fully functioning robotic vehicle design which can be used as a basis for next year's team to make final additions in order enter into competition.

2.1. Aims and Objectives

The overall intention of this project is to design, test and manufacture a USAR robot for use in disaster zones to locate and aid trapped survivors, and to raise awareness for the capabilities of search and rescue robots in these situations.

To achieve this, the aims are as follows;

1. To further develop upon the 2014/15 robotic vehicle design improving its functionality and search and rescue capabilities as the second stage of a 4 year plan.
2. To provide a solid platform to the 2016/17 team for further development with the intent of competing at the 2017 *RoboCup* competition.
3. To raise awareness of the importance of rescue robotics and to inspire the next generation to enter the exciting world of engineering and programming.

The objectives required to meet these aims are;

1. Carry out a critical review of Orion (2014/15 robot) to understand its functionality and determine which aspects will be redesigned and which will be carried forward, saving design and manufacturing time.
2. Ensure a fully functioning robotic vehicle is produced in order to act as a basis for the 2016/17 team, allowing for final additions to be incorporated in order to successful compete at the 2017. *RoboCup* competition.
3. Raise awareness of WMR projects and create relationships between suppliers, the society and institutions.
4. Through outreach events, such as the *2015 Midlands Imagineering Fair*, offer young people the opportunity to gain insights into advanced engineering and technology.

2.2. Team Structure

This year's team consisted of six fourth-year students from various disciplines within the School of Engineering at the University of Warwick. The engineering discipline distribution was; two mechanical, two mechanical & manufacturing, one electronic and one systems.

The robot chassis was split into three modules and generated the individual tasks for the four team members with mechanical based disciplines; the chassis, the drivetrain, the suspension and the dynamic tension system. The entirety of the electronics work was performed by the sole electronic engineer and the systems engineer was responsible for communications, both electrical and mechanical. Collaboration between team members was essential throughout this project, especially between the mechanical members due to the large amount of overlap between their respective tasks.

Each team member also had an administrative role in order to keep the team running effectively and to avoid the time of one member of the team being taken up by all of these administrative tasks. These roles included a project manager, a secretary, a finance director, a sponsorship manager, a social media officer and an outreach officer.

2.3. Project Lifetime

In the time the team had to complete the project, it was clear that there would not be sufficient time to produce a robot that would be ready for competition. The team decided they would build a robot up to a stage where it could be finalised and subsequently taken to the competition by the 2016/17 team. It was therefore important that the robotic vehicle produced by the end of this year was well designed and adaptable to avoid rework for next year's team.

There was 30 weeks in total to complete this project, which included reviewing Orion, designing for Cyclone, manufacturing components, assembling the robot and producing the technical report. The designs for Cyclone were finalised by week 20 and ready for manufacture by week 24, which was later than planned due to complications. The manufacturing was completed by week 30, meaning the robot could not be fully assembled by the 2015/16 team and the onus of the this assembly falls on the 2016/17 team.

2.4. Management and Logistics

The team held regular meetings, with all members initially but the attendance of the entire team was not always necessary and was often counter-productive and so later meetings only involved the team members that were required for the particular discussion topic. There were also weekly meetings with the project supervisor so that all team members could provide an update on project progress. This meeting was often attended by a technician in order to provide manufacturing expertise.

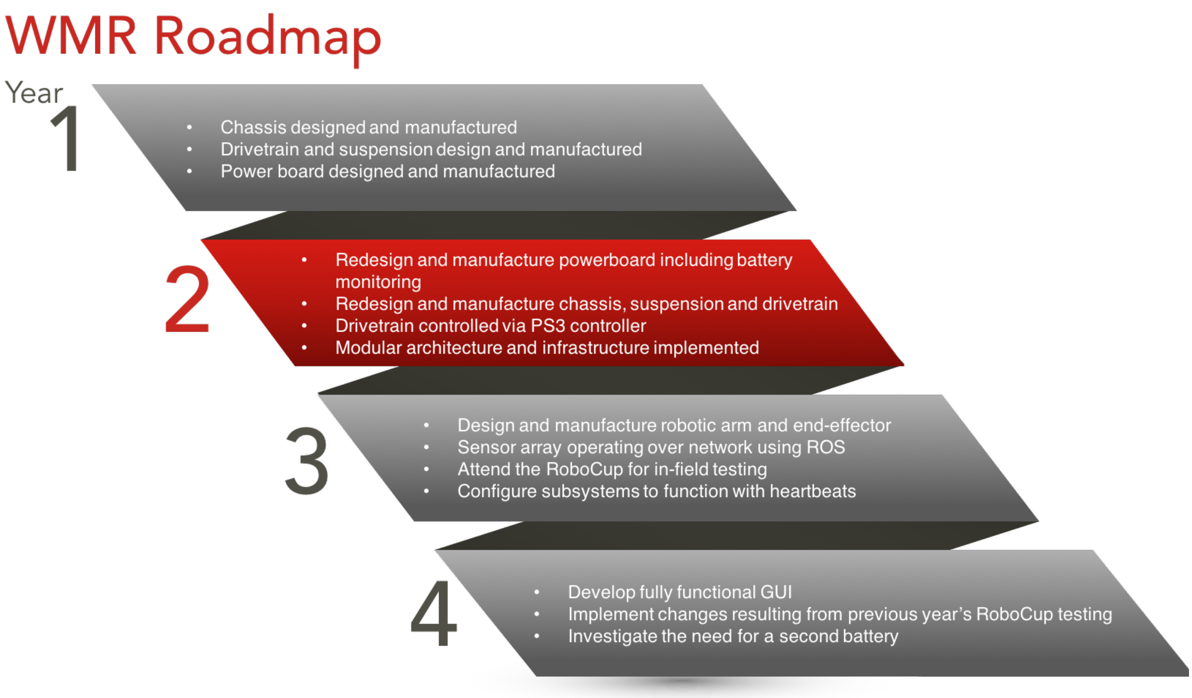

Figure 1: WMR Roadmap

Google Drive acted as the storage facility for all project related files, such as manufacturing drawings and CAD files. Meeting minutes were recorded by the secretary and uploaded to the Drive area following the meeting for members to review. In order to ensure that contact was constant between team members, an instant messaging application called Slack was used to update each other of progress.

For the technical report, each section was written using Google Docs so that comments and changes could be easily made to the documents by the reviewers. Once all sections were completed, the full report was compiled using LaTex, and after several iterations, the final report was completed.

3 Motivation

3.1. Urban Search and Rescue Robotics

The advancement of modern robotics has come a long way since Isaac Asimov [2] formulated his Three Laws in 1941. Now robots are being developed for a wide range of functionalities, including aiding rescue personnel in disaster situations.

Rescue robots are designed to aid response teams by performing tasks such as interacting between casualties and rescue personnel, traversing tough and dangerous terrain to reach casualties and where appropriate automating support activities. Rescue robots work in environments that are hazardous to humans, for example the unstable rubble of a building, where the risk of death or injury is high. The user can perform tasks remotely, eliminating the need for a human to enter these undesirable environments avoiding the needless risk of human life.

Rescue robot designs are tailored to, and will depend upon, the specific task required. These tasks can be split into a number of categories including search, reconnaissance & mapping and in situ medical inspection [3]. All of these require different hardware designs and software configuration, making it hard for one robot to complete multiple tasks. Urban disasters, either natural or man-made, are the most common form of catastrophe.

Recent examples of such disasters are the 2015/16 terrorist attacks across Europe, the 7.8 magnitude earthquake in Nepal in April 2015 and the deadly flash flooding in Texas and Oklahoma in 2015 [4]. With over 350 recorded natural and man-made disasters in 2015 (Figure 2) and thousands of subsequent deaths, there is a tangible need for effective mobile robots to aid in the necessary quick response of USAR. The uneven terrain of an urban disaster zone makes access to survivors hard, or even impossible, for a human team; this is where the USAR robot's capabilities will come into play. They are able to traverse over and around debris to reach survivors and map the area to pinpoint any potentially safe paths for human rescuers, or in some cases extract the survivors themselves.

3.2. DARPA Challenge

The *DARPA Robotic Challenge* drives teams to develop new and innovative robotic platforms to assist humans in USAR [6]. The challenges are built to mimic scenarios within a disaster zone and push the limits of robotic capability. The challenging events, as well as the $2 million

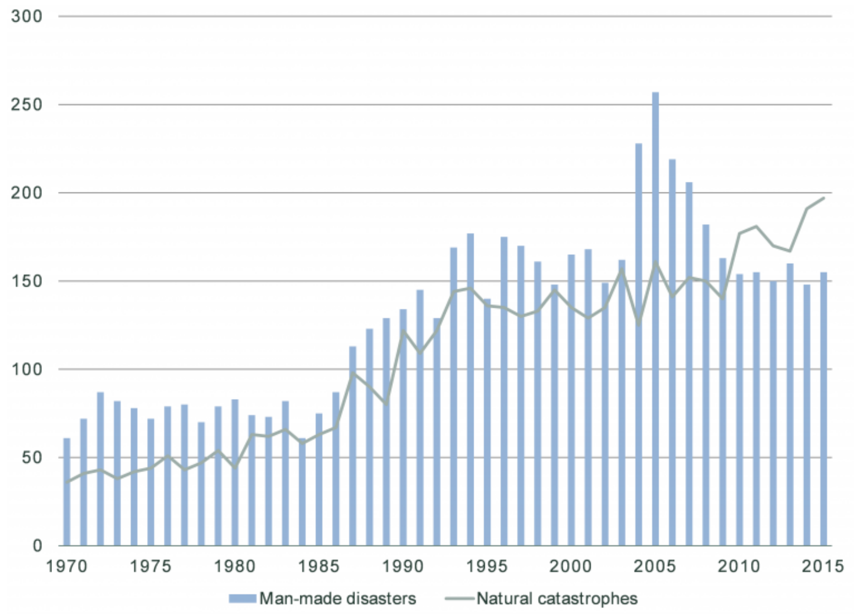

Figure 2: Record of natural and man-made disasters 1970-2015 [5]

prize fund, attracts the very best in advanced robotics organisations and so robotic capability remains on the cutting edge of what's possible; this is welcome news for the rescue community, who will benefit from such advances.

This competition and similar like it are crucial to developments in the field of rescue robotics as commercial funding is low. The onus of developing robotic capability to perform well within disaster zones therefore falls on research institutions such as universities and other privately owned bodies as there is no real commercial value in investing millions into something so specialist.

3.3. Warwick Mobile Robotics

Warwick Mobile Robotics (WMR) began as a project developed by a group of fourth year, multi-disciplinary MEng students at the University of Warwick, which developed an autonomous football team. The WMR team has since moved on from robotic football to the development of a rescue robot platform. Since 2008, groups of MEng students have designed and built USAR robots to compete in the global *RoboCup* competition [7]. Between 2008 and 2013, the teams have developed on the same platform of a large, multi-flipper USAR robot. The 2014 team improved upon this idea by building a smaller and lighter multi-flipper robot (Figure 3 left). The 2015 team took a different approach and focused on designing a miniature USAR robot as seen in Figure 3.

After a thorough review it was found that the 2015 miniature USAR robot (Orion) had a number

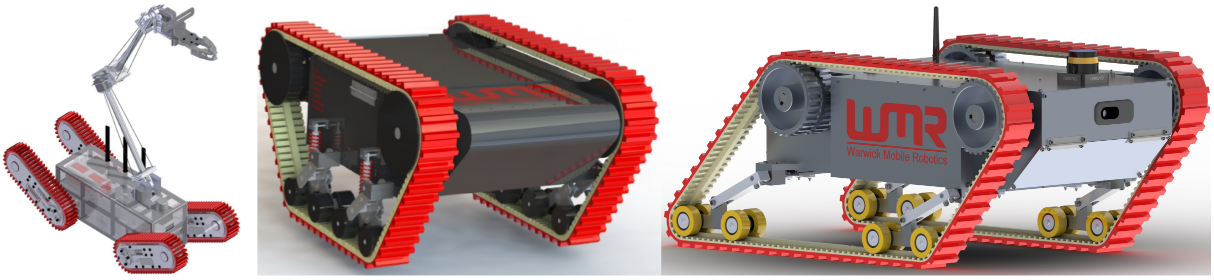

Figure 3: Evolution of the WMR Rescue Robot (2014, 2015, 2016)

of severe faults with its design and so the suggested three year plan was not followed. Instead the 2016 team opted to create a new design of miniature USAR robot building on the better points of Orions design.

3.4. RoboCup Competition

The *RoboCup* competition is an international league where teams compete with one objective: To develop and demonstrate advanced robotic capabilities for emergency responders [8]. The competition is held annually and aims to:

1. Increase awareness of the challenges involved in deploying robots for emergency response.
2. Provide objective performance evaluations of mobile robots operating in complex environments.

The competing teams operate in a simulated disaster zone, working to overcome various obstacles designed to test their manoeuvrability, durability and dexterity. Previous WMR teams have competed at the *RoboCup* competition with a number of victories being recorded. It is expected that the 2017 team will take Cyclone to the next *RoboCup* event. For this reason the *RoboCup* competition guidelines have been considered within the specifications for Cyclone.

3.5. Specification

Working from the previous year's specification and considering the requirements from the *RoboCup* competition, a new specification was created and the requirements split into several subsystems (Figure 4). Although the team does not work on the end effector or arm subsystem, these were kept in mind during design. The full specification can be found in Appendix A.

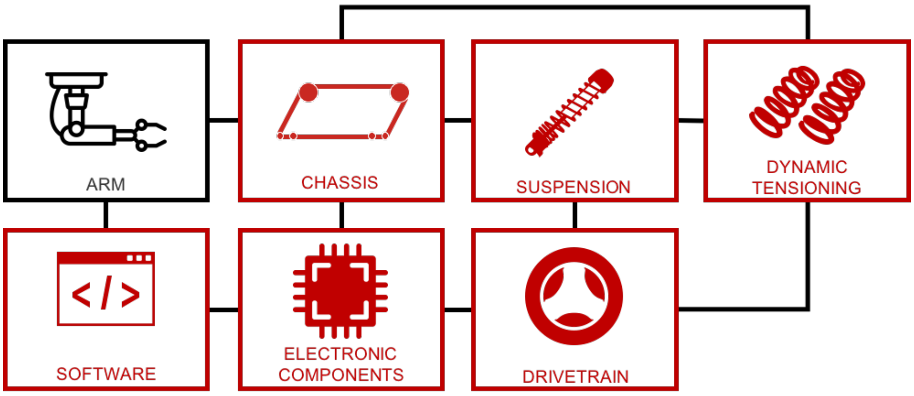

Figure 4: Graphical Representation of Cyclone's subsystems

4 Design

4.1. Design Strategy

During the design process of Cyclone, a strategy was devised to smooth workflow and provide a scientific base on which decisions were made. The strategy shown in Figure 5 ensured that design requirements were met and improved visibility of the design process for each module. This iterative strategy meant that components were changed during the design process to improve performance based on simulation data and input from the workshop staff.

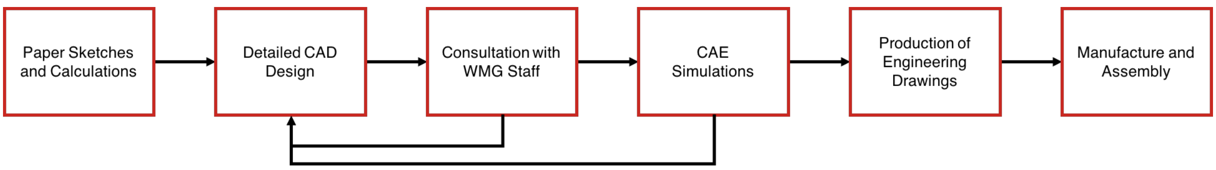

Figure 5: Flowchart of Design Strategy

4.2. Engineering Drawings

SolidWorks was used for its ability to create highly-detailed and accurate 3D CAD models and its ability to generate the 2D engineering drawings used for reference during manufacturing. These drawings specified all geometry and tolerances needed to manufacture each component, as well as notes on the surface finish needed. Figure 6 shows the progression from a CAD model to a 2D engineering drawing and then finally, the finished component.

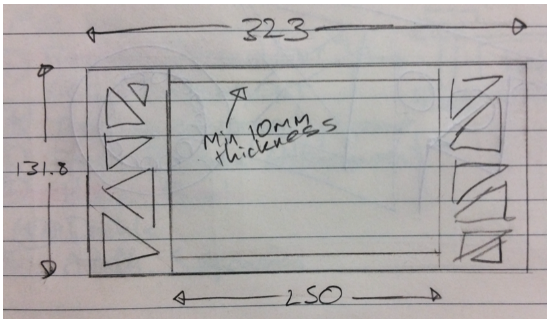

(a) Sketch of Rear Bulkhead

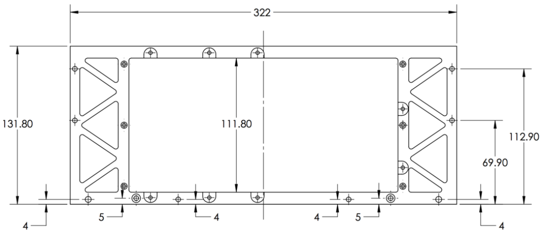

(b) Engineering Drawing of Rear Bulkhead

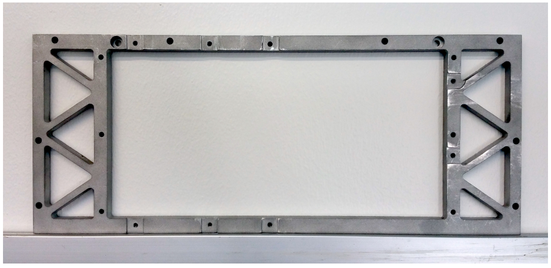

(c) Finished Rear Bulkhead

Figure 6: Progression from initial sketch to Final Part

4.3. Chassis

4.3.1. Chassis Overview

Traditionally, the term chassis refers to a self-propelled subassembly that includes a structure to carry a vehicle's locomotive parts and other components [9]; in the robotics, however, this is simply the structural framework of the robot, a definition adopted by previous WMR teams [10].

The purpose of USAR robots is to assist in environments too difficult for humans to enter, such as irradiated, burning, toxic or collapsed structures. The imperative, therefore, is to design the USAR's containing structure to be rigid and robust, such that any of the above risks are sufficiently mitigated against. A similarly rigid outer shell is often added to ensure that foreign substances, such as dirt and fluids that may interfere with the robot's internal systems, cannot enter the chassis. Thus, in the context of USAR, the chassis exists as a container and shield for internal components. Furthermore, heat dissipation through the chassis allows it to act as a heat sink for energy intensive electronics.

Materials choice represents a key factor in the design of a robot chassis. Similar to in the automotive industry, a balance needs to be struck between weight and rigidity. The result is often some combination of, or choice between, steel and aluminium, with other options such as carbon fibre reinforced polymers, remaining out of the realms of cost-effectiveness for the foreseeable future [11].

Given the risks of damage in the field, the next important consideration is ease of repair and rapid reassembly. Previous WMR teams have placed importance on the manufacturability of the robot's components, as this will facilitate a finished robot by the end of the project [10], [12] and makes for simple component replacement at the *RoboCup* competition. Conversely, a reduction in individual components can have a far greater impact on the component replacement time [13], important in fast-paced search and rescue; this can negatively impact manufacturing lead times further upstream.

Finally, joining processes must be considered. Even the simplest products may be impossible to manufacture from a single piece of material [14], and though it may be possible with some structures to use a single piece [15], the additional machining costs associated with such a decision often make it infeasible. Whilst previous WMR teams have justified the use of mechanical fastenings to allow for disassembly and ease of replacement, if adhesives can be used where appropriate, stress distribution, corrosion and joint degradation could be substantially improved [11].

4.3.2. Critical Analysis of Previous Design

The 2014/15 dimensional requirements, dictated by building regulations and the *RoboCup* specifications, were adhered to in addition to an internal volume requirement of $3.9 \times 10^{-3}\,\mathrm{m}^3$, chosen to ensure both air flow and adequate component space. In spite of this, space was still at a premium as the front and rear areas constrained internal component shape; this led to corner space being under-utilised.

The maximum weight of the robot was set at $25\,\mathrm{kg}$, with $20\,\%$ of this afforded to the chassis. Despite the team's best efforts, the 2014/15 chassis weighed $5.57\,\mathrm{kg}$, $10\,\%$ greater than planned. This was largely a result of the $10\,\mathrm{mm}$ baseplate, chosen despite tests showing empirically that MakerBeam would more than suffice for the robot's application. Furthermore, the robot was encased in a 2mm aluminium shell, thicker than necessary. This increase in weight inevitably impacts other areas of the robot, such as the motor torque, the suspension and dynamic tensioning systems.

The robot's battery was made easily accessible through a battery holder that allowed fast clip-in/out, part of the health and safety considerations. The remainder of the robot's components, however, were difficult to access. Though the removable-top-panel access point was large enough for hands to enter, many components required the removal of additional chassis sections to access and modify the contents.

Where possible, Commercial Off The Shelf (COTS) components were chosen to ensure easy replacement after breakages and to accelerate build-time. The joining methods dictated by components, however, had significant impact on the assembly and disassembly time; many required small screws in hard-to-access locations. Whilst replacement parts could be easily sourced, the changeover itself would take far longer than acceptable in a USAR situation, where time is critical. The chassis also featured examples of redundant components, where MakerBeam was attached to the $10\,\mathrm{mm}$ baseplate; this increased assembly time and chassis weight. Though fabrication was kept to a minimum, and materials were all readily available, the processes used were not as available as initially planned; specialist water-jet cutting was used for a number of mission-critical components.

Before designing Orion's structure, materials were physically tested for their structural feasibility. Though MakerBeam was determined to be the weakest of those tested, it still met the team's strength requirements. Furthermore, it is far cheaper than machining material to a final component shape, and also easier to source. The design was then validated on its structural performance through simulations carried out in Abaqus; a $650\,\mathrm{N}$ drop test and a $250\,\mathrm{N}$ crash test were carried out. These simulations justified both the positioning of MakerBeam components and its use as structural members.

4.3.3. Development of Current Design

The previous chassis shape and configuration were deemed appropriate by the team, though a number of points were to be addressed in the new version:

1. Though the symmetrical shape provided good ground clearance and allowed for stair climbing in either direction, the robot was unstable, with a short tractive length that inhibited maximum operating angle.
2. The shape at the front and rear areas constrained component orientation, complicating component packaging.
3. Heavy plates weighed down the chassis unnecessarily.
4. Joint configuration made reassembly time-consuming and difficult.

These points all required careful consideration to develop a chassis that continued to meet the requirements of the competition with the additional requirements set by the 2015/16 team.

4.3.3.1 A Modular Chassis

The nature of missions carried out by USAR robots is increasingly diverse and thus, the ability to adapt to the mission at hand without substantial reconfiguration time is advantageous. Having the flexibility to quickly change the drivetrain, control electronics or sensors was added to the project requirements. The result of such an approach was a modular framework, shown in Figure 7, that served as the basis for the chassis re-design.

Figure 7: Component distribution

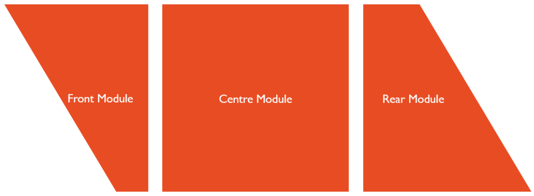

Figure 8: Physical component distribution

4.3.3.2 Parallelogram Shape

Orion's chassis was designed as a trapezium to facilitate bidirectional travel and improve ground clearance. These were both achieved in the implementation, but the tractive length is resultantly short. This impacts the ability to climb slopes, as the centre of mass can easily fall outside of the tractive length causing the robot to topple.

Orion's trapezium design could be adapted by inverting the rear module to create a parallelogram, an approach common with old tanks [16]. Assuming perfect traction and torque, this greatly improves the maximum climb angle achievable.

Thus, the chassis can now be understood in the form shown in Figure 8. The previously described modules would fit well into the overall shape of the robot, and size requirements for each module could be drawn from previous specifications and their respective components. The chassis itself needed to be extended to accommodate larger motors capable of driving the robot. This additional volume and shape reconfiguration, however, also facilitated an $8\,\%$ increase in the volumetric efficiency of the design whilst remaining within the 2014/15 team's maximum length of $580\,\mathrm{mm}$ [10].

4.3.3.3 From MakerBeam to Aluminium Plate

Experience with the previous design, both virtually and physically, made evident the large number of constituent parts in the chassis, assembled in a way that inhibited disassembly. A new requirement was for the reduction in assembly time by minimising the number of separate parts, whilst still allowing for modularity. This was ultimately achieved using aluminium plates, where a greater rigidity is afforded than the MakerBeam frame. These larger pieces were not only stronger, but also allowed for much faster assembly.

4.3.3.4 Weight Reduction

The use of such large plates significantly increased the chassis weight: Light-weighting became imperative. Taking inspiration from single-piece electronics, such as Apple's Unibody MacBook, large areas were designed to be machined away, creating a lattice structure with a solid wall on one face. This, however, presented a challenge in machining time and cost. For the sake of ease of manufacture and fast turnaround from external suppliers, the surface was separated from the structural component, resulting in a structural lattice and a protective shell to enclose the chassis. The strength of the lattice structure afforded a reduction in outer-shell thickness, leaving $2\,\mathrm{mm}$ sheets only where lattice was not present and $0.9\,\mathrm{mm}$ sheet where it was.

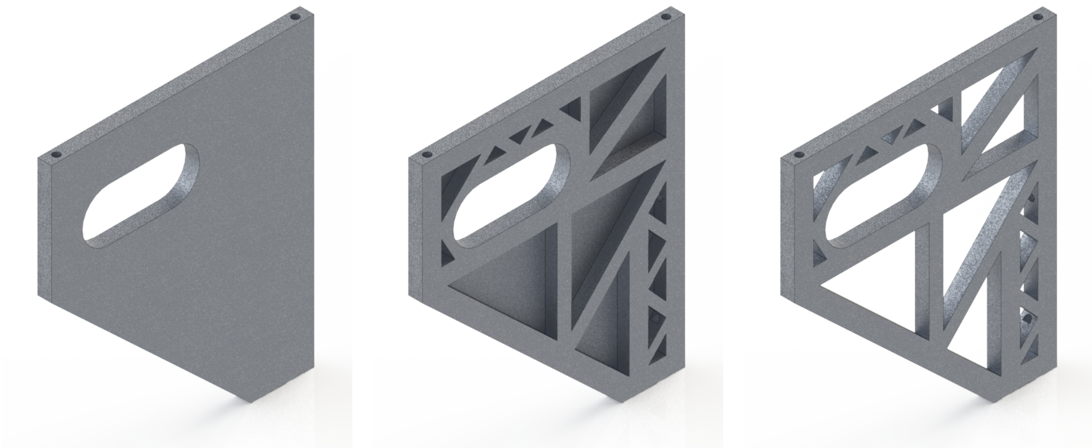

(a) Solid plate (b) Recessed lattice (c) Through-cut lattice

Figure 9: Development of the chassis' structural panels

Where the previous design had called for a uniform thickness of $10\,\mathrm{mm}$ across all structural components, the added strength of the structure achieved through the use of aluminium plate allowed for $6\,\mathrm{mm}$ and $8\,\mathrm{mm}$ plate to be used. The resultant chassis weighed $4.3\,\mathrm{kg}$, over $1\,\mathrm{kg}$ lighter than the previous design.

4.3.3.5 Assembly of the Chassis

To ensure a consistent join, and to add some degree of structural support to the sheet, an adhesive was selected as the joining mechanism. The chosen 2-part epoxy activates on contact to ease the assembly of components and cured in 24 hours. The chassis then made use of bolts to assemble the various plates together. Though not the most efficient joining mechanism, this did greatly facilitate future component replacement, whereas other mechanical joining techniques, such as snap fits and rivets, are harder to reconfigure.

4.3.4. Design Evaluation

4.3.4.1 Fall Resistance Simulation

To meet the requirements Cyclone must survive a drop from 350 mm, for this reason, a simulation representing a drop from this height was performed. The force was applied directly to the underside of the base plates and was calculated using the distance with the suspension bottoming out (34.9 mm). Equation 7 in Section 4.5.4 was used to calculated the applied force. The total force was calculated as 2540 N, which was divided between the rear and centre modules. These two modules were simulated separately due to the interchangeability of the design and so required an understanding of the local response for each.

The drop forces were applied to the base plate where the suspension attaches. The rear bulkhead acted as a fixed boundary condition providing resistance to the forces acting. The resultant stresses and displacements are shown in Figures 10a and 10b for the middle module and Figures 11a and 11b for the rear module, with the maximum stress experienced at 63.23 MPa and 75.00 MPa respectively. The resulting stresses in both modules do not exceed the yield stress of the material, which is 300 MPa [17]. The maximum deflection of the front and centre modules were 0.6470 mm and 0.9030 mm, which can be considered negligible. These simulations add weight to the argument that the chassis would survive a drop of 350 mm.

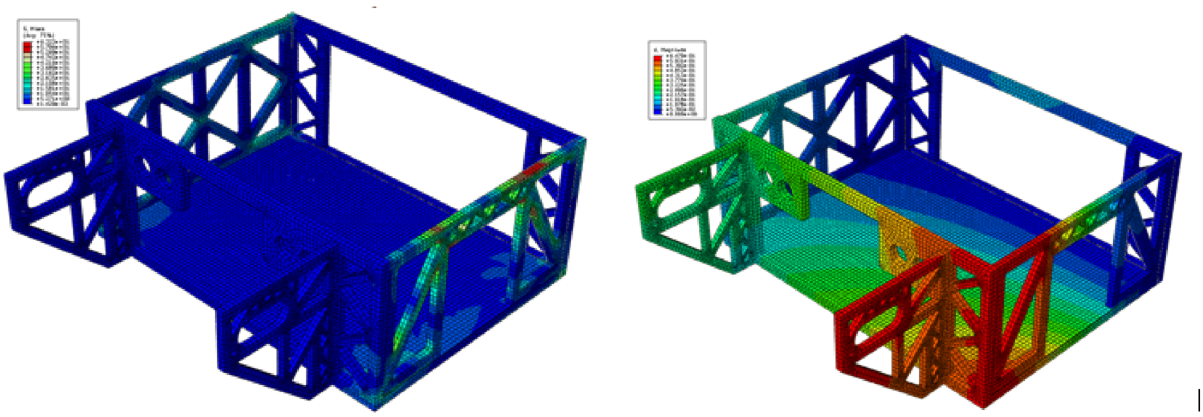

(a) Stress results. (b) Deflections results.

Figure 10: Drop test simulations for the front and middle modules.

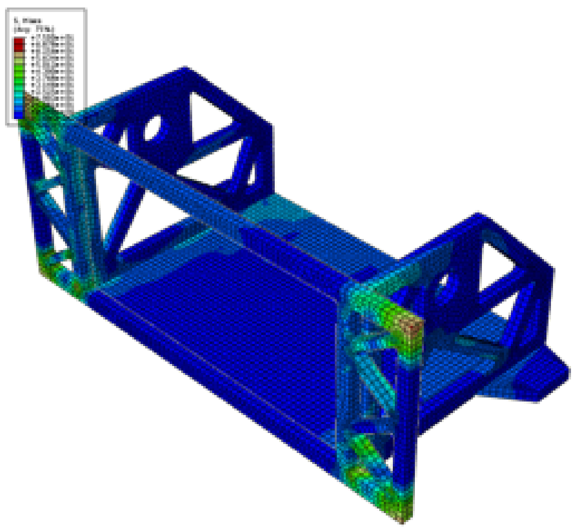

(a) Stress results.

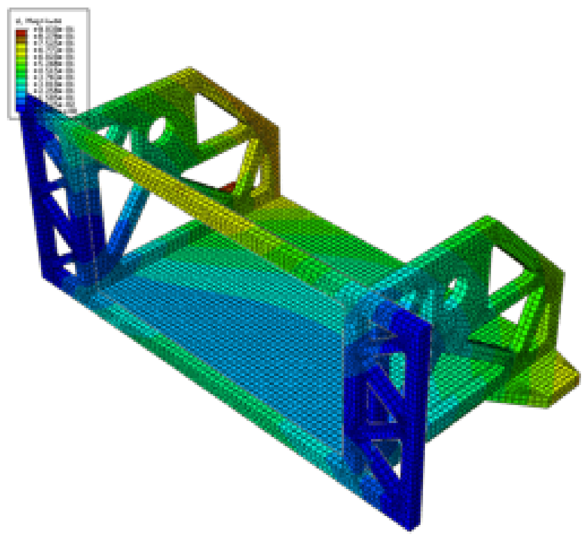

(b) Deflections results.

Figure 11: Drop test simulations for the rear module

4.3.4.2 Crash Resistance Simulation

A simulation was also conducted to test the strength of the chassis under the expected forces of a head-on collision. In this simulation, a force of 250 N was applied to the front of the chassis and the rear axle holes were fixed.

The simulation results were evaluated using the maximum stress and deflection criteria, stated in Section 4.3.4.1. The results of the simulation showed that, under these forces, the chassis would not fail due to the stresses experienced and it would not lose functionality due to excess deflection. The largest stress can be found on the rear bulkhead (Figure 12a), at the location where the drive module side lattices are fixed. This maximum stress of 11.38 MPa is well within the yield stress of aluminium 6082-T6. The maximum deflection is experienced at the location where the force was applied, that is, the front corner of the front side lattice panels. The maximum deflection (Figure 12b) is 0.4253 mm, which will have a negligible affect on the operation of Cyclone. Ultimately, it can be concluded that the chassis is strong enough to survive a head on collision at full speed. From the results to this simulation and those explained in Section 4.3.4.1, the chassis has proven to be suitable for use in urban search and rescue robots.

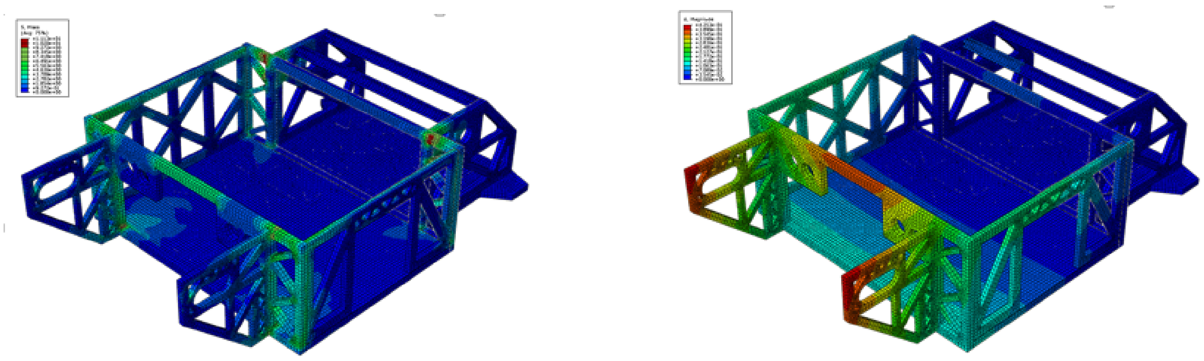

(a) Stress results (b) Deflection results
Figure 12: Chassis crash test simulations

4.3.4.3 Assembly Efficiency

A Boothroyd-Dewhurst analysis was carried out on the chassis to determine the efficiency of its assembly [13]. The results suggested an assembly efficiency of approximately 5 %, an issue for mass-production of such a product. Far more important to the nature of the product's use is the total assembly time, reduced by 85 % from the previous design (Tables H.18 - H.21). This has huge implications on the robot's overall effectiveness in USAR scenarios, where rapid repair is often required for broken components.

4.3.5. Final Chassis and Shell Design

The final design for the chassis and its shell are shown in Figures 13a and 13b. The chassis weight is estimated at 4.396 kg, a 21 % reduction. Furthermore, the modular approach will future-proof the robot, allowing for fast modifications in the field and a reduced development period for new structural layouts.

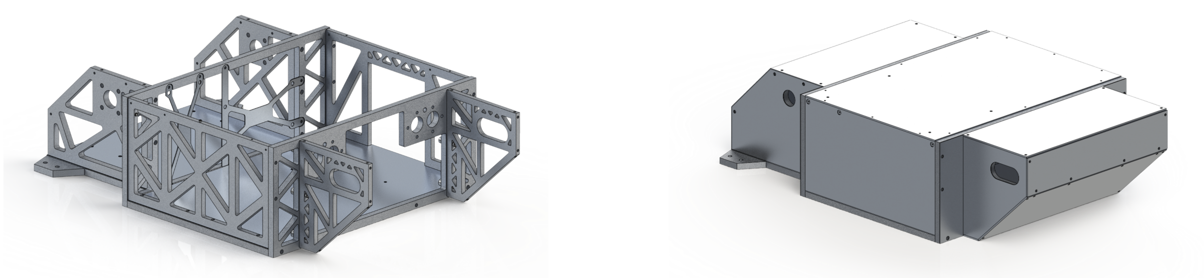

(a) Structural Skeleton (b) Outer Shell
Figure 13: Complete Cyclone's Chassis

4.4. Drivetrain

4.4.1. Rescue Robot Drivetrain

The drivetrain is the system in a motor vehicle which connects the transmission to the drive axle. In regard to a rescue robot the drivetrain is made up of the motors (and their controllers), the drive axles, the drive wheels and the tracks. The drivetrain is a crucial component as without it mobility would not be possible.

Careful consideration must be given to the balance between power and speed. Too little power would render the robot unable to traverse uneven surfaces of disaster zones and not enough speed would result in a prolonged time to survey and manoeuvre any area. The drivetrain of rescue robots are usually tracked to allow easy navigation of unpredictable terrain.

4.4.2. Critical Analysis of Previous Design (2014/15)

Orion's utilised a skid steering system as it was recognised as the best option for the dual tracked robot being built in this project, as it is the simplest and most intuitive method of control. It was therefore carried forward into Cyclone. Skid steering uses two separate motors, one per track, allowing independent control of each.

The material selection for the tracks was sensible and the use of the expertise of the Transdev team was used to select the tracks for Orion, this will be carried forward to Cyclone. The specialist rubber design gives the tracks the flexibility they need not only to travel around the drive wheels and idlers but also to react to the uneven terrain of a disaster zone. This in conjunction with the new suspension design (discussed in Section 4.5) will allow for improved traction when traversing uneven terrain. The track layout of Orion was created with the intention of allowing it to drive whilst upside down, with the track encompassing the area around the body. This invertible design would be void if the addition of a robot arm was carried out and so was not carried forward. After consideration of the profile of Orion's track design it was made clear that the tractive length was too short to allow the robot to climb stairs. The distance between the two points of consecutive steps is $308.8\,\mathrm{mm}$ (Figure 14) and the tractive length of Orion was only $244.60\,\mathrm{mm}$, whereas Cyclones new extended parallelogram track profile allows it to easily climb a standard step.

The motor and gearhead combination for Orion were selected using a worst case scenario of accelerating at $0.3\,\mathrm{m/s^2}$ up an incline of 38° (the incline of a standard step) with an estimated

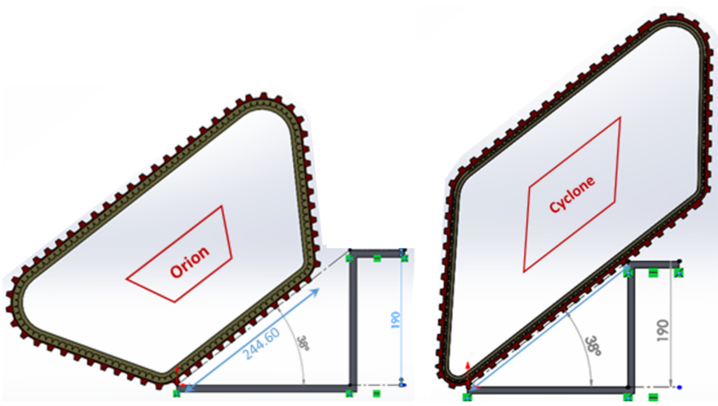

Figure 14: Orion struggling to climb standard stairs

robot weight of 25 kg. This gave a required torque of 4.95 N m per motor. This torque was found by assuming 80 % efficiency of the combination, when in fact the selected combination has an efficiency of 67.76 %, now giving a required torque of 5.79 N m per motor for Orion. The stall torque was also taken into consideration and a motor with a minimum stall torque of 25 N m was suggested (∼5 times worst case torque). With this in mind a motor with a stall torque of 0.588 N m and a gearhead with a 123 : 1 reduction ratio were selected giving an overall stall torque of 72.32 N m (if 100 % efficiency and maximum running is assumed).

Orion's motor system will provide 3.45 N m rather than the 5.79 N m required. Further analysis using a simple force diagram (Figure 15) shows that a total force of 150.99 N is required to hold a weight of 25 kg still on a 38° slope. Equating to 75.5 kg and 3.77 N m per motor, which is greater than the torque that Orion's motors provide.

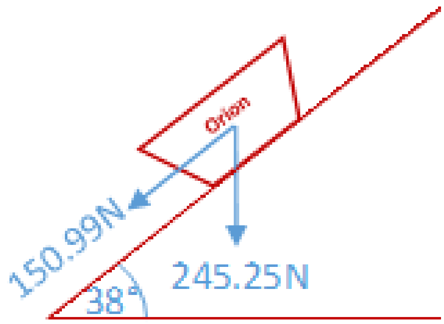

Figure 15: Simple force diagram for Orion on a 38°slope

The speed of Orion's motors was also lacking at a maximum speed of 0.57 m/s. This would not be maintained as it was calculated assuming the battery has maximum charge. Realistically the speed would be around the lower value of 0.43 m/s.

There is always a trade-off between speed and torque but it is hard to see which factor was favoured in the design of Orion's drivetrain as neither the speed nor the torque are sufficient for the successful operation of the robot. For this reason a new motor and gearhead selection was made for Cyclone.

4.4.3. Review of Alternative Drivetrain Designs

There are a number of different methods that can be employed to propel a vehicle, this section will explore these options and justify the chosen one.

4.4.3.1 Propulsion

Firstly, the robot needs a way of converting power to forward momentum. Choosing the best system depends on several factors including the traction, steering, suspension and ground pressure. Three methods of delivering movement were explored; wheels, tracks and legs.

Wheels This is the most common method of movement in ground vehicles. Wheels provide a simple platform for movement as there are limited moving parts involved, only the wheel and drive axle will be turning, meaning fewer components that could be damaged. If there was ever any damage however, the simplicity of design would allow for quick, easy and cheap repair. It would also mean construction, including the suspension element, would be easier and cheaper than a more complicated design such as a tracked variant.

The wheeled design offers a high degree of manoeuvrability allowing the robot to travel at high speeds compared with tracks and legs, due to the lower torque required to start and continue moving. This high degree of manoeuvrability also makes the wheeled robot easy to control with on the spot turns possible (Figure 16). The steering of a wheeled robot could also be carried out using a bell-crank and rack-and-pinion steering linkage [18].

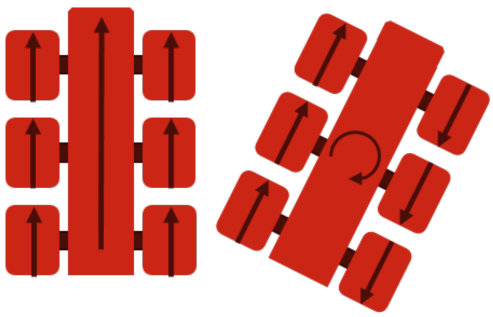

Figure 16: Turning Method of a Wheeled Robot

Because wheels have been around for such a long time they have seen a number of advancements in their design and so there are a number of variants available [19],[20],[21].

Although they have a large variety of designs available and their simplicity makes them cheap and easy to build wheels do have their disadvantages. The main disadvantage is that wheels must be at least twice the height of an obstacle in order to overcome it, so in the case of climbing a standard staircase the wheel must be 380 mm high. Another disadvantage is the small contact area with the ground resulting in reduced traction and also a concentrated weight at specific points making wheeled vehicles unsuitable for soft terrain.

Tracks Tracks are an alternative to the wheeled design although they offer a more complex system. Tracks have a low ground impact as the weight is distributed along the tractive length, ideal for a disaster zone where survivors may be trapped under rubble. The larger footprint of the track offers increased traction and therefore giving a higher performance efficiency compared to wheels. The increased traction coupled with the flexibility of the continuous tracks allows for traversing of rough terrain where a wheeled design would get stuck due to its single contact points [22]. The steering system is as simple as the wheeled system (Figure 17) allowing for on the spot turning and good manoeuvrability.

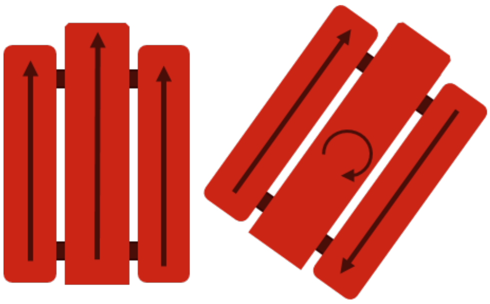

Figure 17: Turning Method of a tracked robot

Although the tracked design is better suited to the rough terrain of a disaster zone it does offer less precise movement and due to the increased traction more power is required whilst turning. The overall design tends to be bulky and heavier and given the more complex nature the build and repair are more costly than alternatives.

Legs were considered but did not seem a practical choice for the time frame offered by this project, see Appendix B for details.

Choice Considering the three options, the best choice for Cyclone would be a tracked drivetrain due to its more rugged nature and greater ability to traverse the uneven terrain it will encounter in a disaster zone.

4.4.3.2 Manoeuvrability

There are a number of ways to steer a two track vehicle and this section will explore the options available.

Dual Drive This is the simplest way to steer a dual tracked vehicle and requires a separate power source (motor) for each track. To steer this system one motor is supplied with more power than the other resulting in one track travelling faster (and so further) than the other causing a turning moment. This design allows the vehicle to perform a neutral turn (turn on the spot), which is useful when navigating the limited space within a disaster zone. The simplicity of the design makes steering intuitive and so the vehicle is easy to operate often using one throttle stick per motor, allowing any unskilled personnel to pick up a controller and operate the vehicle.

This design does come with some disadvantages. Two power sources means double the chance of failure and so reduced reliability compared to just one motor. If one motor was to fail the vehicle would be immobilised and capable of only spinning in circles, rendering it useless. Another issue with two motors is there will be double the weight and with motors tending to be near the drive wheels (at the back) this presents an issue with the centre of gravity. Having two separate motors may cause difficulty in supplying the same amount of power to each track resulting in a less accurate form of control. [23].

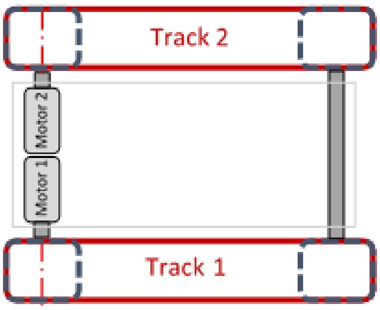

Figure 18: Dual Drive Layout

Clutch Brake This method requires one motor which drives both tracks directly. Turing is achieved by disengaging one track from the motor via a clutch mechanism (Figure 19) in order to slow the disengaged track until it comes to a stop, with the other track still engaged and traveling at the speed of the motor, so causing a turning effect. The disengaged track can also use a brake to bring it to an immediate stop allowing a tighter turning radius. This is another easy method of controlling a tracked vehicle although it is not very efficient. The constant deceleration and acceleration of the tracks also makes manoeuvring slow and inefficient, because slowing and braking the tracks wastes energy. This method also does not allow on the spot turning which would cause problems in the tight areas within a disaster zone [24].

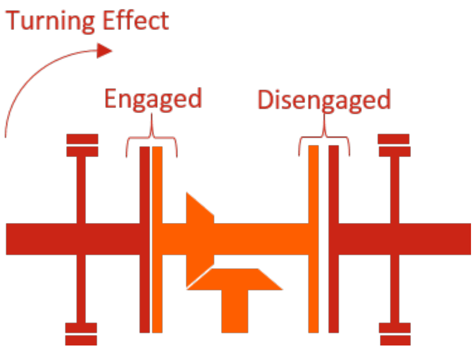

Figure 19: Clutch Brake Layout

Gearing Steering In a gearing steering system a single motor is used to power both sets of tracks through separate transmissions. The tracked vehicle is steered by selecting different gears for each of the tracks. In Figure 20 the 1^{st} gear is engaged on the left and the 2^{nd} gear is engaged on the right, resulting in the left track travelling at a lower speed than the right and so a left hand turning effect. This method allows for a smooth and efficient method of steering and a large combination of gearing ratios so a large number of turning radii. Each transmission can incorporate a reverse gear and so a neutral turn is possible. This method, however, is complex in nature and correct implementation can be time consuming and costly, [24]. Other methods of manoeuvring were considered and can be seen in Appendix B.

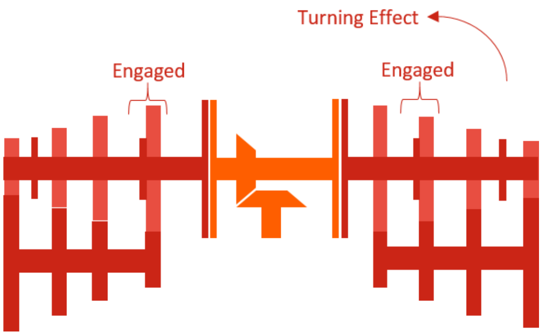

Figure 20: Gearing Steering Layout

Choice Due to the simplicity of its design and ease of use the dual drive option was chosen to power Cyclone.

4.4.4. Design of Cyclone's Drivetrain

Cyclone's drivetrain was created from scratch due to its modular design and the problems inherited from last year, the rear module is solely dedicated to the drivetrain.

The motors for Cyclone were considered against the same worst case requirements as last year, this is accelerating $25\,\mathrm{kg}$ at $0.3\,\mathrm{m/s^2}$ up a 38° incline.

According to the simple force diagram which is equivalent to that of Orions (Figure 15), Cyclone will require a force of $150.99\,\mathrm{N}$ to keep it stationary on an incline of 38°, that is $75.49\,\mathrm{N}$ per motor.

The minimum amount of torque required in this worst case scenario can be found by modifying Figure 15 to a wheel travelling up a slope (Figure 21).The weight of Cyclone and Orion are the same so the same simple force diagram can be assumed. A force balance using Figure 21 will give the following equation;

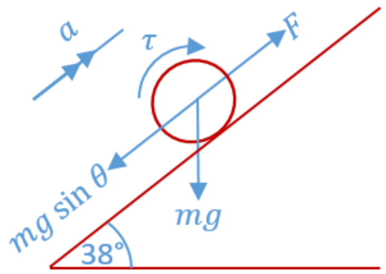

Figure 21: Simple force diagram for a wheel on a 38° incline

$$\sum F_x = F - mgsin\theta = ma \tag{1}$$

Torque ($\tau = F \times r$) can then be substituted into Equation 1 and rearranged to get an equation for the torque up an incline;

$$\tau = (a + gsin\theta)mr \tag{2}$$

Given that there are two motors powering Cyclone working at an efficiency below 100% this should be accounted for and so Equation 2 will be divided by the number of motors (n) multiplied by their efficiency (ϵ) to get Equation 3,

$$\tau = \frac{(a + gsin\theta)mr}{n\epsilon} \tag{3}$$

In order to complete this equation the efficiency of the motors and gearhead combination must be estimated. This was done by using the motor specification information supplied by Maxon Motor [25] [26] and the average efficiencies of likely motors and gearheads that Cyclone would use. The efficiency was estimated to be $60\,\%$, this gives the following result for torque required,

$$\tau = \frac{(0.3 + 9.81 sin38) \times 25 \times 0.05}{2 \times 0.6} = 6.60 Nm \quad (4)$$

That is $6.60\,\mathrm{N\,m}$ per motor to accelerate $25\,\mathrm{kg}$ at $0.3\,\mathrm{m/s^2}$ up an incline of 38^o. The same formula could be used with $a = 0\,\mathrm{m/s^2}$ for Cyclone being held still on the slope, this gives a torque of $6.29\,\mathrm{N\,m}$ (the stall torque).

The speed requirement for Cyclone is modified from the previous 2014/15 project, which required a standard operation speed of $1\,\mathrm{m/s}$. This seemed ambitious given the motor and gearhead combinations available and their torque requirement. This prompted the speed requirement to be lowered to $0.5\,\mathrm{m/s}$ standard operation, which is more achievable. From this information five motor and gearhead combinations were selected outlined in Table 3.

As can be seen in Table 3 the most appropriate combination given the design specifications for Cyclone is the 3^{rd} choice, RE50 $200\,\mathrm{W}$ $24\,\mathrm{V}$ GB motor with GP52C 26:1 gearhead. This motor has the highest speed, the greatest stall torque, the best efficiency and is the cheapest option of the five. This option however does not meet the speed requirement of $0.5\,\mathrm{m/s}$. This compromise was accepted on the grounds that the robot must be able to traverse the uneven terrain of a disaster zone and so torque should take priority, with a nominal torque (maximum continuous torque) of $887.44\,\mathrm{N\,m}$ of the chosen combination which is above that of the worst case torque required.

Figure 22: Cyclone's Gearhead [26]

Figure 23: Cyclone's Motor [25]

The efficiency of the selected combination is $78.02\,\%$ and therefore the calculation for the torque required can be revised using this new efficiency (Equation 5).

$$\tau = \frac{(0.3 + 9.81 sin38) \times 25 \times 0.05}{2 \times 0.7802} = 5.08 Nm \quad (5)$$

That is $5.08\,\mathrm{N\,m}$ per motor for the worst case scenario. The same formula again could be used with a $=0\,\mathrm{m/s^2}$ for Cyclone being held still on the slope, this gives a torque of $4.84\,\mathrm{N\,m}$ (the stall torque). This shows that the selected combination more than meets the torque requirements of Cyclone.

4.5. Suspension

4.5.1. Why Use Suspension?

Suspension allows relative motion between the body of a vehicle and it's wheels. This motion improves road holding by allowing the wheel and tyre to track the contours of the ground, keeping the tyre in contact. Suspension also isolates the body of the vehicle from uneven road surfaces, improving ride quality and comfort. Vibration and impacts on the vehicle are also reduced, lowering the stress on components thus improving lifespan and reliability [27]. Less energy is lost from the vehicle moving vertically and from the wheels spinning in mid-air. Overall, the use of suspension allows a vehicle to travel faster and more safely over rough terrain.

4.5.2. Critical Analysis of Orion's Suspension

The functionality of the Orion's suspension was compromised due to a number of factors in it's design. The coil spring design was said to have $12\,\mathrm{mm}$ of travel, however the actual suspension travel was $0\,\mathrm{mm}$. When loaded, the suspension sagged and caused a bolt head to contact with the outer plate of the suspension mount, preventing the suspension from compressing (this can be seen in Figure 24).

Suspension pre-load could be increased to eliminate sag, however, travel was still severely limited due to the bolt fouling against the outer mounting plate.

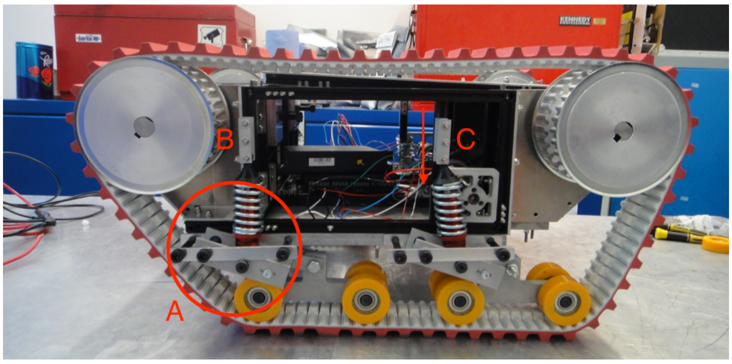

Figure 24: Left Hand Suspension from 2014/15 Technical Report

The design and fixing of the outer mounting plates also caused problems. As can be seen in Figure 24, there is no spacer between the inner and outer mounting plates. When the mounting bolts (A on Figure 24) are tightened they bend the outer mounting plates inwards towards the robot. This increased friction at the swing-arm pivot and thus prevented it from rotating.

The mounting blocks for the top of the coil spring were also flawed. The bolts fixing them to the MakerBeam chassis were perpendicular to the force of suspension compression, without fixation in the axis of compression. This meant that during high compression events the mounting blocks slid upwards, reducing travel to zero. It was found that moving the mounting blocks downwards, illustrated as C in Figure 24 allowed a small amount of suspension travel. This set-up was not ideal however, as it raised the ride height and centre-of-gravity significantly.

Due to the design of the suspension, the outer mounting plates and bolts sit outside the outer line of the tracks, shown in Figure 25. This leaves components vulnerable in the event of a crash or roll-over and increases width.

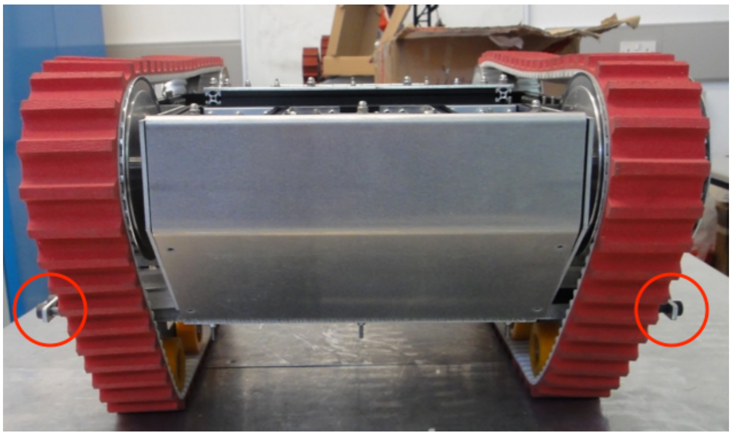

Figure 25: Exposed Suspension Mounting Hardware

The coil springs used did have adjustable pre-load, however there was no mechanism for adjusting the spring rate or ground clearance of the robot without disassembling the whole suspension system and fitting different springs. This meant that the suspension could not be adjusted to better suit terrain conditions, a potentially valuable feature. Furthermore, the robot could not be levelled to account for uneven weight distribution. The coil-spring design did have relatively low un-sprung mass, as well as damping. The damping was beneficial because it stopped the suspension from oscillating following an impact, returning the suspension to the neutral position more quickly.

4.5.3. Review of Possible Alternative Suspension Designs

Several alternative suspension designs were considered to replace the coil spring design. The alternatives were considered on function, manufacturability and weight. All alternatives would have to improve on the current design to be a realistic option.

The first option considered was removing the suspension entirely. Such a design would be the simplest, lightest and most robust as there are no moving parts. However, it was thought that removing it would limit the robot's capabilities.

A second option was modifying the current suspension to rectify it's problems. The suspension design could have been modified to improve performance, for example by installing spacers to prevent the mounting plates from bending inwards. The lack of sag could be addressed by moving the upper coil spring mounting points lower or replacing the coil springs for longer units, however this would further increase the height of the centre-of-gravity. Overall, due to the limitations of the design and lack of robustness and adjustability, a new suspension design was decided to be most appropriate.

Traditional suspension designs for tracked vehicles were then reviewed and considered. The most widely used type is torsion bar suspension [28]. Torsion bar suspension uses a bar mounted to a swing arm to provide a spring action in torsion. One end of the torsion bar is fixed to a swing arm on which a road wheel is mounted and the other end is fixed to the chassis. The torsion bar design has been widely adopted because of its simplicity and the fact it's light weight. Torsion bar suspension also stores more energy for the same weight when compared with other systems, further reducing weight [29]. Torsion bars can be mounted inside the vehicle to protect components from damage, or underneath the vehicle to increase interior volume; this would be suitable for the robot, as maximum interior volume is needed. Another benefit is that the suspension does not protrude past the outside line of the tracks, minimising vehicle width. Although the torsion bars may be vulnerable to damage sitting outside the chassis, the components are simple to replace and so this downside is accepted [29].

The spring rate of torsion bars can be changed by changing either the diameter or length of the bar. It would be possible to include a mechanism to change the torsion bar length to adjust the spring rate and therefore the ride height, allowing the robot to be levelled. Such adjustability would also allow the pitch of the chassis to be changed depending on terrain conditions, improving tractive performance [30]. A shorter torsion bar has a higher stiffness and therefore higher spring rate (See Appendix C.1).

There are disadvantages, however. Torsion bars do not self-damp [29], so either dampers will need to be separately included in the design or not used altogether. Not using dampers for a fast-moving tracked vehicle would be infeasible, however, the robot travels at a maximum speed of

$0.35\,\mathrm{m/s}$ and will weigh less than $25\,\mathrm{kg}$. Firstly, it is likely that the robot will be travelling too slowly for any large oscillations to be induced and secondly there will be a degree of coulomb damping [31] in the suspension system. Secondly, the spring rate of torsion bars is linear, not progressive as coil springs are [29]. For larger vehicles progressive spring rates are preferable, however it is an acceptable compromise in return for a robust and simple suspension system.

Overall it was deemed that the advantages of torsion bar suspension, namely; simplicity, low weight, robustness, the potential for adjustability, no reduction in internal volume and good packaging outweighed the disadvantages of no inherent damping and having linear spring rate. For these reasons, a torsion bar configuration was chosen for Cyclone.

4.5.4. Design of Cyclone's Torsion Bar Suspension

When designing the torsion bar suspension it was a priority to keep all parts as simple as possible. Reducing complexity would make the design and manufacturing phases shorter, improve reliability and make in-field maintenance and repair more simple. The current suspension was analysed to determine which components could be reused. It was decided to reuse the idlers from the previous design and retain the same swing arm length of $80\,\mathrm{mm}$.

Firstly, the amount of suspension travel had to be determined. Orion had a total spring travel of $25\,\mathrm{mm}$, allowing a maximum compression of $12\,\mathrm{mm}$, as springs are not recommended to be compressed more than half of their travel [12]. Cyclone should have travel greater than the total spring travel of Orion.

Under maximum compression (following a $350\,\mathrm{mm}$ drop) a swing angle of 20º $(0.35\,\mathrm{rads})$ (θ_1 in Figure 26) from the starting position (S in Figure 26) to the horizontal gave $27.4\,\mathrm{mm}$ travel, calculated using Equation 6. This travel was 2.25 times that of Orion. The suspension was able to rotate a further 4.64º $(0.081\,\mathrm{rads})$ (θ_2 in Figure 26) past the horizontal before bottoming out. This zone is not intended for normal operation and is there to prevent the suspension from running out of travel and contracting the shell. Worked equations can be found in Appendix C.2.

$$Travel = sin(\theta) \times L \tag{6}$$

Having determined the length of the swing arm and the swing angle, the force of the $350\,\mathrm{mm}$ drop was calculated given a robot weight of $25\,\mathrm{kg}$ (Equation 7). The force was calculated to be

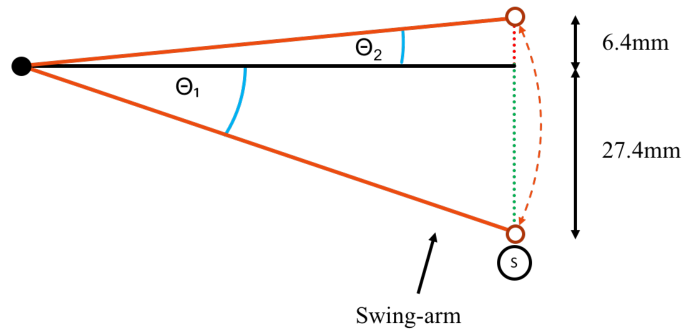

Figure 26: Suspension Compression Path

738 N (3 S.F) per corner, giving a torque (Equation 8) on the torsion bar of 62.7 N (3 S.F). The calculations for force and torque are detailed in Appendix C.3.

$$Force = \frac{m \times g \times h}{stopping\ distance} \times \frac{1}{4} \tag{7}$$

$$Torque = F \times d \tag{8}$$

The polar moment of inertia of a torsion bar of a given cross-section was calculated, as well as the length of bar needed to allow a 20° swing angle for three materials (magnesium, aluminium and stainless steel). The sections considered were circular and rectangular and the dimensions of the torsion bar and blade were modified in an Excel model to give a suitable length of bar that would allow for good adjustability. Equations 9 and 10 calculate the polar moment of inertia. Worked equation can be found in Appendix C.4.

$$Circular\ section : J = \frac{\pi(d^4)}{32} \tag{9}$$

$$Rectangular\ section : J = \frac{bh}{12}(b^2 + h^2) \tag{10}$$

Torsion bar lengths were calculated for all materials (Equation 11). The results showed that the most suitable materials for a torsion bar were either a 6 mm diameter aluminium rod, needing a length of 49.0 mm to absorb the fall or a steel torsion blade (6.35 mm by 2 mm) needing to be 52.4 mm in length (Appendix C.5). Both options give a wide range of adjustability along the 99 mm blade length. Worked calculations are detailed in Appendix C.5.

$$Length = \frac{\theta(J \times G)}{T} \tag{11}$$

The steel blade was more suitable because of the higher sheer modulus of steel (79 GPa) against aluminium (25.5 GPa) [32], which is critical as the torsion bars will experience significant shear force. Furthermore, from a manufacturability standpoint it would be easier to fix a flat blade to other components than it would be for a cylindrical bar. Using a steel torsion bar was investigated but found to be unfeasible due to the small diameter required for a good range of adjustability.

A rail system with a movable anchor point for the torsion blade was designed to allow the effective length to be varied to adjust spring rate and therefore travel and ground clearance. The rail system was made from MakerBeam. There were concerns that the MakerBeam and MakerBeam bolts would not withstand the tensile and compressive forces produced during suspension compression. Simulations were carried out on the MakerBeam rails, bolts and tuning block using Autodesk Inventor Fusion. One of the M3 MakerBeam bolts was subjected to a tensile force of $391.5\,\mathrm{N}$, the other to a compressive force of the same magnitude. This represents the $783\,\mathrm{N}$ impact force on each suspension assembly if not allowed to compress, when dropped from $350\,\mathrm{mm}$.

The MakerBeam experienced a maximum stress of $98.97\,\mathrm{MPa}$, Figure 27. MakerBeam is manufactured from 6063-T6 aluminium, which as a yield strength of $215\,\mathrm{MPa}$ [33]. This gives a factor of safety of 1.2. This was a "worst-case scenario", during operation the suspension should never be completely locked out, therefore the stress on the MakerBeam would be significantly less.

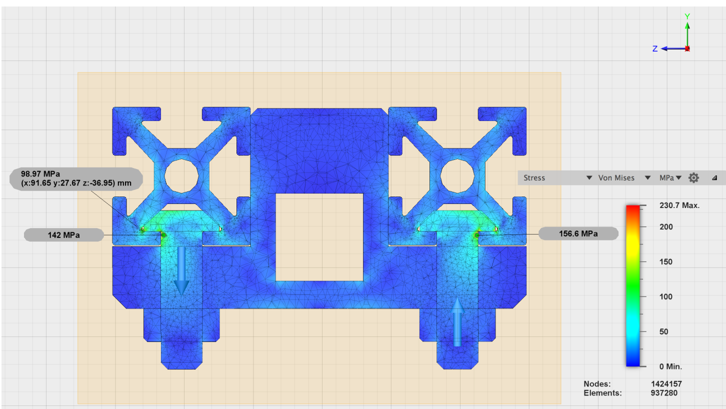

Figure 27: MakerBeam Rail and Fixing Simulation

The M3 screws fixing the tuning block to the MakerBeam experienced a maximum stress of $156.6\,\mathrm{MPa}$, (Figure 27). The yield strength of an M3 alloy steel screw is $945\,\mathrm{MPa}$ [34], therefore the stress that will be exerted on the screws during normal operation will not exceed the yield stress of the fixings and has a factor-of-safety of 6.0.

4.5.5. Simulation of Suspension Components

To assist the design and validation of the suspension components, further simulations were carried out. The service conditions of the components were known and were used to form the basis of these simulations.

4.5.5.1 Blade Adapter Simulation

Figure 28 is a simulation applying $783\,\mathrm{N}$ (the calculated force on one suspension assembly when dropped from $350\,\mathrm{mm}$ in the y-axis to the smaller diameter section of the blade adapter. As before, this simulates a worst-case scenario where the suspension is not allowed to function, transferring all force into the blade adapter. The maximum stress was $134.9\,\mathrm{MPa}$, lower than the yield stresses of 6063-T6 aluminium ($215\,\mathrm{MPa}$) [33] and silver steel ($640\,\mathrm{MPa}$) [35] that were considered for the component. The decision was made to manufacture the component from silver steel as it allows a greater factor of safety of 4.7.

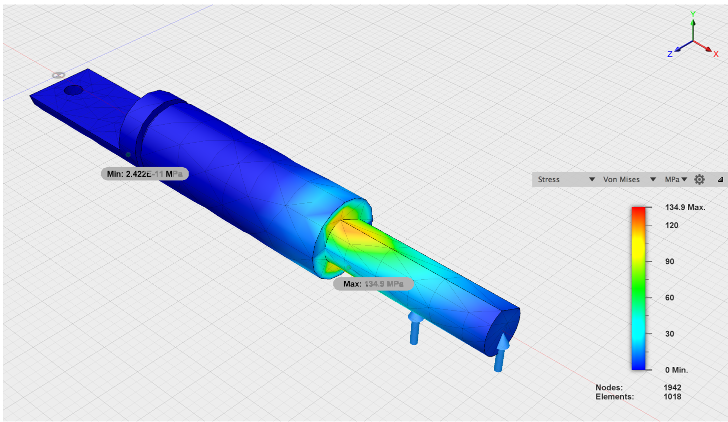

Figure 28: Simulation of the Blade Adapter

4.5.5.2 Torsion Blade and Blade Adapter Simulation

Simulations investigating the shear stress on the blade adapter and torsion blade were also carried out. When a torque of $62.66\,\mathrm{N\,m}$ (the torque when dropped from $350\,\mathrm{mm}$) was applied to the blade adapter, the maximum shear stresses on the blade adapter were $4996\,\mathrm{MPa}$ ($4.996\,\mathrm{GPa}$), and $-8945\,\mathrm{MPa}$ ($-8.945\,\mathrm{GPa}$), which can be treated as $8945\,\mathrm{MPa}$ ($8.945\,\mathrm{GPa}$). The shear modulus of steel is $79\,\mathrm{GPa}$ [32], giving a factor of safety of 8.8. The average shear stress on the blade adapter was around $1000\,\mathrm{MPa}$ ($1\,\mathrm{GPa}$) and around $2200\,\mathrm{MPa}$ ($2.2\,\mathrm{GPa}$) on the torsion blade, as seen in Figure 29, and will therefore have an even greater factor of safety. This means that during normal operation, the shear stresses exerted on the blade adapter and torsion blade will not cause mechanical failure.

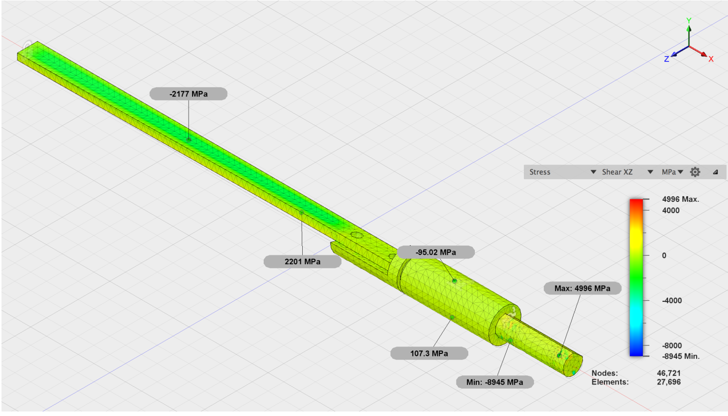

Figure 29: Simulation of the Torsion Blade and Blade Adapter

4.5.6. Suspension Design Summary

The torsion bar suspension set-up fitted to Cyclone was designed using the lessons learnt form Orion as guidance. The problems highlighted in the critical analysis of the suspension are all problems which could disable the robot in the field and the new design sought to address these. The torsion bar suspension, although without damping, did address the issues of the coil spring design and would provide a more robust system that is also simpler. Table C.11 in Appendix C.6 compares the suspension systems of Orion and Cyclone. The final torsion blade suspension design is shown in Figure 30.

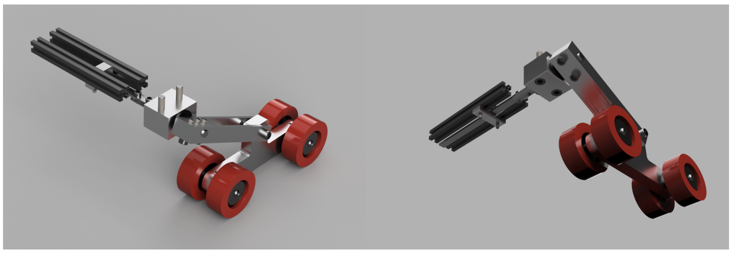

Figure 30: Final Torsion Blade Suspension Design, including Idlers

4.6. Dynamic Tensioning

4.6.1. What is Dynamic Tensioning?

When a suspension system in tracked vehicles contracts or extends slack is produced to as a consequence; this could result in derailment if not counteracted. Tensioning systems work in tandem with the suspension to ensure that tracks are always sufficiently taught. In static systems, track tension may only be adjusted whilst the vehicle is stationary, whereas dynamic systems facilitate control whilst the vehicle is in motion.

4.6.2. Analysis of Orion's System

Orion used a static tensioning system to counteract the slack in the tracks by means of an adapted screw used to position the components which hold the front axles, the pillow blocks. Although simplistic, and therefore easy to design and implement, the static nature of Orion's tensioning system resulted in an impractical solution for it's intended purpose: to control the tension of the tracks whilst in motion. During operation, if Orion's suspension contracted in reaction to any uneven surface, there would be a high risk of track-derailment.

4.6.3. Design for Cyclone's System

The decision was made to adapt Orion's static system to allow for dynamic functionality. This system is contained within the front module and ensures that changes in the track tension due to the motion of the suspension are sufficiently counteracted. Each track's tension is independently controlled which is imperative for crossing rough, uneven terrain.

Many of the components were reused but required reworked, however, this kept the design simple and thus saved on both design and manufacturing time. Each system consists of a pillow block, two springs and two spring rods. The front axles, onto which the wheels are fixed, are then placed through the pillow blocks to complete the dynamic tension system seen in Figure 31. The system is held in place by linear bearings which are bolted to the bulkhead, connecting the front module to the centre module. The rods, which are inside the springs, pass through these bearings and are then able to move freely in a linear motion to enable the system to perform its functionality. The system is installed in such a way that it will work in conjunction with, but in a reverse manner to, the suspension. When the suspension is compressed, the dynamic tensioning springs will extend to remove the resulting slack, by pushing the axle forward, and vice versa during suspension extension. The installation of this system will lower the risk of track derailment whilst the robot is in operation and thus avoid the manual collection of Cyclone by rescue personnel from potentially hazardous environments.

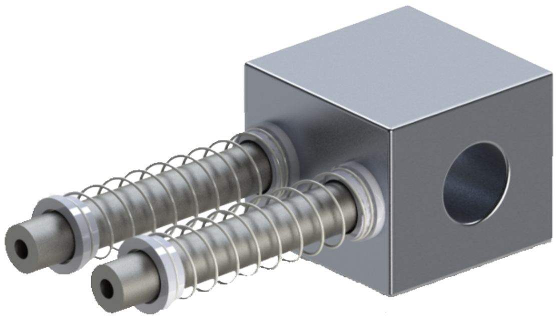

Figure 31: Cyclone's Dynamic Tension System Assembly

Springs were chosen as the method of applying a force to the pillow blocks to push the front axles forward to tension the tracks. This was found to be the simplest way to provide a force and is easily implemented onto the design adapted from the previous year.

In order to fully adapt the previous design to that of Cyclones, its faults had to be corrected. This was namely, the poor selection of bearings. The linear bearings in the pillow blocks of Orion were replaced with rotational bearings more suited to the rotational motion of the axles. Linear bearings were also used in the bulkhead to allow for the smooth movement of the rods through the bulkhead.

During design, it was discovered that there was the risk of beaching if the dynamic tensioning system contracted too far, therefore exposing the frame of the robot. To avoid this, the frame was altered to give a shallower profile and a simple stopper was installed in the front module to prevent the springs from contracting too far.

In order to decipher which type of spring was required, specifications had to be identified. The main requirement is that the total spring rate of each system must not be larger than that of the suspension and so not preventing the suspension from performing its own function. The spring rate was therefore calculated for the suspension using the polar moment of inertia, the Young's modulus and the length of the steel blade. The equations for the spring rate are shown in equations (12) and (13).

$$Spring\,rate = \frac{J \times G}{L} \tag{12}$$

$$Spring\,rate = \frac{4.69 \times 10^{-11} \times 200 \times 10^{9}}{0.0524} = 179.0N/m \tag{13}$$

There are four torsion blades in the suspension, which equates to the number of springs used within the dynamic tension systems. Therefore, the spring rate for each of the four springs (two per track) needed to be less than $179.0\,\mathrm{N/m}$ calculated from equation (13). The suppliers, Lee Springs, catalogue springs used $\mathrm{N/mm}$ as the units for the spring rate, therefore the spring rate was converted to $0.179\,\mathrm{N/mm}$. The second requirement is that the springs should allow for the same amount of travel as the suspension to ensure the track tension does not suffer as a result. The maximum travel for the suspension (if the suspension bottoms out) is calculated to be $33.9\,\mathrm{mm}$, and therefore the travel of the dynamic tensioning systems will be at least $33.9\,\mathrm{mm}$. It was advised by the manufacturers that the recommended travel (as seen in Table 1) of the springs should be no more than $80\,\%$ of the difference between its free length and closed length if compressed for a continuous period as this will affect its performance. However, since the required travel of $33.9\,\mathrm{mm}$ is only going to be necessary in very rare occasions when the suspension bottoms out, providing the recommended travel of the springs was at least equivalent to the usable travel of the suspension, $27.4\,\mathrm{mm}$, they could be accepted. Due to the confined space within which the dynamic tensioning system is located, the free length of the springs is also a factor to consider, this length is limited to $64\,\mathrm{mm}$. The springs require an inner diameter larger than $10\,\mathrm{mm}$ in order to fit over the rods.

There was a limited availability of springs that fit these requirements. However, after consultation with Lee Spring, two different types were chosen, seen in Table 1. This allowed for testing of both springs and ultimately LP032K06S316 was chosen for the dynamic tensioning.

Table 1: Parameters of Spring Choices [36], [37]

Parameters	**Spring Type**	
	LP032K06S316	LP29K06S316
Outside Diameter (mm)	13.716	13.716
Inside Diameter (mm)	12.904	12.980
Wire Diameter (mm)	0.812	0.736
Free Length (mm)	50.800	50.800
Closed Length (mm)	10.718	8.737
Recommended Travel (mm)	32.066	33.650
Spring Rate (N/mm)	0.170	0.130

4.7. Electronics

4.7.1. System Overview

The electronics architecture has been improved from the design proposed by the WMR 2014/15 team.

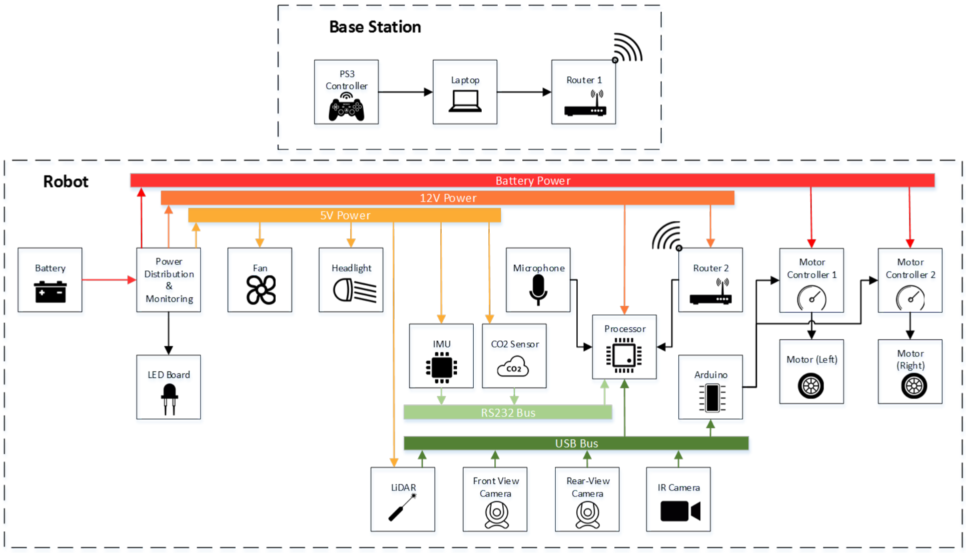

Figure 32: Electronics Systems Diagram

The key differences include the addition of a second router at the base station. This approach has been implemented to overcome the ”connectivity issues” that many past WMR teams have experienced at the competition. The new router has superior performance over a laptop’s Wi-Fi card and so will improve the connectivity between the robot and the base station.

A second key difference is the removal of the bulky 8-to-1 USB splitter. This device limited the speed that the USB peripherals could run at, bottle-necking 8 data streams into 1, due to the maximum capable speed on USB 2.0. To ensure good quality video streams, it is proposed the RS232 ports of the robot’s computer are utilised. Both the CO_2 sensor and Inertial Measurement Unit (IMU) have compatible RS232 outputs.

It was discovered that a single threaded microcontroller could not reliably support the control of the motors whilst pseudo-simultaneously monitor the sub-systems. Therefore, this has been split into two, with a dedicated device driving the motors.The monitoring of the sub-systems has moved onto a new board, which also incorporates the power distribution that had to be redesigned.

4.7.2. Processor

A quintessential component within the robot is the processor board. This board runs the Ubuntu Operating System (OS) and the ROS master software, so is responsible for managing each of the subsystems simultaneously, whilst maintain a live feed of information to the base station laptop. A range of processor boards were considered and the results against the requirement criteria are given in Table 2.

Table 2: Processor Comparison [38, 39, 40]

General		**Power Supply**		**Processing**			**I/O Capability**	
Processor Board	Dimensions (mm)	Voltage (V)	Power (W)	Chipset	Speed (GHz)	DDR3 (GB)	USB	Other
Axiotex PICO831	100 x 72	5	15	Intel Atom N2800	1 86	4	4	2x RS232
Intel NUC5i5MYBE	115 x 111	19	65	Intel Core i5	2 3	16	6	-
Axiotex PICO842	100 x 72	12	10 8	Intel Celeron J1900	2 42	8	4	2x RS232

Last year's WMR team chose the PICO831 board as the robot computer. This board utilises an Intel Atom N2800 chipset released in 2011 [41] and supports up to 4GB of DDR3 RAM. However, modern boards can support more RAM allowing Cyclone to have improved video-streaming capabilities. As this board had not been purchased, alternative processors were considered.

The Intel NUC board was a good choice as it supports 16GB of RAM. In addition, its processor runs 23 % faster, not to mention its additional two USB ports compared to Orion's processor. However, this comes at the detriment of this board drawing over four times as much power. It was decided therefore that the more recent, PICO842 board utilising the Intel Celeron J1900 released later in 2013, was the best option [42]. This processor, coupled with the AX93283 I/O expansion board [43], provides a fast processing platform at a low power consumption with Gigabit Ethernet capability so was an ideal choice for Cyclone.

4.7.3. Motors

The WMR project team of 2014/15 set to use Maxon EC-4 pole 323217 motors coupled with the Maxon ESCON P/N 409510 controllers. It was discovered that these motors were not suitable for our robot, as discussed in greater detail in Section 4.4. Therefore, a new set of motors (plus gearhead) that could provide a greater torque were required. The new motors were also selected to be compatible with the existing controllers purchased by last year's team. Table 3 provides a summary of the motor/gearhead combinations that were investigated.

The results show the theoretical speeds and current requirements for each of the motor/gear

Table 3: Motor & Gear head Comparisons [44, 45, 46, 25, 47, 48, 49, 26, 50, 51]

General		Motors	Gearhead		Summary					
Type	Option	Efficiency (%)	Reduction	Efficiency (%)	Min Speed (rpm)	Max Speed (rpm)	No Load Current (A)	Stair Climb Current (A)	Length (mm)	Cost (£)
Motor:136203 w/ Gear:203127	1	80	126	72	45.3	62.7	0.59	6.82	215.6	554.15
Motor:136204 w/ Gear:203127	2	80	126	72	34.8	48.2	0.46	5.26	215.6	554.15
Motor:370356 w/ Gear:223087	3	94	26	83	52.4	72.5	0.38	4.31	206.4	460.21
Motor:305015 w/ Gear:203127	4	90	126	72	30.5	42.2	0.32	3.62	155.4	505.63
Motor:305015 w/ Gear:326669	5	90	123	70	30.4	42.0	0.33	3.82	155.2	526.09
Orion's (2014/15) selection										
Motor:323217 w/ Gear:166945	-	88	122.8	70	77.9	107.8	0.90	10.28	122.7	718.70

combinations. Mechanically the best motors are option 1, as they provide the most torque with option 5 providing the least torque. Conversely, from an electronics perspective, the power required to achieve those torques have almost the inverse relationship. Option 4 and 5 appear enticing due to their low power consumption, but this does come at a penalty on speed, which may be too slow for the robot's operation.

Therefore, it was decided that to satisfy both mechanical and electronic requirements, option 3 would be the motors of choice. The 94 % efficient DC 370356 motors coupled with the 83% efficient 223087 gear head, are approximately 27 % more efficient than Orion's motors. This is important to maximise the robot's battery life.

4.7.4. Motor Drive Processor

The DC motors are managed via ESCON 50/50 P/N 409510 motor controllers. The motor velocity commands can be input by either an analogue or Pulse Width Modulation (PWM) signal. Cyclone utilises the PWM functionality, as is boasts significant advantages particularly due to its insensitivity to noise. This trait is common across all digital signals, which has lead to their abundant usage in modern day electronics.

It was decided that the ATMega328 microcontroller on the Arduino Uno platform was suitable for this application. This low-cost microcontroller is smaller and requires less power when compared to the Arduino Mega 2560 board; as proposed by the WMR 2014/15 team. In addition, an Arduino can be easily integrated with the ROS environment, plus software development is made simpler with the intuitive Arduino IDE.

4.7.5. Sensor Array

In order for the robot to compete at the RoboCup, it needs to be equipped with a range of sensors as more points will be awarded to robots with the greatest capabilities. Cyclone's architecture has been designed to handle a comprehensive range of sensors. Previous WMR builds provide a proven sensor array design, but a revision of these are essential in order to take advantage of the latest cutting edge technology, plus ensuring their compatibility with Cyclone's ROS driven system. Appendix D.1 gives a summary of the sensors selected for use within Cyclone.

4.7.6. Battery Monitor Board

4.7.6.1 Overview

The 2014/15 WMR team designed and manufactured a power distribution board. The intention was for it to provide regulated power at 12 V or 5 V to each robot subsystem. However, after a critical analysis of the board it was decided a redesign was needed for the following reasons:

1. When tested, the 12 V regulator was not producing the required output. It would require major board modifications, which are not easy to do on buried PCB traces.
2. The max current output from the 12 V regulator was too small and it would not have been capable of powering all the systems requiring this voltage.
3. The 5 V regulator was not appropriate for the design, due to over-cautious estimations of it's output power requirement. This meant it would operate at a much lower efficiency than expected. This would severely reduce the robot's battery life and the power lost would cause the regulator to dissipate a greater amount of heat.
4. There was no consideration for how battery monitoring and automatic shutdown of the robot could be implemented. Additionally, there was no consideration for how a master power switch and E-Stop button would be integrated.
5. There were redundant current limiting fuses that would not have blown in the event of an over-current draw.
6. The board has no raw battery voltage output, which is required for the motors or may be required in the future design of an arm.

4.7.6.2 Principle Operations

A new integrated battery distribution & monitoring board was therefore designed, with the schematic given in Appendix D.2. The robot utilises Lithium Polymer (LiPo) batteries due to their compact size, large capacity and high discharge rate. These are volatile as they use dry electrolyte polymer sheets, which can burst or catch fire if mistreated [52]. So each of the battery's cells are monitored to ensure they stay within their safe operating conditions, whilst also ensuring their maximum power is drawn from them.

It is for this reason that an ATMega328 microcontroller is integrated on the board. It has 6x 10-bit Analogue-to-Digital Converter (ADC) inputs, which are used to monitor each of the cells to an accuracy of $4.88\,\mathrm{mV}$. The microcontroller updates an LED array with the current battery voltage, in addition to sending messages back through ROS to display this level on the operators Graphical User Interface (GUI). Should the warnings be ignored, the microcontroller will automatically shut down the entire robot, to ensure the safety and longevity of the battery.

An additional safety feature is the monitoring of sub-system's ”heartbeats.” The electronic systems output periodic pulses when operating correctly, which can be monitored. In the event of a software glitch, the ”heartbeat” is not received, and the operation of the robot is likely to be unknown and uncontrollable. In this event the microcontroller will shut down the robot as a precaution. The battery status LED would begin with an error code so that the reason for the shutdown is known.

Additional hardware safety features including an emergency stop and master power on/off switch have been included like many previous successful WMR designs.

4.7.6.3 Voltage Regulators

The 2014/15 team made conservative estimations regarding the power drawn from each device. These were based on the worst-case scenario and proved to be inaccurate, as they were not reflecting the true power drawn. Table 4 shows the updated power requirements, which have been measured using a bench power supply.

Table 4: Cyclones Power Requirements [53, 54, 55]

Device	Voltage (V)	Max Current (A)	Safety Margin (+20%) (A)
Motor (x2)	Battery	8 6	10 32
Motor Controllers (x2)	Battery	0 172	0 2064
		Total	**10.5264**
Processor	12	0 9	1 08
Arduino (Motors)	12	0 1	0 12
Front Camera	12	0 5	0 6
Rear-View Camera	12	0 5	0 6
IR Camera	12	0 5	0 6
		Total	**4.2**
Router	5	1	1 2
LiDAR	5	0 5	0 6
IMU	5	0 07	0 084
CO_2 Sensor	5	0 2	0 24
Headlight	5	0 35	0 42
Fan	5	0 236	0 2832
		Total	**1.6272**

Changes to the processor board, motors and router coupled with these conservative estimates meant the regulators were no longer suitable. The 12 V TRACO TEL30-2412 could provide a maximum output current of 2.5 A however, Cyclone requires 4.20 A so this regulator needed to be replaced [56].

Their GE EHHD024A0A41 can provide 24 A at 5 V, which is far greater than the 1.63 A required by the robot. This meant that the regulator would be working at only at 70 % efficiency (see Appendix D.3) [57]. So for these reasons a new set of regulators was considered, with a comparison between the new and old robots regulators given in Table 5.

Table 5: Regulators Comparison between Orion and Cyclone [56, 57, 58, 59]

Part	Output Voltage (V)	Max Output Current (A)	Dimensions (Inch)	Efficiency (%)
WMR Power Distribution Board 2014/15				
TRACO TEL30-2412	12	2.5	2 x 1	91
GE EHHD024A0A41	5	24	2.3 x 0.9	≈70
WMR Power Distribution Board 2015/16				
TRACO TEN60-2412N	12	5	2 x 1	92
TRACO TEN40-2411N	5	8	2 x 1	91

The TRACO TEN60-2412N and TRACO TEN40-2411N have been selected due to their high efficiency and small footprints. These rugged regulators satisfy the temperature requirements of the board with a wide operating range of −40°C to 80°C. Their maximum current outputs are greater than those calculated in Table 4 to this is to allow for future expansion, with the inclusion of a robot arm.

4.7.6.4 Current Protection

An over-current protection fuse has been incorporated into the design. The 20 A Littelfuse was selected, such that if the current drawn exceeded the expected maximum, allowing for a 20 % margin, then it will blow and cut the power to the robot.

4.7.6.5 Connectors

This design requires many types of connectors, due to the number of mixed signals utilised in the design. All the connectors used within the robot were sourced from WMR sponsor, Harwin. A full list of connectors and how they meet their associated requirements is given in Appendix D.4.

Harwin's MixTek range of connectors can support up to 20 A of current through each pin so suffice the power distribution operations. Conversely, It was decided that their L-Tek range was suitable for all the low power signals. All of the connectors contain either, a screw terminal lock in or a friction latch (12 to 14N of force) [60]. This is to ensure a reliable connection, even under the shock and vibration conditions the robot will be subject to at the competition.

4.7.6.6 Trace Sizings

The track widths on the board needed to be sized to suffice the power requirements previously stated. The trace sizings calculated in Table 6 are based on the worst-case scenario using the IPC-2221 standard [61].

Table 6: Trace Sizings & Wire Thicknesses Required for each Power Line

Trace	Max Current (+20% safety margin) (A)	Trace width Single-Sided (mm)	Trace width Double-Sided (mm)	Wire Thickness (AWG)	Current Carrying Capability (A)
Battery	13.78	7.35	3.68	12	34
12V	4.2	1.43	0.71	14	24
5V	1.63	0.39	0.19	14	24
Signals	¡ 0.03	Negligible	Not Necessary	22	5

These widths have been calculated on the standard trace thickness of $1oz.ft^{-2}$ (≈35 µm), allowing for a 20°C rise of an external track when conducting; with an assumption of 25°C ambient temperature [62]. The board design utilises double sided traces to minimise trace width, with the plated through holes to electrically connect the two. It was decided that there were enough through-hole connections, such that resistance between the traces on each layer was negligible, so no additional shorting vias were required.

In addition, traces have been made as short as possible in order to reduce their resistance. A high parasitic resistance would lead to a voltage drop along the trace, introducing floating ground issues, as well as dissipating lots of power. Traditionally, a multi-layer board is used to minimise these effects, but the additional cost and complexity is not required for this build.

4.7.6.7 Wire Sizings

The wires carrying the current to and from the board also need to adhere to these power requirements. Table 6 shows the wires thickness, in American Wire Gauge (AWG), selected from each part of the board [63].

4.7.6.8 Board Dimensions

Considerations to minimise the amount of board real-estate were required to create a compact design that adhered to the mechanical dimensions. The central section of the robot is $212\,\text{mm} \times 322\,\text{mm} \times 122\,\text{mm}$, so the board was sized to $120\,\text{mm} \times 120\,\text{mm}$. Therefore, the board can be rearranged in many orientations, allowing future teams to alter the internal arrangements with ease. The Ultiboard layout is given in Figures 33a and 33b.

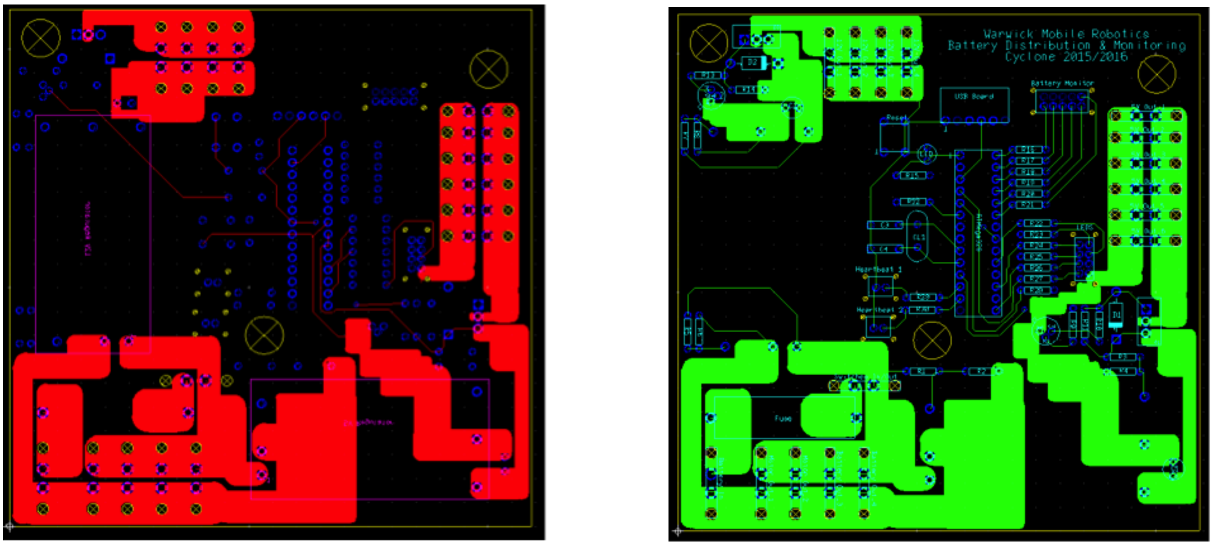

(a) Bottom-Side (b) Top-Side

Figure 33: Battery Monitoring Board PCB Design

4.7.6.9 Usability & Testability

The board was designed to allow for maximum testability, plus to have the ability for modifications. Extra ”dummy” components were incorporated into the design with their pads laid out. The intention was to not fit these components, but have the ability to do so if required.

All components were selected to be through hole, allowing for ease of soldering and debugging of the board during testing. In addition, decoupling capacitors were added to the outputs of the regulators. Their purpose is to reduce the voltage ripple on the output, such that a smooth, constant voltage is delivered to the remaining circuitry.

4.7.6.10 Component Placing

Care was taken when placing the components in order to separate the high power ”noisy” circuitry, from the sensitive digital micro-controller circuits. In the design’s layout, it was thought the regulators were placed on the backside of the board. The intention was that these would be fixed to the robot casings, to aid with heat dissipation, whilst the connectors on the other side would still be easily accessible to the rest of the sub-systems. However, there was a misinterpretation with the software and the regulators were not placed on the bottom of the board as expected.

4.7.6.11 Final Design

The design was sent for manufacture at Euro circuits. They were selected as they could provide plated through holes, on a short-lead time, for at a reasonable price. The returned blank PCB was then populated with components, with the soldering done in-house by hand, as shown in Figure 34.

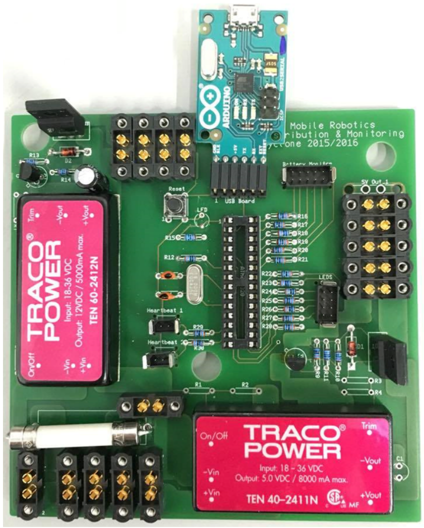

Figure 34: Battery Monitoring & Distribution Board

4.7.7. LED Board

A second board was manufactured in the School of Engineering. This board consists of 6-power status LEDs and a robot status LED. This single-sided board was designed so that the LEDs are placed externally from the battery board and can be made visible through the robots chassis. All the routing is on a single-side however, the connector is orientation on the bottom side. This is so it can be connected on the inside of the robot, with the LEDs facing out of the robot. There are 4 mounting holes to allow the board to be fixed, with spacers, to the robot using M3 screws.

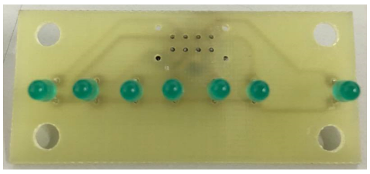

Figure 35: LED Board

4.8. Communications

4.8.1. Wireless Network

There are different protocols of wireless specification 802.11. They encompass a range of frequencies and therefore effective distances [64]. The latest infrastructure, 802.11ac, can transmit data at greater speeds with less interference compared to its predecessors due to a higher operating frequency [65]. However, this higher frequency comes to the detriment of a reduced range [66]. Therefore, the 802.11n will still be used given its flexibility despite having lower data transmission rate.

4.8.2. Data Rate

The routers capabilities have been analysed based fundamentally on the amount of data that needed to be communicated to and from the robot. This data includes the operator's controls and real-time information, such as audio, mapping and video streams. The Kush Gauge methodology [67] was used to calculate the video streaming data requirement. Cyclone will use 720p cameras with medium motion video at 30 frames per second.

$$(1280 \times 720) \times 2 \times 30 \times 0.07 = 3,870,720bps \approx 3,870kbps \tag{14}$$

The total data rate that Cyclone needs to support is 15Mbps. This includes 3 cameras, a LiDAR, IMU, audio and the controls to command the robot. This value is likely to be closer to 20Mbps after the inclusion of the robot arm, and accounting for packet losses.

4.8.3. Further Considerations

The router must also conform with the dimensions and weight limitations imposed by the chassis's requirements. A further factor to be considered is the power consumption. The selected routers should operate at either $12\,\mathrm{V}$ or $5\,\mathrm{V}$ to ensure compatibility with the power distribution board.

Lastly, Cyclone could benefit from the use of a non-commercial, high-powered router. This can improve the robot's range but it operates by emitting at a higher frequency. This has been found to be harmful to bystanders and must therefore remain within EU regulations for electromagnetic frequencies [68].

4.8.4. Orion's Router

The specification of the router selected by last year's team is given in Appendix E.14. This router did not fulfil robot's requirements for two reasons. Firstly, the 2014/15 team purchased a router with the belief it operated at 5 V. However, upon testing it was discovered that it required a 24 V supply and therefore was incompatible with their own power distribution board. Secondly, the router was limited to the 2.4 GHz range, which reduces its usable frequency bands. At the *RoboCup*, due to the number of competitors using the WiFi infrastructure, the option to operate on the 5 GHz range would be beneficial as a more reliable network could be set up, with less interference.

4.8.5. Selecting Cyclone's Router

The routers, detailed in Appendix E.15, all fulfill Cyclone's requirements. Three routers were selected for testing to determine, which was the most suitable (see Table 7). The Buffalo AirStation AC433 was small in size and weight. However, it was limited to 150 Mbps data rate. The second router, the ZyXEL NBG6503, could reach wireless data rates of up to 300 Mbps, plus this router has the added advantage of detachable antennas. The third router, D-Link DWR-118, has mobile internet capabilities, giving a wider range of wireless frequencies as well as supporting Gigabit Ethernet (1000 Mbps). These ports allow faster Local Area Network (LAN) data transfer compared to standard ports at 100 Mbps. Each of these routers were tested in order to determine the maximum range they can communicate (see Section 7.2).

Table 7: Comparison of selected router's Specifications

Parameter	**Value**		
Name	Buffalo	D-Link	ZyXEL
Dimensions (mm x mm x mm)	45.0 × 45.0 × 15.0	148.5 × 113.5 × 25.0	159.0 × 111.0 × 23.0
Weight (grams)	19	194.3	230
Wireless Speed 802.11 n/ac (Mbps)	150/433	150/433	300/433
Power Supply (DC)	5V USB Powered	12V/1.5A	12V/1A

4.9. Software

4.9.1. Robot Operating Software (ROS)

4.9.1.1 Overview

Robot Operating System (ROS) is an open source platform that runs on Linux distributions and allows for the rapid development of robot software. The system offers many other tools that are advantageous when testing and debugging software [69]. It is for these reasons that the system has been adopted for use in Cyclone.

4.9.1.2 Suitability

Its operations are based on individual executable nodes of code that can communicate. A node is language independent and is used to perform a particular function; such as communicating with a sensor. An advantage is that experts publish nodes, which can be accessed by the ROS community, which with minor modifications can interface with complex hardware within your own system. This means that rather than developing all the code from scratch, much of the complex interfacing and communications are handled by ROS.

Additionally, ROS was selected for Cyclone due to its integrated features. It can store ”bags” of data that can be reviewed and replayed multiple times to aid with debugging [70]. This facility is one that will also be useful come the Robocup, as the competition has a requirement to submit the data files gathered in order to score points.

4.9.1.3 Distributed Computing

The ROS architecture has been designing to allow for distributed computing, allowing nodes to run on separate hardware to form a robot system. This is all possible due to the ROS master, which utilises its XMLRPC form parameter service, to act as a database for nodes to communicate on a network.

4.9.1.4 Communications Protocol

A ROS topic is the name given to a set of messages that can be published or subscribed to. The data is then asynchronously communicated between nodes relating to that topic, with multiple nodes capable of publishing or subscribing at once. Alternatively, direct, synchronous peer-to-peer messaging can be established through the use of ROS services.

The ROS master is implemented via XMLRPC, which is a HTTP-based stateless protocol, meaning each packet of data is considered to be unrelated [71]. The transportation of data is done using standard Transmission Control Protocol/Internet Protocol (TCP/IP) sockets. The data messages consist of a header, which contains the message type and routing information, followed by the actual data [72]. This is a reliable method to transfer data that is suitable for the Robocup competition, given the issues experienced by previous WMR teams with unreliable communications connections. However, the alternative User User Datagram Protocol (UDP) can support greater data rates, which is ideal for streaming multiple camera feeds. It achieves this by having less ”handshaking” and no acknowledgement packets meaning data can be lost, but this trade-off between protocols can be experimented with for the competition.

4.9.2. Motor Control

The aim for WMR 2015/16 was to design a robot that could be remotely operated from a Play Station 3 (PS3) controller. In order to achieve this, ROS needs to interface with the PS3 controller, and then pass the relevant data onto the Arduino, which controls the motors. Figure 36 shows how each of the scripts interacts.

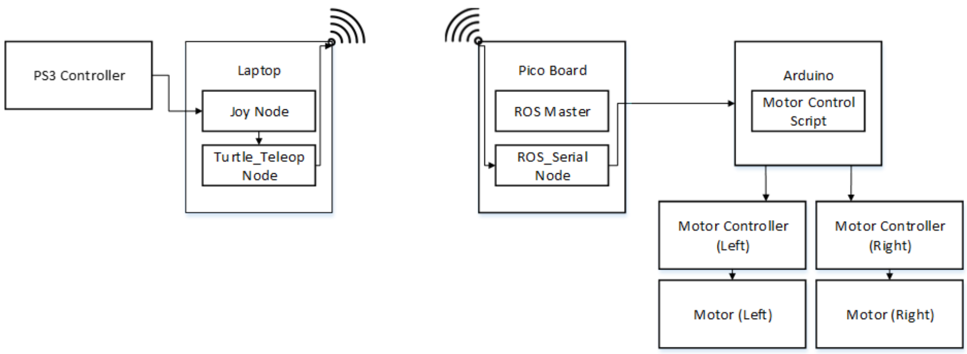

Figure 36: Cyclone’s Software Overview

4.9.2.1 Joy Node

The PS3 controller interfaces to ROS through the ”joy” node, written in C++. This node handles all the header packets, data and requirements for interfacing with the laptops USB port. The node decodes the incoming data stream and publishes the ”joy” topic, containing the button information, in the form of a structure, with each button assigned an ID number.

4.9.2.2 Turtle_Teleop Node

Cyclone will be controlled via the two analogue sticks; with the left and right sticks operating their respective motors, similarly to how a tank operates to achieve an improved turning circle. This data is passed from the joy node as a 16-bit integer, which is converted and published as a scaled floating-point number between 1 and -1. This node is run on the laptop to filter out all the other button data, so that less bandwidth is required across the network. The data sent is on the topic named ”velocity”, in the form of a structure so that it can be adapted for additional controls in the future for say, an arm.

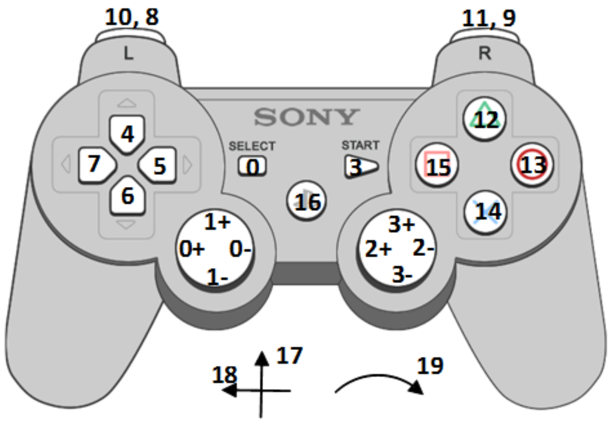

Figure 37: PS3 Controller’s ID References

4.9.2.3 ROS_Serial Node

This node is used to handle the communications with the Arduino, in a similar manner to operation of the joy node. The data is sent via a UART connection, into the input buffers of the Arduino as soon as it is received.

4.9.2.4 Arduino Motor Controller Script

The final script is run on the Arduino UNO and is responsible for converting the incoming velocity messages to a PWM signal to drive the ESCON P/N 409510 controllers. The most recent content of the Arduinos 280-byte input buffer is read in using the ”Spinonce” ROS function [73]. The buffers are monitored at a faster rate than the incoming data to avoid overflow, and a high data rate is maintained to maximise the systems responsiveness. Each data value is scaled to an 8-bit number that is converted to a PWM signal with varying duty ratio. A high duty ratio increases the speed in the forward direction, whilst reducing it increases the speed in the reverse direction, centred about a 50:50 ratio with the motors still. In order to stay within the controllers safe operating range, the duty ratio is rationalised between the bounds of $90\,\%$ to $10\,\%$. A more detailed overview of this script is given in Appendix F.1.

4.9.2.5 Launch Files

Launch scripts have been written to start up all the nodes at once. The whole system has been consolidated into two launch files, one for the Pico board and a second of the laptop. These scripts start up all the nodes on that machine at once, rather than having to run each script individually in a new terminal. They have been designed such that in the future more scripts can be incorporated and launched simultaneously.

4.9.3. Battery Monitoring

The ATMega328 microcontroller on this board is responsible for monitoring the battery cell voltages, updating the LED display, monitoring sub-systems heartbeats, communicating with ROS and being capable of shutting down the robot in an emergency. The software was written in the Arduino IDE, with the software flow illustrated in Appendix F.2.

The 6 ADC pins connected to each of the LiPo battery cells are sampled. The ADC samples have a best resolution of $4.88\,\mathrm{mV}$, however as this device is relatively cheap the samples can vary by 3-4 times this value. So in order to maximise the accuracy, each cell is sampled 5 times with its average value being stored.

The subsystem's heartbeats are also monitored by utilising the 'millis()' function. Each signal is sampled every $500\,\mathrm{ms}$, which corresponds to $1\,\mathrm{Hz}$ heartbeats. The frequency is determined based on the time it takes for the code to complete one-iteration of the software loop; due to Arduino devices having only a single thread, with instructions executed sequentially. The battery cell sampling takes $300\,\mathrm{ms}$, with the remaining code taking $7.5\,\mathrm{\mu s}$ to $37.5\,\mathrm{\mu s}$. This is calculated based on the clock speed of $20\,\mathrm{MHz}$ ($50\,\mathrm{ns}$ per instruction), with somewhere between 150 to 750 instructions per cycle. The code will always be in the position to sample the heartbeats after $500\,\mathrm{ms}$, so Cyclone is capable of shutting itself down $0.5\,\mathrm{s}$ from a sub-system failing. In this event the status LED flashes at a frequency of $2\,\mathrm{Hz}$.

When the software has gathered all the necessary data, it displays this information for the user on the LED panel. It illuminates a number LEDs with $0.9\,\mathrm{V}$ intervals between each from $19.8\,\mathrm{V}$ to $25.2\,\mathrm{V}$, corresponding the battery voltage. If the battery voltage is less than $20.7\,\mathrm{V}$, this is considered low and the LED, which is normally on will flash at $1\,\mathrm{Hz}$.

It is ensured that each cell voltage is above their minimum safe value, which is $3.3\,\mathrm{V}$ for LiPo batteries, as has been discussed previously. If any cell is below this value, the trigger flags are set to cut the power to the robot. When the robot is disabled, the software enters its low power function where it is the only thing still powered from the battery. The status LED flashes four times as fast ($4\,\mathrm{Hz}$), to alert the operates the issue that has occurred.

Table 8: Battery monitor board status LED codes

Battery Monitor Status LED Codes				
LED Status	Permanently ON	Flashing 1 Hz	Flashing 2 Hz	Flashing 4 Hz
Meaning	Normal Operation	Low Battery	Sub-system Heartbeat Failure	Dangerously Low Cell Voltage

4.10. Thermal Modelling

The thermal properties of the robot were evaluated to ensure the electronic components would remain within their safe operating conditions. If the temperature rises too high it risk the failure of these devices, putting a rescue mission in jeopardy. A thermal model was therefore created to determine if Cyclone required a cooling system.

4.10.1. The Lumped Sum Approach

The Lumped Sum Approach is the simplistic model that has been adopted to simulate the internal temperature characteristics within the Robot. The internal air and each of Cyclone's major components were modelled as thermal capacitors. The generated heat is then dissipated via the chassis, which has been modelled as six parallel resistances (Figure 38a). Nodal analysis [74] and was used to combine these components to a simplified 'lumped' electrical model [75] (Figure 38b).

$$\begin{aligned} q_1(t) &= q_i(t) - q_r(t) \\ C\frac{d}{dt}\theta_1(t) &= q_1(t) \\ q_r(t) &= \frac{1}{R}(\theta_1(t) - \theta_A(t)) \end{aligned} \tag{15}$$

q_i is the heat flow into the robot, C is the internal capacitance, R is the sum of the resistances of the shell and θ_A is the ambient temperature.

It has been assumed that all the heat will dissipate via the metal casing, as the body shell is sealed with is no air gaps. The external air is also considered to be sufficiently large, so it does not need to be modelled as a capacitor, but instead it acts as a thermal sink at a constant ambient temperature. In order to achieve the worse-case results, the battery was modelled to dissipate all of its energy as heat.

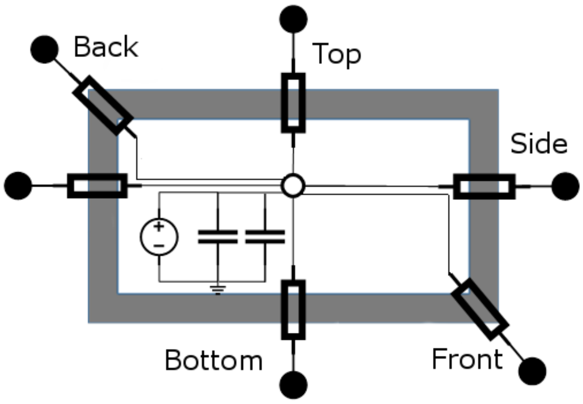

(a) Cyclone's shell represented with electrical components.

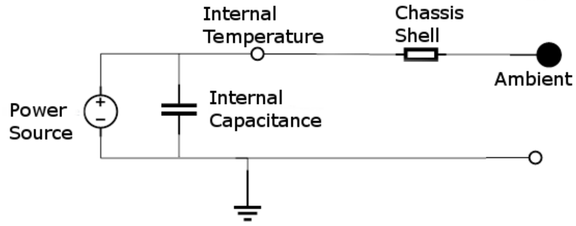

(b) Reductions to create a simplified electrical model.

Figure 38: Thermal model diagrams or Cyclone

4.10.2. Results and Analysis

The model was created in Simulink using the values given in Appendix G.1 with the full derivation of the thermal parameters give in Appendix G.2. An initial 100 second period allows the system to reach its steady state conditions, based on the ambient temperature of $24\,°\mathrm{C}$. The battery discharges all of its power over the following 80 seconds, which is based on the maximum discharge rate and capacity of the battery.

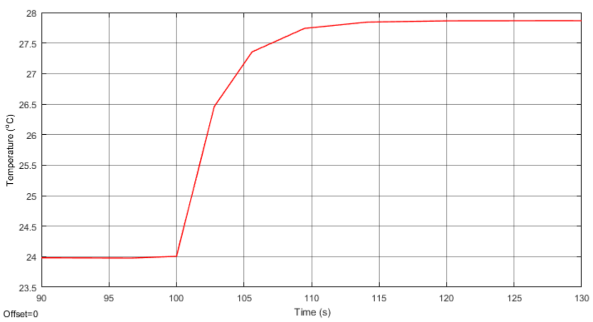

(a) Battery Starts Dissipating

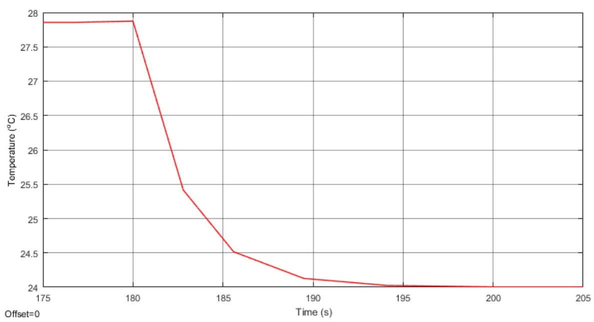

(b) Battery Stops Dissipating

Figure 39: Thermal response of the system

These show that in the worse-case scenario, Cyclones internal temperature will increase by $3.9\,°\mathrm{C}$, until it reaches equilibrium where the rate the energy is lost to the environment equals the energy dissipated by the heat source (Figure 39a). Figure 39b shows that the internal temperature returns to ambient 15 seconds after the battery has dissipated all its power.

The model is a simplistic thermal view of Cyclone, which gives a broad overview of the heating effects during its operation. Based on these results it can be concluded that Cyclone will not require a cooling system. However, individual electronic components have not assessed. In order to achieve this, a more detailed 3-D model using complex CAD software such as Abaqus is required. These results may indicate that a specific electronic component approaches its safe operating limiting, therefore actions must be taken to mitigate this excessive heating; such as fixing the components to the chassis or the inclusion of a dedicated fan to move hot air away from this individual component. Under these circumstances the cooling should remain within a closed system, to ensure that Cyclones specification is adhered to.

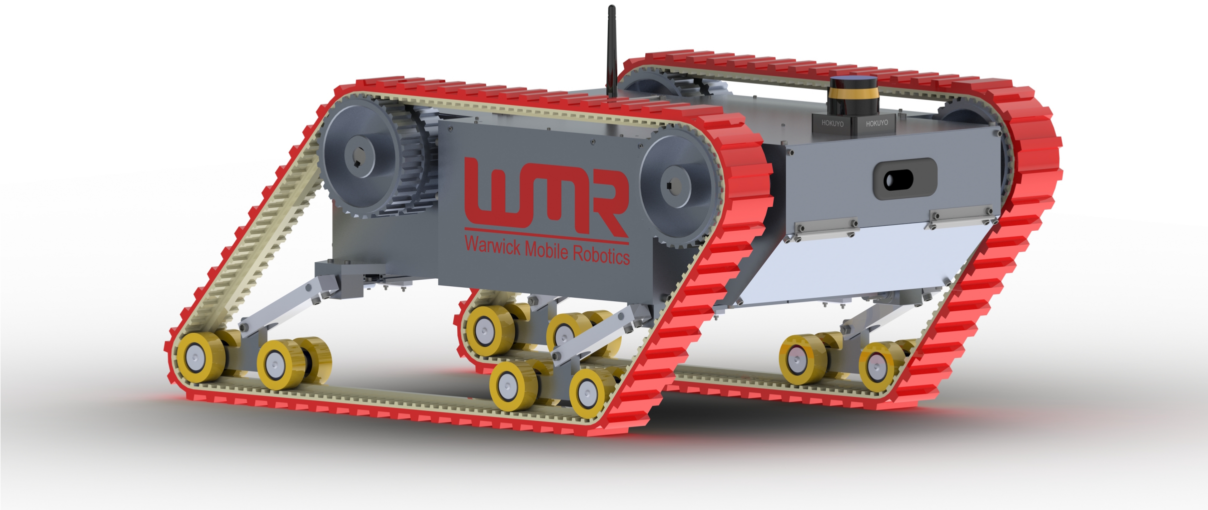

Figure 40: Rendered CAD image of Cyclone

5 Final Design

High-level collaboration between team members, suppliers and technicians helped to realise the final design for Cyclone. This design was subsequently fabricated and assembled by the team to create the M-USAR robot shown in Figures 40 and 41. Although manufacturing was commenced, it was not fully completed and tasks remain for the 2016/17 team to finalise.

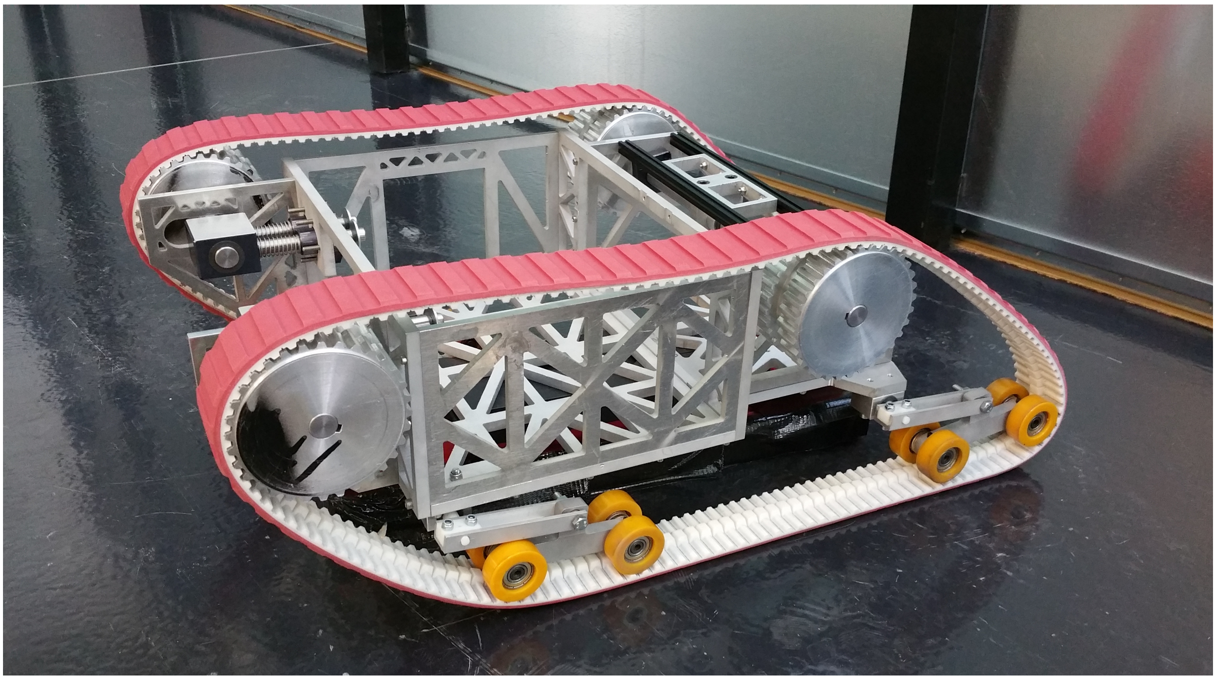

Figure 41: Cyclone

The aspects of particular achievement as perceived by the team are numerous and diverse. The modularity of the chassis has allowed rapid assembly and can be easily adapted to take on varying rescue tasks. The chassis has been manufactured from aluminium lattices, reducing weight when compared to Orion whilst improving structural integrity. The dynamic tensioning system envisioned by the 2014/15 team has been modified and implemented, working in tandem with a fully adjustable torsion blade based suspension system. Regarding the drivetrain and electronics, the $152\,\%$ more powerful motors and their associated control systems have been integrated, allowing wireless operation from a range of $30\,\mathrm{m}$. Battery and health monitoring have been implemented, these systems both display the status of the robot on an LED panel on the robot and feed data back to the operator. In addition to this, further hardware and software safety features have been integrated into the battery distribution board.

6 Manufacturing

6.1. Design For Manufacture

6.1.1. Overview of Design for Manufacture

Design for manufacture considers the limitations of manufacturing processes and materials early in the design process to ensure that these factors are not overlooked [76]. Concurrent engineering aims to integrate all stages of product development (Figure 42). The goal is to reduce lead-time and improve interdepartmental communication to benefit the business and its customer.

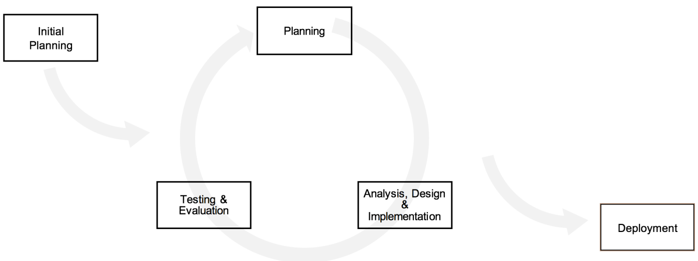

Figure 42: Concurrent Engineering, Adapted from Kusiak, [76]

Using DFMA more time is spent in the early design stages (concept design) to establish the performance criteria and parameters. This reduces changes made further into the product life-cycle and reduces costs, as 70 % are committed in the design stage [13]. DFMA can reduce to the time to market by up to 40 %, whilst intelligent and careful design is the greatest factor in reducing cost [13].

6.1.2. Concurrent Engineering and Design for Manufacture for Cyclone

The modular nature of Cyclone allowed concurrent engineering to be used; design work was split between group members and carried out simultaneously. The interactions between modules were considered from the outset to minimise changes later on. Time was spent to ensure that design concepts, CAD design and design analysis were resolved to reduce design changes during the later stages of the project. Furthermore, because the WMR USAR project runs from year-to-year, potential future developments had to be taken into account. For example, the chassis, suspension and motors were designed to be capable of supporting the additional weight of a robotic arm, again reducing costs and design changes incurred during the project life-cycle, this also fed into Design for Assembly (Section 6.3). There are a number of principles of Design for

Manufacture, as described by Chang et al. [77]. These were applied to Cyclone as is detailed below:

1. *Reduce total number of parts.*

   Orion used over 20 MakerBeam sections to make up just the central chassis section and over 40 fixings. Cyclone has 5 plates making the central chassis section and 12 bolts. The reduction in parts count reduced design complexity and simplified it as there were fewer part interactions to consider.

2. *Develop a Modular Design*

   Modules were defined as discrete mechanical systems. Cyclone was comprised of six modules: front, mid, rear, drivetrain, suspension and dynamic tensioning. The modularity meant work could be carried out concurrently. A further benefit was that, if one module was delayed, the others could progress unaffected.

3. *Parametric Modelling*

   Inherent in the use of concurrent engineering techniques is the knowledge that changes to designs and their dimensions are inevitable. Intelligent use of CAD software can, therefore, substantially mitigate the lost time in redesign. Parametric modelling, in which the dimensions of CAD parts are created with the knowledge of positions of key diameters and lengths, allows for structural components to self-modify upon these changes. Figure 43 demonstrates the motor controller holders, that required modification to accommodate changes in hole spacing. The structural members in this part were defined using equations and parameters based on the location of features and contact points, meaning that these dimensions are all that need to be modified for future changes.

4. *Use of Commercial Off-the-shelf Components*

   The advantages of standard components are the cost and time benefits. Standard components do not require extensive engineering effort, allowing focus to be on other areas. Some examples in Cyclone were the processor, Igus bearings, motors and motor controllers.

5. *Design Parts to be Multifunctional*

   By designing parts to be multifunctional the parts count and complexity of the robot could be reduced. An example of this was using the chassis itself as a heat-sink. Electronic components, such as the motor controllers, were positioned against large surfaces of the chassis to draw away heat and dissipate it though the chassis to the environment.

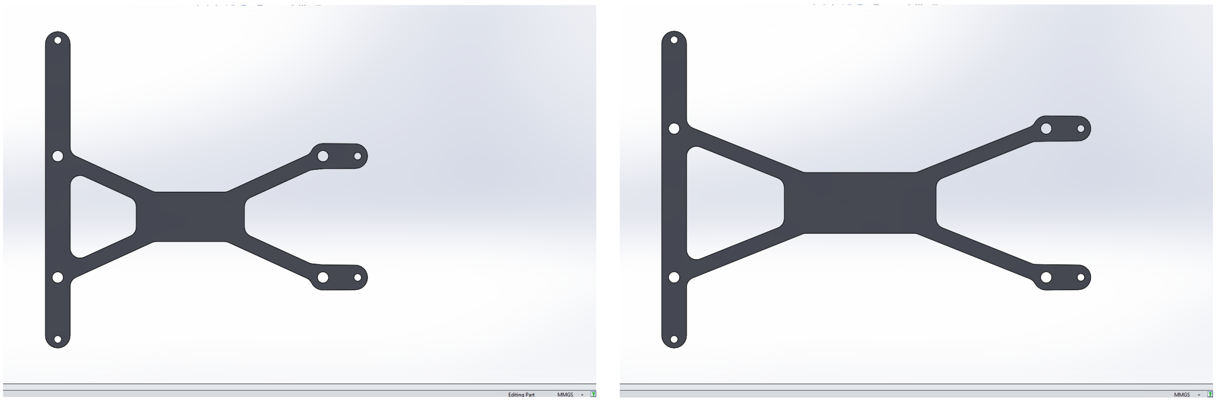

(a) Iteration 1 (b) Iteration 2

Figure 43: Development of the motor controller holders

6.2. Materials Selection

6.2.1. Principles of Materials Selection

Materials selection is the process of establishing a link between the properties required of a component and the materials available, defined by two points [78]:

1. *"Identifying the desired attribute profile and then*
2. *Comparing it with those of real engineering materials to find the best match"*

The designs' performance requirements were examined to determine the constraints placed on materials choice. Ashby material property charts were then used to significantly narrow the choice of materials, ruling out those that did not meet the requirements. The materials left over were ranked against their ability to fulfil the performance criteria of the design using Pugh matrices.

6.2.2. Materials Selection using Properties Charts

Materials selection for Cyclone was primarily based on the Ashby material property charts. These charts plot material properties against each other to give ratios that are invaluable for selecting a material; examples are strength-density and Youngs modulus-density.

The desired properties for each component were considered and then the applicable Ashby chart used to determine the most appropriate materials. The most commonly used chart was strength-density, as high strength and low weight were required for the majority of components. The chart of Youngs modulus against density was also used as high stiffness was needed to withstand the stresses subjected to parts during operation.

Figures 44 show how the Ashby charts were used to select a suitable material for the chas-

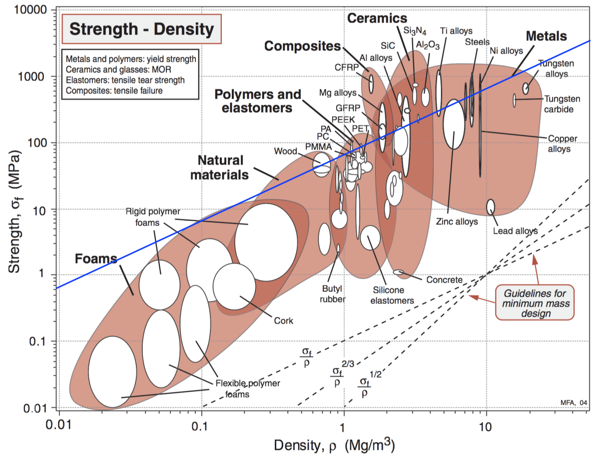

(a) Strength-Density, [78]

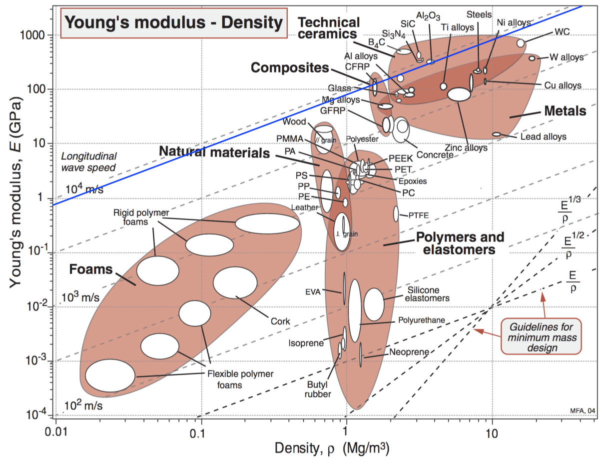

(b) Stiffness-Density , [78]

Figure 44: Ashby Charts

sis. The criteria were high strength-to-weight and stiffness-to-weight. The default material was taken to be aluminium, as it was used extensively in Orion (as both plate and extrusions (MakerBeam)). The design guideline for minimum weight was moved upwards to coincide with aluminium and the other materials the new (blue) line intersected evaluated in Pugh matrices.

Possible materials were titanium, steels, carbon fibre reinforced plastic, nickel alloys (Inconel) and magnesium. These were then ranked on further criteria in a Pugh Matrix (see Appendix H.1, Table H.17). Aluminium was taken as the baseline and the alternatives ranked either positively or negatively against it. The material with the highest overall rank is the most suitable material, however the result must be critically considered. According to the table, CFRP was the most suitable material based on its favourable mechanical properties. However, in terms of manufacturability it is difficult and time consuming to work with. Therefore, manufacturability was effectively worse than one - mark. Because of this CFRP, was not considered and aluminium chosen as the most suitable material, as it scored the next highest.

Material selection for some parts was carried out using different methods. For example, material selection for the torsion blades was done using a formula to calculate the length of a torsion bar for a given material's Youngs modulus. The material which gave a good range of adjustability was chosen, which was steel. Stainless steel was ultimately chosen for the materials corrosion resistance, which was needed as the torsion blades are exposed to the environment on the underside of the robot.

In summary, the materials selection process was carried out to determine the most appropriate material for each component. This method of materials selection is beneficial because it incorporates a scientific approach to materials selection, which is often carried out using a gut feel approach. Using the Ashby charts meant that the most important performance criteria were considered first and all materials compared against to give a broad range of possible materials which could then be narrowed down to find the most suitable material.

6.3. Design For Assembly

Design for assembly is an important consideration in the creation of new products, especially those destined for mass-production. Although the Cyclone design is not intended for mass-production, design for assembly and disassembly has been an important consideration in the choice of joining methods, their locations and the number of individual parts. A boothroyd analysis has been carried out for the front module to look at assembly efficiency and assembly time (Appendix H.2, Table H.18).

It is considered best practice, where assembly is concerned, to remove the need for extra assembly steps if similar materials are used and there is no relative motion between the parts nor need for the parts to be separate [13].

6.3.1. Joining Techniques

The final stage of manufacture of the robot was the means by which each constituent part was joined together. Whilst there are myriad factors to consider in joining techniques can be categorised as follows [79]:

Performance Considerations: Such as strength, stiffness, yield and stability in different environments.

Production Considerations: Such as strength, stiffness, yield and stability in different environments.

Use Considerations: Such as design for disassembly, operating environment, lifecycle impact, reparability and durability.

Safety Considerations: Such as flammability, toxicity, noise, vibration and harshness.

Ultimately, all of these factors, and more, must be taken into account. Within the context of the USAR student project however, cost can be considered a large limiting factor and, fortunately or unfortunately, greatly simplifies the process.

6.3.1.1 Joining Considerations for Cyclone

The requirement for easy disassembly maintains the need for non-permanent joining techniques for a considerable number of parts. Screws and bolts have, therefore, remained the cornerstone of the WMR assembly methodology, especially for the internal components and the module joints, that may require replacement or frequent reassembly.

Many of the bearings have been fitted using interference fits for process simplicity, whilst maintaining a high joint strength. Forces can be limited by dimensional control over the diameters.

Finally, the chassis has made use of adhesives to bond sections of the aluminium shell to the lattice structure. This was to help reduce the number of bolts required for the overall assembly, helping to reduce the weight. Welding has has not been used within the assembly of Cyclone as there has not been a functional need for the process.

6.4. Manufacturing Strategy

The robot was made up of 5 sub assemblies, all of which needed parts to be manufactured. A manufacturing priority list was used to stagger manufacture of parts to make best use of the time available. Figure 45 graphically represents the priority list. The highest priority parts were those of the chassis as it is the core of the robot. The drivetrain sub-assembly was manufactured next, allowing the electronics to be installed and in-situ testing to be carried out. Manufacture of the suspension and dynamic tensioning system commenced after the chassis and drivetrain were completed and whilst the electronic testing was carried out. The full priority list can be found in Appendix H.3, Table H.22.

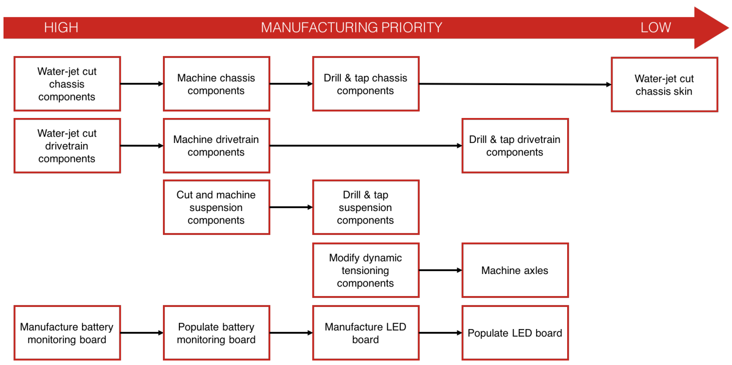

Figure 45: Graphical Representation of Manufacturing Priority

6.4.1. Use of Partnerships

Where possible, manufacturing partnerships were utilised. The large chassis components were waterjet cut by Aquajet Ltd. Waterjet cutting of sheet metal is far quicker than solely using

CNC machining. Taking advantage of partnerships reduced overall project costs. Use of specialised knowledge allowed the team to avoid decisions which may otherwise have introduced complexity and increased lead time.

6.5. Manufacturing Process

Parts were manufactured using a number of techniques to achieve close tolerances and excellent surface finish. Once parts were received from the waterjet cutter they were milled to the final dimensions, media blasted to achieve the desired surface finish and were drilled and tapped for mechanical fasteners. The manufacturing processes used are detailed in Appendix H.23.

6.5.1. Rapid Prototyping

Though not initially designed for Rapid Prototyping (RP), the technique was used to manufacture a number of components to enable a minimum working example to be built in time for the report deadline. RP allowed multiple components to be manufactured in a very short time-frame, rather than the length time-frames required for manual machining.

6.5.2. Manufacturing Challenges

The precision required to align components made manufacturing a challenge; misalignment could impact both assembly and performance. This was dealt with by careful dimensioning and tolerancing to ensure manufacturing accuracy. Another challenge was packaging; the new motors were far larger than the motors used in Orion. This meant that materials had to be carefully considered to reduce part volume to fit the drivetrain parts within the rear module. Finally, the time taken to manufacture the components was a challenge. There were many components to manufacture, which required prioritisation and careful scheduling. Significant care was taken to ensure that components were manufactured in the most appropriate order.

As the project progressed, delays occurred with increasing regularity. To mitigate against these issues, first by taking responsibility for processes, to alleviate the work of technicians, and then to find alternative processes to achieve a ”minimum working robot.” This minimum working robot relied heavily on rapid prototyping to guarantee physical components in time for the report deadline.

7 Testing

7.1. Electronics Testing

7.1.1. Control Results

The control of Cyclone's motors using a PS3 controller over a network was tested. Figure 46 shows the successful ROS node connections, generated from the in built ′rqt_graph′ function. This was achieved with the 2 launch files as discussed previously. Each of these files were launched from the laptop, by connecting to the robots Pico board via a Secure Socket Shell (SSH).

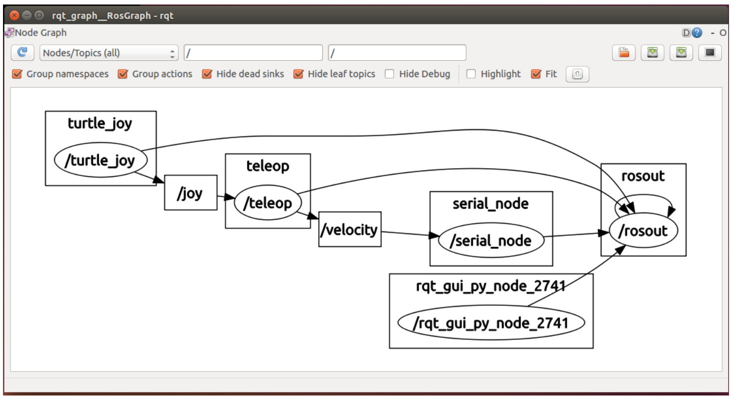

Figure 46: rqt_graph results of the ROS network

7.1.2. Control Critical Analysis

In order to achieve the best results with Cyclone, continuous testing was performed over the entirety of the project. One issue that was overcome, was the inherent PWM jitter due to the use of a low-cost Arduino micro-controller. This caused the motors to judder at zero velocity, as the duty ratio was not exactly 50:50. So not only would the robot move when it was expected to be stationary, but this also induced a large current draw due to the rapid changes in inertia. This was overcome by the introduction of an enable signal, to effectively turn the motors off at 0 rpm.

Secondly, there was an issue with ground loops and the correct galvanic isolation. These ground loops caused a difference in potential in the ground lines so the PWM signal output was floating. In addition, by reconfiguring the grounding scheme it prevented a large conducting current path through the communications ground line. An issue faced by last years team was inadequate grounding of the controllers units, which caused the USB controller IC within the device to blow.

7.1.3. Battery Monitoring Critical Analysis

The battery monitor board was tested and proved to produce the expected regulated outputs in addition to; being capable of shutting down the motors, monitoring the cell voltages and updating the LED board.

However, some modification were needed which were found through testing. The board output a stable 12 V but, this dropped once loaded by the Pico board. This was overcome by changing the value of R14, so the zener diodes reverse breakdown voltage was still reached at increased loads. Furthermore, the on-board LED was holding the micro-controller in reset, by not allowing enough current to flow into the ATmega328 pin; this was also resolved by changing the resistor value.

Besides these only aesthetics would need to be modifying on a 2^{nd} revision of the board. This would include, increasing the distance between the connectors to allow the wires greater freedom of movement and to allow the underlying silkscreens to be seen.

Finally, the regulators were intended to reside on the reverse side of the board to aid with heat dissipation to the chassis. However, due to a misunderstanding in the software they were mounted on the topside. This does not alter the performance of the board, but would be desirable to have them where they were intended.

7.2. Communications Testing

The three selected routers were tested in order to determine their maximum range whilst maintaining Cyclones payload, which was previously calculated at 20 Mbps. If the communication speed falls below this the robots responsivity and the video streaming quality will rapidly deteriorate.

The open source iPerf software, used to test the router, could support a data rate up to 1Gbps. However, the current setup cannot support gigabit transmission across the whole system. The laptop bottlenecks the communication capability as it is limited to 100 Mbps.

7.2.1. Router Results

The three routers were tested under two conditions; first, covered by a 4 mm aluminium sheet and then uncovered. The aluminium sheet was used to imitate the robots shell. Based on the attenuation caused by the metal, the team could decide on the best location for the router.

Furthermore, two communications protocols (TCP and UDP) were tested to determine the best approach for Cyclone's applications. Figures 47a and 47b show the results attained from the test.

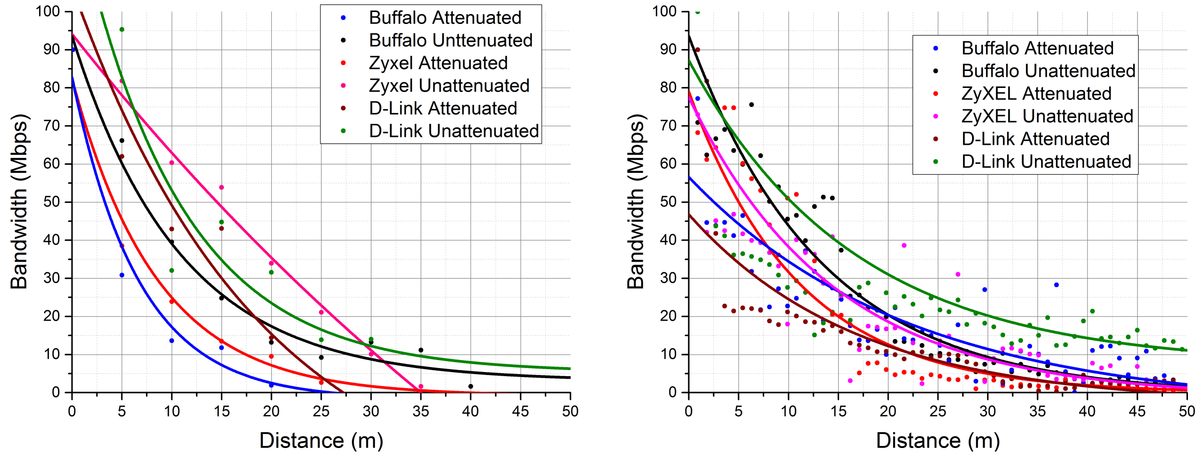

(a) The UCP Protocol (b) The TCP Protocol

Figure 47: Router performance results

7.2.2. Router Critical Analysis

The results show that the speed of communication is proportional to the distance between the router and the laptop. The wireless interference present on the universities campus is a good representation of the conditions the robot will be subject to at the *RoboCup* (Figure 48).

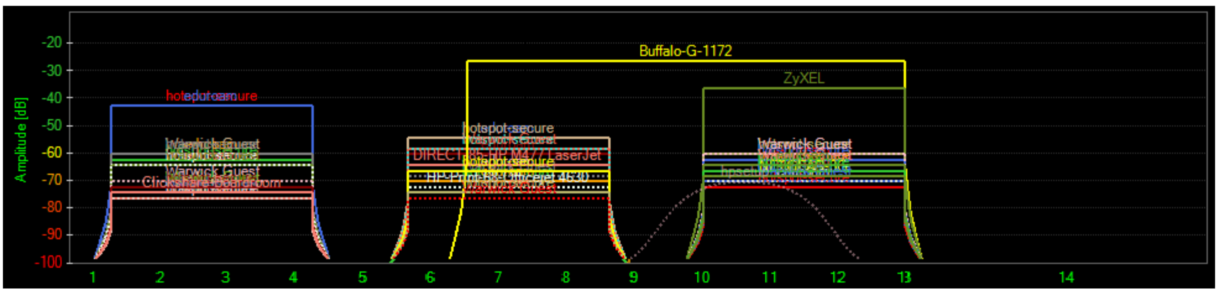

Figure 48: An University environment, displaying a wide range of wireless access points.

The D-link utilising the TCP protocol, when uncovered could support 20 Mbps up to 30.0 m, however was limited to 13.5 m when attenuated. This outperformed the other two routers using the TCP although the ZyXEL prevailed when UDP was adopted. This sustained communications for an uncovered range of 26.0 m or 12.5 m when attenuated. Overall, placing the routers within the shell caused approximately a 45 % to 55 % drop in Cyclone's range.

The Buffalo appeals due to its small size and weight and therefore it's can be placed outside the robot, allowing a range of 20.0 m. This has a greater range compared to the other routers by approximately 5.0 m if they are in-cased within the shell. However, the larger routers' antennas can be protrude out of the shell and under these circumstances the D-Link router prevails. Cyclone will therefore use the D-Link router for the competition as this will allow for the greatest range using TCP protocol.

However, it is suggested that next years team investigates the addition of a flexible or mounting antenna. This will increase the range further in addition to being more durable should Cyclone topple. Furthermore, as Cyclone increases its capabilities a greater data rate may be required. The latest Gigabit Ethernet is not support throughout the system due to the bottleneck on the base-station laptop.

Table 9: Comparison table of the routers performance

Protocol	**TCP**				**UDP**			
Distance	**Unattenuated (m)**		**Attenuated (m)**		**Unattenuated (m)**		**Attenuated (m)**	
Bandwidth (Mbps)	20	10	20	10	20	10	20	10
Buffalo	20.0	30.0	20.0	32.5	18.0	27.5	9.0	12.5
D-Link	30.0	50.0	13.5	22.5	22.5	35.0	18.0	22.5
ZyXEL	19.0	27.5	15.0	22.5	26.0	30.0	12.5	17.5

7.3. System Testing

Upon the completion of Cyclone's assembly, a series of system test procedures was planned to be carried out to ensure the design meets the specification. For the 2015/16 build, this involves making sure the robot is operational in three aspects: durability, controllability and mobility.

It is expected that the systems testing will be finalised by the next years team. So in order to assist them, the team wrote detailed manuals to ensure they can get up to speed with the project as fast as possible. This includes instructions on how to boot the electronics so the robot can be controlled. It is essential that the test results and methodologies are recorded, so that the source of any failures can be addressed.

8 Critical Review of The Cyclone Project

8.1. Project

The 2015/16 WMR team were multidisciplinary allowing for a well-equipped and capable cohort ready to tackle the monstrous task ahead. The team developed an extremely close knit relationship allowing for a smooth running project allowing for reaction to any unexpected arisings. As mentioned, the previous robot, Orion, underwent a complete redesign in order to provide the 2016/17 team with a solid platform to allow further development. This added considerable pressure to the 2015/16 team, especially given the team had been reduced by two members and ultimately resulted in the manufacture and assembly of Cyclone suffering. A large importance was placed on the electronic aspect of the project given the 2014/15 team came nowhere close to a functioning electronics or control system, this created significant work for the sole electronics engineer who was arguably conducting the work of two individuals. On top of the large amount of work involved in designing and manufacturing Cyclone a new sponsor, Harwin, was acquired through creating and maintaining a solid rapport with both the marketing team and the resident experts. This resulted in receiving the majority of electronic components at no charge. The relationship with the existing sponsors were preserved and strengthened resulting in a number of cost savings and publicity.

8.2. Design

Cyclones design was well resolved, however, it resulted in the birth of a number of intricate components creating a further challenge to the manufacturing process concerned with these components. If design work had been completed by January 2016, as initially planned, ample time would have been left to manufacture all components allowing time for full assembly and testing. This deadline was not adhered to due to a number of unforeseen occurrences due to complexities in the component design and manufacturing responsibilities, as well as the fact that this goal was maybe rather ambitious. Cyclones design is a vast improvement on Orion, as it focused on removing and improving upon flaws that severely limited the capability of Orion. Given the complexity of components it would have been prudent to have produced a rapid prototype version of Cyclone early in the product before final manufacture in order to verify designs and test the mechanical interaction of components, something which is difficult using software based tools. The use of RP would have allowed an increase of design iterations allowing one part to be manufactured in the final material. Currently, under high load conditions (continuously climbing stairs) Cyclones battery life is 20 minutes, this extends to 30 minutes under normal operation. The robot currently carries one battery, however, if a robotic arm were added, the inclusion of a second LiPo battery would be required to retain the current life, despite the added weight.

8.3. Manufacture

A number of difficulties arose with the manufacturing of Cyclone due to an initial lack of insight into the manufacturing processes and their lead times, as well as late design changes. This resulted in group members taking manufacturing responsibilities upon themselves, gaining training in a number of techniques including media blasting, milling, drilling and tapping. This could have been avoided if in depth discussions were had early on in the design process, ensuring the team and technicians fully understood the implications each design of component had on manufacturing. This would have also brought to fruition the material requirements and any tolerances needed for the machining of each component. The team could have taken advantage of the University and WMGs reputation and contacts to explore potential outsourcing of manufacturing of final components. In the future the use of selective laser sintering could be explored as well as the RP suggested previously. Although a fully complete robot was not produced by the end of the 30 week project time frame, there is a solid platform for the 2016/17 team to build upon, including copious amounts of final designs and engineering drawings.

8.4. Lessons Learnt

- Allow for extra contingency time when sending off materials for manufacture.
- Ensure a better flow of manufacturing by sending off less labour intensive pieces early to allow for extra time to design the more complex components. This would eliminate the risk of backlog in the workshop.
- Make use of rapid prototyping for design verification.
- Ensure that material is bought with enough contingency for manufacturing tolerances.

9 Future Recommendations

Cyclone requires further work before it is ready to compete at the *RoboCup* competition which the designed platform facilitates.

1. **System Integration**

   To ensure Cyclone functions as expected, a set of system integration tests must be carried out. These need to be conducted in the following criteria;

   (a) **Mobility and Control** - To test Cyclone's ability to climb stairs and traverse a variety of terrains and obstacles.

   (b) **Health Monitoring** - To ensure the battery monitoring board is working as expected and components are operating within a safe temperature range.

2. **Mechatronic Considerations**

   Additional mechatronics for future builds should include;

   (a) **Robotic Arm** - To assist in search and rescue operations, Cyclone would benefit from an arm with interchangeable end-effectors to adapt to the particular task. This arm should be lightweight to ensure the centre of gravity remains within the robot's base over all terrains. Potential functionalities the arm could have are;

      i. Provision for an additional sensor array for heightened reach.

      ii. Assisting in the removal of small obstacles.

      iii. Providing supplies to personnel or casualties.

   (b) **Thermal Health Monitoring** - To ensure components are operating within a safe temperature range, means of monitoring these components may be investigated.

3. **Sensor Implementation**

   In order to assist in detecting survivors, Cyclone requires the use of several sensors that can be integrated with the ROS software, these should include, but are not limited to;

   (a) **LiDAR** - will allow Cyclone to detect and map it's surroundings for use by rescue personnel.

   (b) **IMU** - Used in conjunction with the LiDAR to determine Cyclone's position and orientation, to enhance the mapping capabilities.

   (c) **Infra-Red Camera** - will allow Cyclone to detect survivors or hazards by means of thermal imaging.

   (d) **CO_2 Sensor** - will allow Cyclone to detect survivors trapped under debris by detecting their breath.

4. **Software Integration**

   Complex ROS nodes will be required to interface with the sensor array. Furthermore, a Human Controllable Interface (HCI) should be designed to assist operators to control, monitor and gather information from Cyclone and should have the following functionalities;

   (a) **Health Monitoring** - To feedback Cyclone's health for when the LED panel is out of visible range.

   (b) **Mapping** - Required for submission at the RoboCup, which allows operators to gain an visualisation of hard to access disaster zone.

   (c) **Human Detection** - SMART software to collaborate sensor data in order to pin point survivors and their condition.

   (d) **Fail Safe** - To integrate a dead man's switch into the control software to stop prevent operation of the robot unless the left and right triggers on the PS3 controller are depressed.

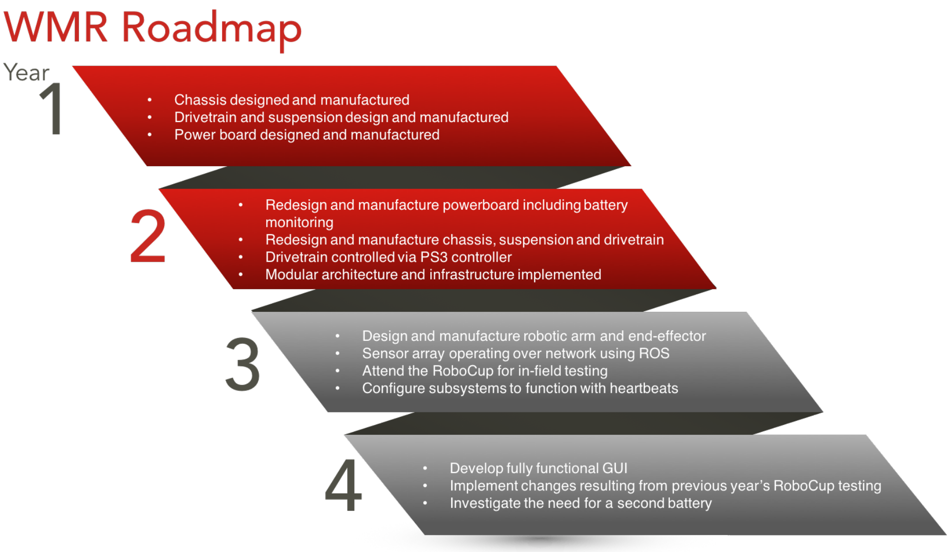

Figure 49: WMR Roadmap

10 Conclusion

Having completed the second year of a four year plan, the WMR team is confident that, come April 2017, Cyclone will be competition ready. The design work and implementation carried out this year has more than fulfilled the requirements of a year-long design and build project, delivering across a number of key areas.

The modular approach adopted throughout the design phases of the project allowed for the fast development of the project, and ensured that the team worked towards a common goal. The intelligent use of collaborative engineering tools ensured that the team were able iterate continuously throughout the project whilst consulting all involved parties and ensure the successful integration of the constituent subsystems. Though significant challenges were faced in translating design intent into physical components, the team ensured that sound understanding of the processes involved was gained, to best represent components and feasibly manufacture a fully functional robot under tight time constraints.

Complications in the manufacturing timeline risked throwing the project off-course and hindering its ability to deliver within the timeframe, but by modifying parts for ease of 3D print fabrication techniques and taking responsibility for sections of the manufacture the team were able to deliver on the project with minimal compromise.

Achievements of the project, such as reducing the weight by a fifth, the 85 % improvement in assembly time and the near-doubling of battery-life prove that the essential work carried out in developing upon the previous year's foundations was of monumental success.

A long-standing technical partnership with Maxon Motor was strengthened, and a new relationship with Harwin forged. These industrial sponsorships will continue to be of great benefit to the WMR project in the coming years. The 2015/16 WMR team have introduced a new generation of young engineers to the field of mobile robotics, as well as representing the discipline at University open-days and events, further expanded upon in the Cost Benefit Analysis report.

As highlighted in the critical review, the project is not without issue; optimistic ambition drove the team to over-zealous goals. The responsibility now lies with the 2016/17 team to further develop the platform to the point at which the robot can be operated effectively by non-experts, intrinsic to a USAR's ability to save lives.

11 References

[1] A. Davids, "Urban search and rescue robots: From tragedy to technology," *IEEE Intelligent Systems*, vol. 17, no. 2, pp. 81–83, 03 2002.

[2] I. Asimov, *I Robot, Science fiction short series*. United States: Gnome Press, 12 1950.

[3] B. Siciliano and O. Khatib, *Handbook of Robotics*. Berlin, Germany: Springer Science and Business Media, 2008.

[4] E. Shapiro, "A look back at some of the major natural disasters in 2015," *Constructor Quarterly*, no. 1, 2015.

[5] M. Gallucci, "Natural disasters and catastrophic events racked up $92b in global economic losses in 2015: Report," *IB Times*, no. 1, 2016.

[6] DARPA, "Darpa robotics challenge," Jan 2015. [Online]. Available: http://www.theroboticschallenge.org/

[7] WMR, "Warwick mobile robotics: About us," Apr 2016. [Online]. Available: http://www2.warwick.ac.uk/fac/sci/eng/meng/wmr/about/

[8] RoboCup, "Robocup: Rescue robot," Jan 2014. [Online]. Available: http://www.robocup2014.org/?page_id=968

[9] G. Genta and L. Morello, *The Automotive Chassis*. Turin, Italy: Springer, 2009.

[10] L. Dawson, C. Fox, M. Galbusera, P. Martin, M. Nkere, A. Popat, R. Saunders, and J. Strutton, "Urban search & rescue robotics: The design and development of a miniature, urban search & rescue robot," Tech. Rep. [Online]. Available: http://www2.warwick.ac.uk/fac/sci/eng/meng/wmr/projects/rescue/reports/1415reports-copy/wmr_technical_report_2014-15.pdf

[11] G. Davies, *Materials for Automobile Bodies*. United Kingdom: Butterworth-Heinemann, 2012.

[12] C. Chavasse, A. Parkin, T. Whales, L. Rutter, J. Yardley, V. Dhanji, and J. Aljafri, "Urban search & rescue robotics," Tech. Rep. [Online].

Available: http://www2.warwick.ac.uk/fac/sci/eng/meng/wmr/projects/rescue/reports/1314reports/wmr_technical_report_2013-14.pdf

[13] G. Boothroyd, P. Dewhurst, and W. A. Knight, *Product design for manufacture and assembly, Third edition (manufacturing engineering and ma..*, 3rd ed. United States: CRC Press, 12 2010.

[14] S. Kalpakjian and S. R. Schmid, *Manufacturing Engineering and Technology*. Singapore: Pearson, 2010.

[15] P. McClean, "Apple details new macbook manufacturing process," Oct 2008. [Online]. Available: http://appleinsider.com/articles/08/10/14/apple_details_new_macbook_manufacturing_process

[16] B. Perrett, *German Light Panzers 1932-42 (New Vanguard)*. Osprey Publishing, 1998. [Online]. Available: http://www.amazon.com/German-Light-Panzers-1932-42-Vanguard/dp/1855328445%3FSubscriptionId%3D0JYN1NVW651KCA56C102%26tag%3Dtechkie-20%26linkCode%3Dxm2%26camp%3D2025%26creative%3D165953%26creativeASIN%3D1855328445

[17] Aalco Metals Ltd. (2016, March) Aluminium alloy 6082 - t6 t651 plate. Cobham, Surrey, United Kingdom. [Online]. Available: http://www.aalco.co.uk/datasheets/Aalco-Metals-Ltd_Aluminium-Alloy-6082-T6T651-Plate_148.pdf

[18] P. Hornback, "The wheel versus track dilemma," *Armor Magazine*, vol. 107, no. 2, pp. 33–34, 1998.

[19] D. Swart, "R/c omniwheel robot," *Make:*, vol. 40, no. 1, 2014.

[20] Robu.In, "Transdev," Apr 2016. [Online]. Available: http://robu.in/product/152mm-aluminium-mecanum-wheel-right/

[21] Sparkfun, "Sparkfun: Wheels, wheel 42x19mm," Apr 2016. [Online]. Available: https://www.sparkfun.com/products/8899

[22] D. Calin, "Introrobotics: Wheels vs continuous tracks: Advantages and disadvantages," Jan 2014. [Online]. Available: http://www.intorobotics.com/wheels-vs-continuous-tracks-advantages-disadvantages

[23] W. E. Johns, "Tracked vehicle steering," Jan 2003. [Online]. Available: http://www.gizmology.net/tracked.htm

[24] P. Edwards, "Differentials, the theory and practice," *Constructor Quarterly*, no. 1, pp. 46–49, 1988.

[25] Maxon Motor, "Maxon motor, 370356, specification," Jan 2015. [Online]. Available: http://www.maxonmotor.co.uk/maxon/view/product/motor/dcmotor/re/re50/370356

[26] Maxon motor, "Maxon gear, 223087, specification," Jan 2015. [Online]. Available: http://www.maxonmotor.co.uk/maxon/view/product/gear/planetary/gp52/223087

[27] R. N. Jazar, *Vehicle dynamics: Theory and application*. New York, NY: Springer-Verlag New York, 2009.

[28] G. Mastinu and M. Plochl, Eds., *Road and off-road vehicle system dynamics handbook*. Boca Raton, FL: CRC Press, 04 2011.

[29] G. Hohl, "Torsion-bar spring and damping systems of tracked vehicles," *Journal of Terramechanics*, vol. 22, no. 4, pp. 195–203, 01 1985.

[30] J. Y. Wong and J. PrestonThomas, "Investigation into the effects of suspension characteristics and design parameters on the performance of tracked vehicles using an advanced computer simulation model," *ARCHIVE: Proceedings of the Institution of Mechanical Engineers, Part D: Transport Engineering 1984-1988 (vols 198-202)*, vol. 202, no. 34, pp. 143–161, 06 1988.

[31] B. N. Persson, *Sliding friction: Physical principles and applications*, 2nd ed. New York: Springer-Verlag Berlin and Heidelberg GmbH & Co. K, 2000.

[32] S. H. Crandall, N. H. Cook, R. R. Archer, N. C. Dalh, F. A. McClintock, E. Rabinowicz, and G. S. Reichenbach, *Introduction to the mechanics of solids: In S.I.Units*, second edition ed., S. H. Crandall, N. C. Dahl, and T. J. Lardner, Eds. United States: McGraw Hill Higher Education, 04 1978.

[33] J. R. Davis, Ed., *ASM speciality handbook Aluminium and Aluminium alloys: Aluminium and Aluminium alloys*, 3rd ed. United States: A S M International, 07 1993.

[34] Unbrako, "Socket products engineering guide," Tech. Rep., 2004. [Online]. Available: http://unbrako.com/docs/engguidepdf

[35] E. H. Smith, Ed., *Mechanical Engineer's Reference Book*, 12th ed. United Kingdom: Butterworth-Heinemann, 03 1994.

[36] Lee Spring. (2016) Compression spring specifications - lp 032k 06 s316. [Online]. Available: http://www.leespring.co.uk/uk_product_spec.asp?partnum=LP032K06S316&springType=C&subType=

[37] Lee spring. (2016) Compression spring specifications - lp 029k 06 s316. [Online]. Available: http://www.leespring.co.uk/uk_product_spec.asp?partnum=LP029K06S316&springType=C&subType=

[38] Intel Corporation. (2014) Intel tregistered nuc kit nuc5i5myhe and board nuc5i5mybe mini pc. Intel. [Online]. Available: http://www.intel.com/content/www/us/en/nuc/nuc-kit-nuc5i5myhe-board-nuc5i5mybe.html

[39] Axiomtek. (2016) Pico830 - pico-itx sbc with intel atom pocessor n2600/n2800. [Online]. Available: http://www.axiomtek.com/Default.aspx?MenuId=Products\&FunctionId=ProductView\&ItemId=1036

[40] Axiomtek. (2016) Pico842 - pico-itx sbc with intel celeron j1900/n2807 (bay trail). [Online]. Available: http://www.axiomtek.com/Default.aspx?MenuId=Products\&FunctionId=ProductView\&ItemId=8955\&upcat=137

[41] Intel. (2015) Intel®atom™processor n2800 (1m cache, 1.86 ghz) specifications. Intel®ARK (Product Specs). [Online]. Available: http://ark.intel.com/products/58917/Intel-Atom-Processor-N2800-1M-Cache-1_86-GHz

[42] Intel. (2016) Intel®celeron®processor j1900 (2m cache, up to 2.42 ghz) specifications. Intel®ARK (Product Specs). [Online]. Available: http://ark.intel.com/products/78867/Intel-Celeron-Processor-J1900-2M-Cache-up-to-2_42-GHz

[43] Axiomtek. (2016) Ax93283 - i/o board for pico-itx board. [Online]. Available: http://www.axiomtek.com/Default.aspx?MenuId=Products\&FunctionId=ProductView\&ItemId=8979

[44] Maxon Motor. (2016) Motor. [Online]. Available: http://www.maxonmotor.co.uk/maxon/view/product/motor/ecmotor/ec4pole/323217

[45] Maxon Motor. (2016) Motor. [Online]. Available: http://www.maxonmotor.co.uk/maxon/view/product/motor/ecmotor/ec/ec45/136203

[46] Maxon Motor. (2016) Motor. [Online]. Available: http://www.maxonmotor.co.uk/maxon/view/product/motor/ecmotor/ec/ec45/136204

[47] Maxon Motor. (2016) Motor. [Online]. Available: http://www.maxonmotor.co.uk/maxon/view/product/motor/ecmotor/ec4pole/305015

[48] Maxon Motor. (2016) Gear. [Online]. Available: http://www.maxonmotorusa.com/maxon/view/product/gear/planetary/gp32/166945

[49] Maxon Motor. (2016) Gear. [Online]. Available: http://www.maxonmotor.com/maxon/view/product/gear/planetary/gp42/203127

[50] Maxon Motor. (2016) Gear. [Online]. Available: http://www.maxonmotor.com/maxon/view/product/gear/planetary/gp32/326669

[51] Maxon Motor. (2016) Controller. [Online]. Available: http://www.maxonmotor.co.uk/maxon/view/product/control/4-Q-Servokontroller/409510

[52] RCHelicopterFun. (2008) Understanding rc lipo batteries. RCHelicopterFun.com. [Online]. Available: http://www.rchelicopterfun.com/rc-lipo-batteries.html

[53] M. Yamamoto and Mori, "Scanning laser range finder urg-04lx-ug01 (simple-urg) specifications," Tech. Rep., 08 2009. [Online]. Available: https://www.hokuyo-aut.jp/02sensor/07scanner/download/pdf/URG-04LX_UG01_spec_en.pdf

[54] FLIR Inc., "Photon user's manual," Tech. Rep., 2008. [Online]. Available: http://www.flir.com/uploadedFiles/CBI/Documents/41200350010Rev100.pdf

[55] MTi, "The mti is a miniature size and low weight 3dof attitude and heading reference," Tech. Rep., 2011. [Online]. Available: https://www.xsens.com/wp-content/uploads/2013/11/mti-leaflet.pdf

[56] JP Zblin, "Ten30 datasheet," Tech. Rep., 2014. [Online]. Available: http://assets.tracopower.com/20160407154341/TEN30/documents/ten30-datasheet.pdf

[57] "Ehhd024a0a hammerhead* series; dc-dc converter power modules," Tech. Rep., 03 2014. [Online]. Available: http://www.mouser.com/ds/2/167/EHHD024_DS-357318.pdf

[58] "Ten60n datasheet," Tech. Rep., 2015. [Online]. Available: http://assets.tracopower.com/20160407154341/TEN60N/documents/ten60n-datasheet.pdf

[59] "Ten 40n series 40 watt input specifications," Tech. Rep., 2015. [Online]. Available: http://assets.tracopower.com/20160407154341/TEN40N/documents/ten40n-datasheet.pdf

[60] Harwin. (2016) Harwin. Harwin. [Online]. Available: https://www.harwin.com/products/M80-8810245/

[61] "Ipc-2221a generic standard on printed board design association connecting electronics industries ®," Tech. Rep., 2003. [Online]. Available: http://www.ipc.org/TOC/IPC-2221A.pdf

[62] Advanced Circuits. (2016) Pcb printed circuit board file creation calculator. [Online]. Available: http://www.4pcb.com/trace-width-calculator.html

[63] Engineering Toolbox.

[64] IEEE Computer Society, "Ieee standards for local and metropolitan area networks: Overview and architecture." New York, IEE, 2014. [Online]. Available: https://standards.ieee.org/findstds/standard/802-2014.html

[65] R. Abdelrahman, A. Mustafa, and A. Osman, "A comparison between ieee 802.11a, b, g, n and ac standards." *IOSR Journal of Computer Engineering (IOSR-JCSE)*, vol. 17-5, pp. 26–29, 2015.

[66] Litepoint, "IEEE 802.11ac: What Does it Mean for Test?" October 2013. [Online]. Available: http://www.litepoint.com/wp-content/uploads/2014/02/80211ac_Whitepaper-1.pdf

[67] K. Amerasinghe, "H.264 for the rest of us." San Francisco, 2009.

[68] R. Stam, "Comparison of international policies on electromagnetic fields (power frequency and radiofrequency fields)," May 2011.

[69] ROS. (2014, 05) ROS - introduction. [Online]. Available: http://wiki.ros.org/ROS/Introduction

[70] ROS. What is ros. [Online]. Available: http://www.generationrobots.com/en/content/55-ros-robot-operating-system

[71] ROS. (2014, 06) Ros - technical overview. [Online]. Available: http://wiki.ros.org/ROS/Technical\%20Overview

[72] ROS. (2013, 04) Ros - tcpros. [Online]. Available: http://wiki.ros.org/ROS/TCPROS

[73] ROS. (2011, 10) Ros aerial - overview - limitations. [Online]. Available: http://wiki.ros.org/rosserial/Overview/Limitations

[74] G. Sidebotham, *Heat Transfer Modeling, An Inductive Approach*. New York, United States: Springer International Publishing Switzerland, 2015.

[75] N. Kovanova, "Thermal systems; system modelling analogies." Mar 2015. [Online]. Available: http://www2.warwick.ac.uk/fac/sci/eng/eso/modules/year3/es3c8/resources/

[76] A. Kusiak, Ed., *Concurrent engineering: Automation, tools, and techniques*. New York: Wiley, John & Sons, 12 1992.

[77] T.-C. Chang, R. A. Wysk, B. Hsu-Pin, and H.-P. Wang, *Computer- aided manufacturing*, 3rd ed. United States: Pearson Prentice Hall, 06 2005.

[78] M. F. Ashby, *Materials selection in mechanical design*, third edition ed. Amsterdam: Elsevier Butterworth-Heinemann, 2005.

[79] D. Hughes, "Design for manufacture lecture resources," Apr 2016. [Online]. Available: https://www2.warwick.ac.uk/fac/sci/eng/eso/modules/year3/es3a8/resources

[80] S. Hazra, "Quora: Is there any benefit to legged robots over wheeled ones?" Feb 2015. [Online]. Available: https://www.quora.com/Is-there-any-benefit-to-legged-robots-over-wheeled-ones

[81] School of Engineering, *Engineering Data Book*. Coventry, England: University of Warwick, 2014. [Online]. Available: http://www2.warwick.ac.uk/fac/sci/eng/eso/students/guidance/handbook/7th_e_edition-with_covers.pdf

[82] Thermal Hazard Technology, "Determining the specific heat capacity of a battery pack." Bletchley, England, Mar 2016.

Appendices

A Specification

Working from the previous years specification and bearing in mind the requirements from the RoboCup competition, a new specification was created and the requirements were split into the following sections of the robot; chassis, drivetrain, robotic arm, electronics, software, power.

The robot has been built upon specifications based around the following aspects;

1. Dimensions, Weight, and Clearance
2. Durability
3. Accessibility
4. Control
5. Communication
6. Detection
7. Mapping
8. Mobility
9. Visualisation

NOTE: Definitions used throughout this specification

SHALL It is required

SHOULD It is recommended

MAY It is optional

Table A.10: Specification of Cyclone

Parameters			
ID	**Type**	**System**	**Value/Description**
P1	Weight	N/A	Mass shall not exceed 25 kg
P2	Weight	N/A	The robot shall be deployable by one person
P3	Dimensions	N/A	The robot shall be capable of turning with a standard door width

P4	Dimensions	N/A	The external dimensions shall not exceed: $410.0\,\mathrm{mm}$ width $580.0\,\mathrm{mm}$ length
P5	Dimensions	N/A	The internal volume shall be flexible to allow storage of all vulnerable components
P6	Clearance	N/A	Ground clearance shall be minimum of $100\,\mathrm{mm}$
P7	Clearance	Powertrain	The robot shall climb stairs with a step height of $190\,\mathrm{mm}$ and angle of $38°$
P8	Accessibility	N/A	The robot shall be easy to maintain whilst out in the field
P9	Accessibility	Power	An operator shall change the battery within $30\,\mathrm{s}$

Functionality

ID	**Type**	**System**	**Value/Description**
F1	Durability	Chassis	The robot shall survive an impact from a drop from a $350\,\mathrm{mm}$ height
F2	Durability	Chassis	The robot interior components shall not be vulnerable to sand and dust
F3	Durability	Chassis	All vulnerable components shall be inside the shell - Advice: This should include motors, processor board, battery, etc.
F4	Durability	Chassis	There should be no exposed wiring
F5	Durability	Chassis	A simulation of overheating and cooling shall be provided
F6	Durability	Powertrain	The robot may use a system to ensure efficiency of mobility and control
F7	Durability	Electronic	The robot shall have means to operate in the dark
F8	Mobility	Powertrain	The robot shall drive at $1\,\mathrm{m/s}$
F9	Mobility	Powertrain	The robot shall accelerate at $0.3\,\mathrm{m/s^2}$

F10	Mobility	Powertrain	The robot shall supply sufficient torque to climb stairs
F11	Mobility	Powertrain	The robot shall traverse over both solid and soft terrain The traction provided by the robot shall traverse over mud, hard floor, etc
F12	Mobility	Powertrain	The robot shall traverse over uneven terrain.
F13	Control	Powertrain	There should be controlled positioning provided by the motors
F14	Control	Powertrain	The robot should maintain high precision and accuracy of movement Advice: Controlled positioning
F15	Control	Software	The robot shall be tele-operated controlled when out of sight
F16	Control	Software	An operator shall control the robot remotely
F17	Control	Software	The robot shall respond to a remote operator
F18	Communication	Software	An operator shall command the robot remotely
F19	Communication	Software	The robot shall send data to a remote operator
F20	Communication	Software	The robot shall receive data from a remote operator
F21	Communication	Software	An operator should be able to locate the robot
F22	Communication	Electronic	The robot may have a secondary back-up method of communicating data.
F23	Communication	Power	The robot shall tell the operator the percentage of power remaining within the battery
F24	Mapping	Electronic	The robot shall have full functionalities of a LiDAR
F25	Mapping	Software	The robot shall have the functionality to generate a 3D map of an area
F26	Detection	Software	The robot shall visually detect a human personnel

F27	Detection	Software	The robot shall non-visually detect a human personnel Advice: CO_2
F28	Detection	Software	The robot shall be able to detect it's surroundings- Advice: Walls, holes, doors etc.
F29	Visualisation	Electronic	The robot shall have visualisation for tele-operated control
F30	Visualisation	Electronic	The robot may have visualisation for tele-operated control from the rear
F31	Visualisation	Electronic	The robot shall have visualisation in the dark
F32	Visualisation	Electronic	The robot shall have thermal visualisation

B Drivetrain

Propulsion

Legs are becoming more common in robot designs and so were also considered for Cyclone.

Legs are the most agile of the three options and rather than being able to perform at high speeds, they enable the robot to react quickly to any outside forces or changes in environment, allowing a change in pose or principal orientation. This reactiveness allows for an extremely stable platform for the robot when walking over ice, mud, rocks etc. Limbs (of a robot) also allow a greater solution space giving more options when traversing uneven surfaces and obstacles (Figure B.50). The limbs of the robot could also be utilised to climb vertical surfaces allowing the exploration of areas tracked or wheeled robots could not reach (Figure B.51) ([])

Figure B.50: Solution Space of a legged robot [80]

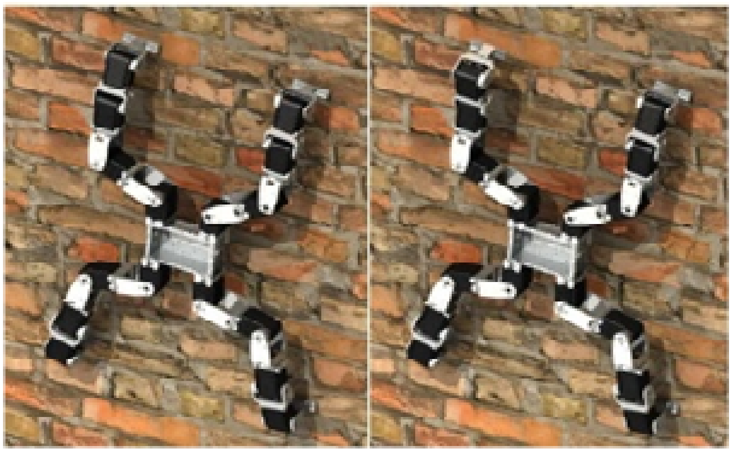

Figure B.51: Legged Robot Climbing a vertical surface [80]

As well as the physical advantages, a limbed robot would be a more sensible choice in terms of set-up and cost for a disaster extraction, because no local infrastructure would have to be set up, like paths and open passages.

The limb design is still in research and so is currently expensive and extremely time consuming to get right on a project dealing with such unpredictable environments. This is the main downfall of this type of design.

Manoeuvrability

Braked Differential This is a simplified version of the clutch-brake drive shown in Figure 19, but differs in that the two axles are driven through a differential and so the clutches are removed. When one axle is slowed or stopped, the differential acts to transfer all the motion to the remaining 'free' axle and so results in a turning effect. This method is less efficient than the clutch-brake system, given the brake dissipates the energy of the track and the motor. The braked differential method is harder to control and straight line travel may become a problem as the system can become unpredictable. However, its simplicity makes up for these faults. [24].

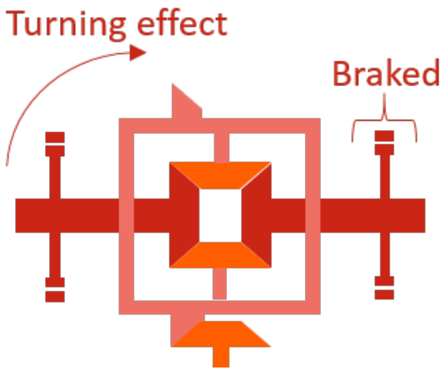

Figure B.52: Braked Differential Layout

Double Differential This is a more refined version of the standard braked differential system. This method adds a second transmission between the steering input of the transmission and the motor. This allows the differential gears to run at several different speeds resulting in a large range of track speed combinations. This will allow for a great number of turning radii making this system well suited for fast steering vehicles. This system is used for all modern fast track-layer steering transmissions due to its efficiency, turning radii possibilities (including a neutral turn) and its stability (it wont self-steer) [24].

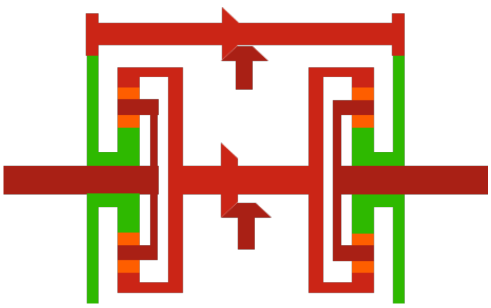

Figure B.53: Double Differential Layout

C Suspension

C.1. Formula for Spring Rate of Torsion Bar Suspension Systems

$$k = \frac{\pi \times d^4 \times G}{32L} \tag{C.1}$$

$k = spring\,rate\,(N/m), d = diameter\,(m), G = Young's\,modulus\,(N/m^2), L = length\,(m)$

C.2. Worked Calculation of Travel

$$Travel = sin(\theta) \times L$$

$$Travel = sin(0.35) \times 80 = 27.4mm$$
$$Travel = sin(0.082) \times 80 = 6.4mm$$
$$Total\ Travel = 33.8mm$$

C.3. Worked Calculation of Drop Force and Torque or Torsion Bars

$$F = \frac{m \times g \times h}{stopping\ distance} \tag{C.2}$$
$$\frac{25 \times 9.81 \times 0.35}{0.0274} = 3132.775N$$
$$\frac{3132.775}{4} = 783.189N \approx 783N$$
$$T = F \times d \tag{C.3}$$
$$T = 783.189 \times 0.08 = 62.66Nm$$

C.4. Worked Calculations of Polar Moment of Inertia

$$Circular\ section : J = \frac{\pi(d^4)}{32} \tag{C.4}$$
$$J = \frac{\pi(0.006)^4}{32} = 12.72 \times 10^{-11} m^4$$
$$Rectangular\ section : J = \frac{bh}{12}(b^2 + h^2) \tag{C.5}$$
$$J = \frac{0.00635 \times 0.002}{12}(0.00635^2 + 0.002^2) = 4.69 \times 10^{-11} m^4$$

C.5. Worked Calculations of Torsion Bar Length

$$Length = \frac{\theta(J \times G)}{T} \tag{C.6}$$

$$\theta = Twist\ angle\ (radians), J = polar\ moment\ of\ inertia(m^4),$$

$$G = Young's\ modulus(N/m^2), T = Torque(Nm)$$

$$Aluminium\ bar : L = \frac{0.35(12.72 \times 10^{-11} \times 69 \times 10^9)}{62.66}$$

$$L = 0.0490m = 49.0mm$$

$$Steel\ blade : L = \frac{0.35(4.69 \times 10^{-11} \times 200 \times 10^9)}{62.66}$$

$$L = 0.0524m = 52.4mm$$

C.6. Orion & Cyclone Suspension Comparison

	Orion 2014	**Orion 2016**
Travel	12mm	27mm
Ground Clearance	100mm	93mm
Adjustability	Fixed travel & ground clearance	Adjustable travel & ground clearance
Pivot Points	16	8
Parts Count	16	16

Table C.11: Comparison of Orion's and Cyclone's Suspension

D Electronics

D.1. Cyclone's Sensor Array

Table D.12: Cyclone's Sensor Array

Sensor	Part		Own or Required	Interface
	Company	Part Number		
LiDAR	Hokuyo	URG-04LX	Own	USB
IR Camera	Photon	160	Own	USB
Front-View Camera	-	-	Required	USB
Rear-View Camera	Microsoft	LifeCam HD-3000	Own	USB
IMU	Xsens	MTi-28A53G35	Own	RS232
CO2 Sensor	DFR	SEN0159	Own	RS232
Microphone	-	-	Required	Microphone
Headlight	-	-	Required	-

D.2. Battery Monitor Board Schematic

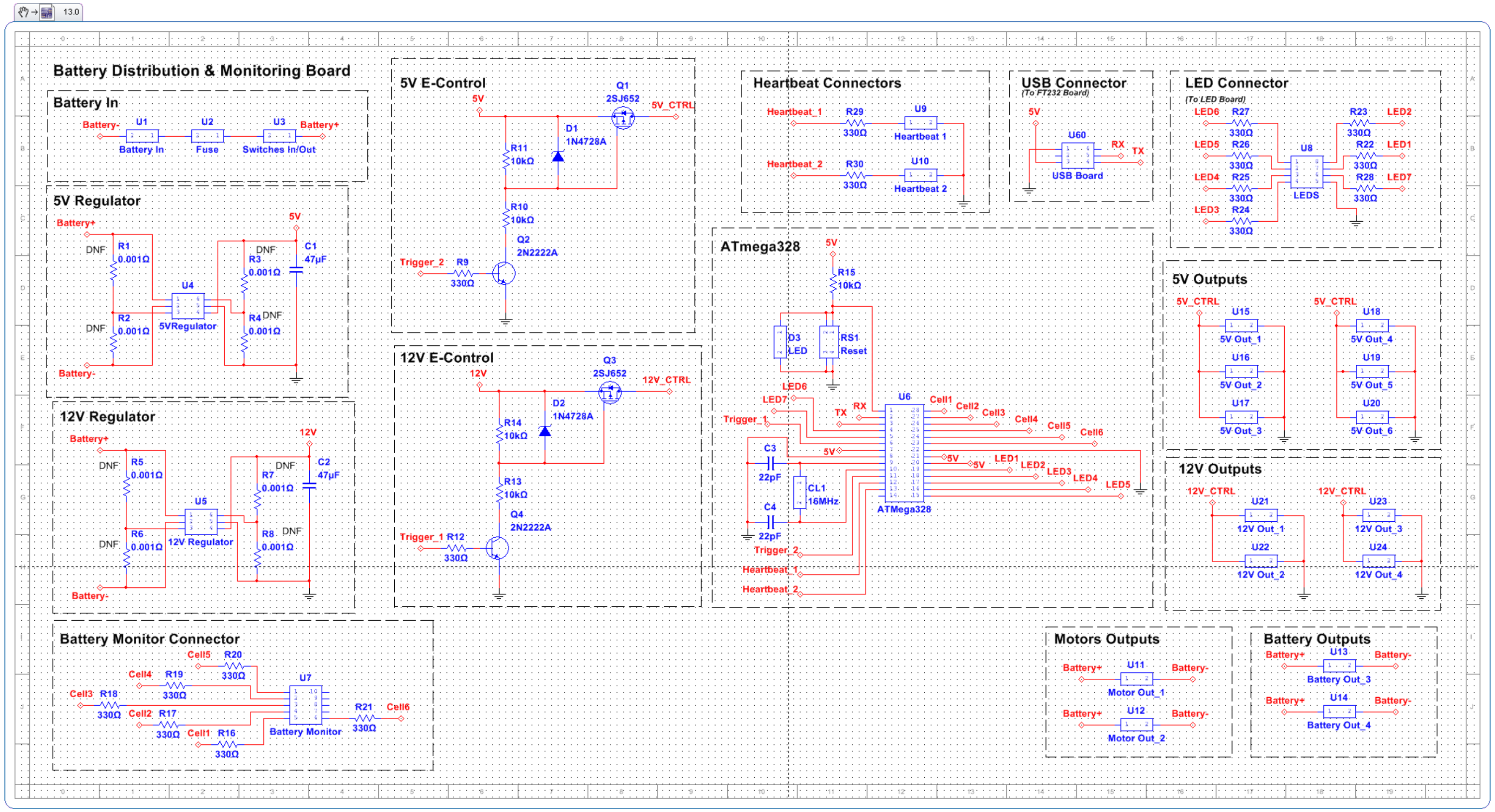

Figure D.54: Battery Monitor Board Schematic

D.3. GE EHHD024A0A41 Efficiency against Output Current

Figure D.55: GE EHHD024A0A41 Efficiency against Output Current

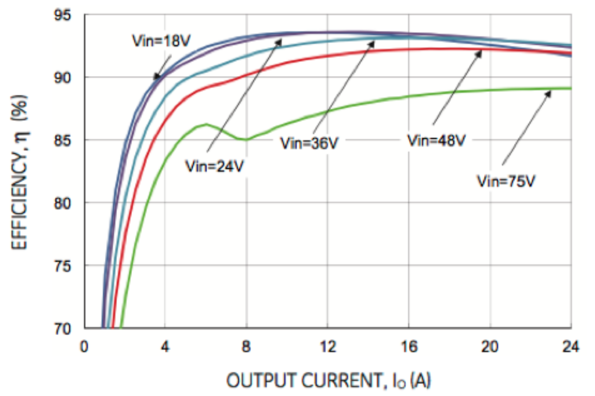

D.4. Cyclone's Battery Monitoring Board Connectors

Table D.13: Harwin Connectors Used on Cyclones Battery Monitoring & Distribution Board

Purpose	Part Number	Gender	Quantity	Reason for Selection
Power	M80-5000000M2-02-331-00-000	Male	16	Max current 20A per pin
Power	M80-4000000F1-02-325-00-000	Female	16	Mating half
Heartbeat	M80-8810245	Male	2	Friction Latches
Heartbeat	M80-8990205	Female	2	Mating half
LED Board	M80-8630842	Male	2	Friction Latches
LED Board	M80-8890805	Female	2	Mating half
Battery Mon	M80-8631042	Male	1	Friction Latches
Battery Mon	M80-8891005	Female	1	Mating half
USB Board	M20-9710645	Male	1	Compatible pin pitch to USB board

E Communications

E.1. Orion's Router

The 2014/15 team purchased a router with the following specifications:

Parameter	**value**
Dimensions	$162 \times 132 \times 30$ mm
Weight	221g
Wireless Protocols	802.11 b/g/n
Frequency	2.4GHz
Wireless Speed	$<$ 150Mbps
Wireless Range	$<$ 100+ m
Wireless Output Power	19 dBm
Power Supply	5V 2A adapter (included)

Table E.14: Specifications for the airRouter AR unit

E.2. List of viable routers for Cyclone

Table E.15: Cyclone's specifications based on the following routers

Name	**Dimensions** (mm x mm x mm)	**Weight** (grams)	**Wireless Speed** 802.11 n/ac (Mbps)	**Power Supply** DC (V)	(A)
Archer C7	$243.0 \times 160.6 \times 32.5$	<Unknown>	450/1300	12	2.5
Buffalo Airstation AC433	$45.0 \times 45.0 \times 15.0$	19.0	150/433	5V USB Powered	
D-Link DAP-1665	$147.0 \times 108.0 \times 278.0$	222.0	<1200	12	1
D-Link DIR0510L	$140.0 \times 59.0 \times 16.0$	154.0	<750	5	1.8
D-Link DWR-118	$148.5 \times 113.5 \times 25.0$	194.3	150/433	12	1.5
ZyXEL NBG6503	$159.0 \times 111.0 \times 23.0$	230.0	300/433	12	1

E.3. Testing the Routers

Each router's performance was evaluated using iPerf, a software tool that measures in the throughput bandwidth of a system, by following the procedure below:

1. Set up network as below and iPerf started on both computer and laptop.
2. Set up Laptop as iPerf server and computer as a client
3. At 5m intervals test the UDP network
   (a) Evaluate bandwidth and data loss of network
   (b) Repeat with aluminium cover to simulate robot chassis

F Software

F.1. Motor Controllers Arduino Software Diagram

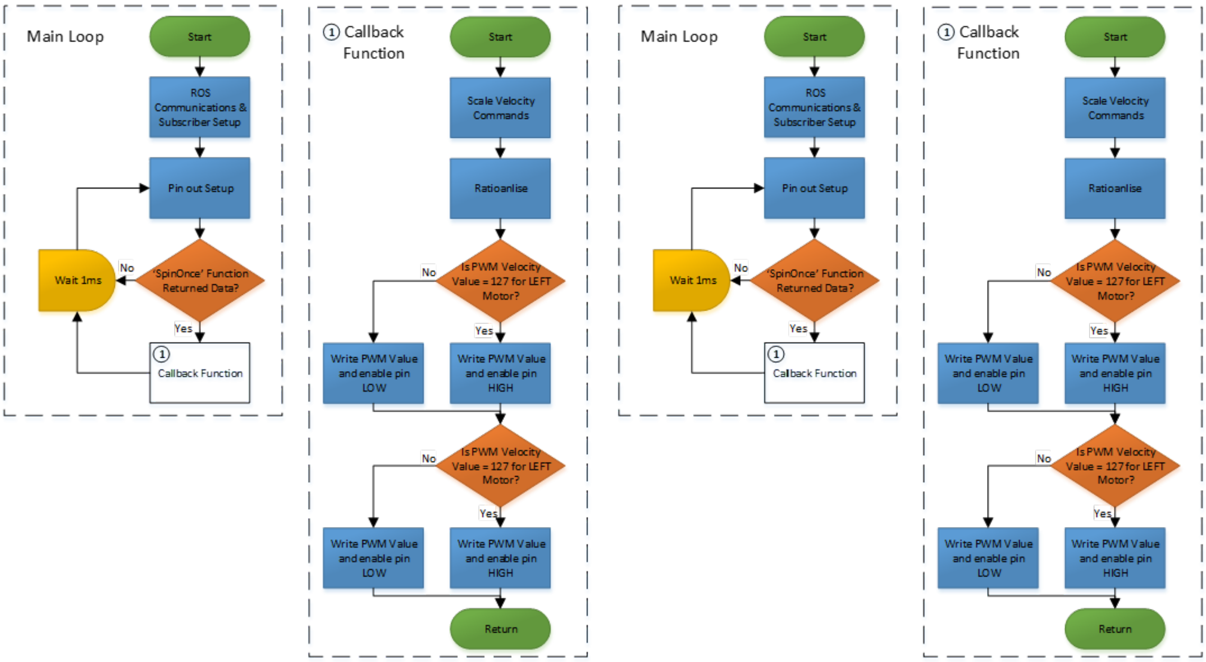

Figure F.56: Software diagram of the Ardunio script used to control the motors

F.2. Battery Monitor Board's Ardunio Software Diagram

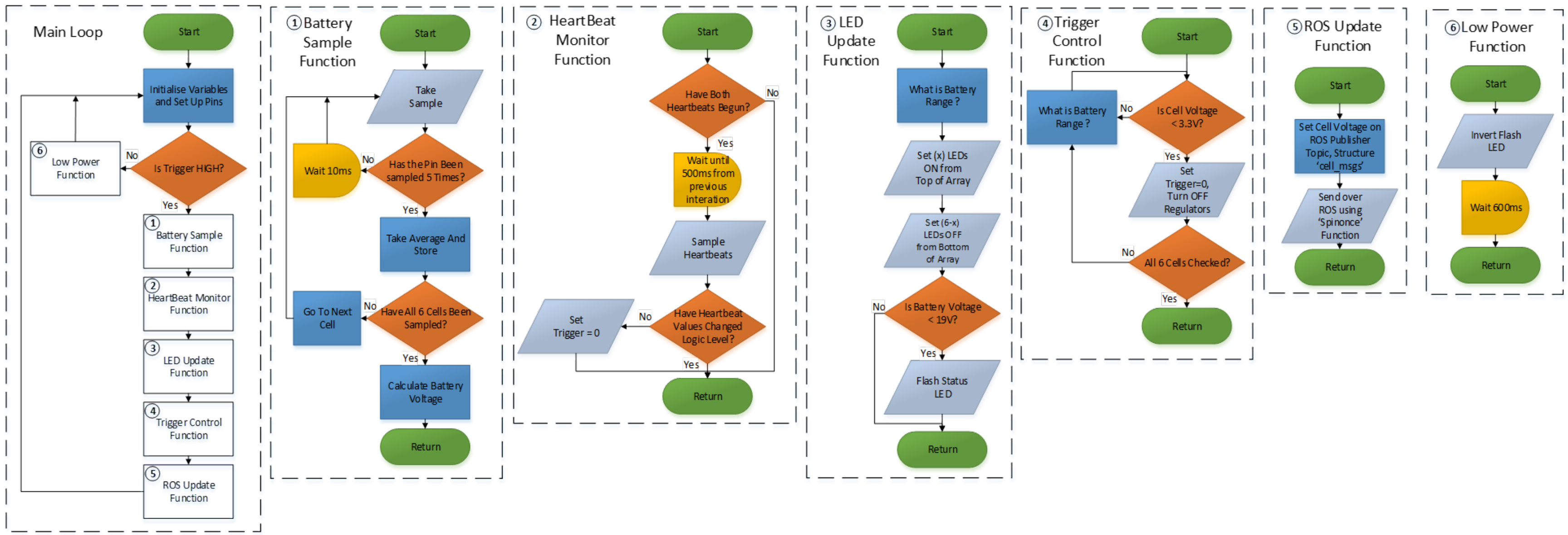

Figure F.57: Software diagram of the Ardunio script, which is run on the Battery Monitoring Board

G Thermal

G.1. Thermal Model Dataset

The thermal model was creating using following values[81]:

Table G.16: Table of values used to create the lumped sum thermal model

Name	**Algebraic Symbol**	**Value**
Ambient Temperature (K)	θ_A	297
Shell Resistance		
Aluminium thermal conductivity ($Wm^{-1}K^{-1}$) [17]	α	180
Top Area (m^2)	A_t	0.510×0.322
Top Thickness (m)	d_t	0.002
Base Area (m^2)	A_b	0.510×0.322
Base Thickness (m)	d_b	0.008
Side Area (m^2)	A_{rl}	0.510×0.132
Side Thickness (m)	d_{rl}	0.002
Front and Back Area (m^2)	A_{fb}	0.132×0.322
Front and Back Thickness (m)	d_{fb}	0.004
Internal Capacitance		
Density of Air (kgm^{-3})		1.2922
Volume of internal Air (m^3)		0.002 68
Mass of internal Air (kg)	m_{air}	0.003 463
Specific Heat Capacity of Air at constant pressure ($Jkg^{-1}K^{-1}$)	σ_{air}	718
Aluminium Mass of internal (kg)	m_{al}	4.4
Aluminium Specific Heat Capacity ($Jkg^{-1}K^{-1}$)	σ_{al}	913
Mass of Lithium Polymer Battery (kg)	m_b	0.265
Specific Heat Capacity Lithium Polymer Battery ($Jkg^{-1}K^{-1}$) [82]	σ_b	820
Battery Characteristics		
Capacity (mAh)		5000
Discharge Rate (C)		45
Voltage (V)		25.2
Power (Js^{-1})	q_i	5670
Time to fully Discharge (s)		80

G.2. Background

There are two basic elements of thermal modelling; resistors and capacitors. These, fundamentally, can be modelled in the same same way as an electrical system [75]. Where Heat flow rate $q(t)$ is an equivalent to current with units in W or Js^{-1} temperature, $\theta(t)$ is an equivalent to voltage with units in K. As such, thermal storage:

$$C\frac{d}{dt}\Theta(t) = q(t) \tag{G.1}$$

$$C = m\sigma \tag{G.2}$$

Where Mass (m) and Specific Heat (σ)

And thermal Resistor

$$q(t) = \frac{1}{R}\theta_{12}(t) \qquad \theta_{12}(t) = \theta_1(t) - \theta_2(t) \tag{G.3}$$

Where R is the path of the cross-sectional area A with length d through the material

$$R = \frac{d}{A\alpha} \tag{G.4}$$

A batteries parameters are given by its capacity (mAh), the nominal voltage (V) and the discharge rate (c). With the discharge rate being constant, the time a battery would last is given, in hours, by:

$$\frac{1}{DischargeRate} \tag{G.5}$$

The power of a battery can be calculated by multiplying the capacity, voltage and discharge rate in watts or joules per second. This can also be the equivalent of heat flow.

$$Capacity \times Voltage \times DischargeRate \tag{G.6}$$

The total energy of a battery can be found by calculating capacity and voltage, giving watt hours. Watt hours can then be multiplied by 3600 to give joules.

$$Capacity \times Voltage \times 3600 = Energy \tag{G.7}$$

For the Robot Model 38;

$$\begin{aligned} q_1(t) &= q_i(t) - q_r(t) \\ C\frac{d}{dt}\theta_1(t) &= q_1(t) \\ q_r(t) &= \frac{1}{R}(\theta_1(t) - \theta_A(t)) \end{aligned} \tag{G.8}$$

q_i is the heat flow into the robot, C is the internal capacitance, R is the sum of the resistances of the shell and θ_A is the ambient temperature.

$$R = \Sigma\frac{d}{A\alpha} = \frac{1}{\frac{A_b\alpha}{d_b} + \frac{A_t\alpha}{d_t} + 2\frac{A_{fb}\alpha}{d_{fb}} + 2\frac{A_{rl}\alpha}{d_{rl}}} \tag{G.9}$$

α is equal to the thermal conductivity of the metal. The length and area varying on the panels.

$$C = \Sigma m\sigma = m_{air}\sigma_{air} + m_{al}\sigma_{al} + m_{batt}\sigma_{batt} \tag{G.10}$$

m is the mass and σ is the specific heat capacity.

$$q_i = mAh \times V \times C \tag{G.11}$$

Additionally, the time it takes for the battery to fully discharge is the time it takes to discharge completely.

$$Time = \frac{1}{C} \times 3600(s) \tag{G.12}$$

H Manufacturing

H.1. Materials Selection

Table H.17: Pugh Matrix for Chassis Material Selection

Material	**Weighting**	**Al Alloy**	**Stainless**	**Ni Alloy**	**Ti Alloy**	**Mg Alloy**	**CFRP**
Weight	5	S	-	-	-	+	+
Strength	4	S	+	+	+	-	+
Stiffness	4	S	+	+	+	-	+
Corrosion Resistance	2	S	+	+	+	-	+
Manufacturability	5	S	-	-	-	-	-
Cost	3	S	S	-	-	-	-
Weighted Sum of Positives		0	10	10	10	5	15
Weighted Sum of Negatives		0	12	13	13	18	8
Total		0	-2	-3	-3	-13	7

H.2. Design for Assembly

A Boothroyd-Dewhurst analysis has been carried out to assess the assembly times of Cyclone and a best case assembly time for Orion. Cyclone's calculated assembly time is 617.73 s, whilst Orion's is 4629.92 s.

Table H.18: Boothroyd-Dewhurst analysis of Cyclone's Front Module

		Manual Handling		**Insertion**		**Operation Time**	
Item	**QTY**	**Code**	**Time (s)**	**Code**	**Time (s)**	**Single (s)**	**Total (s)**
Attach sideplate to bulkhead	2						
Place bulkhead upright on table	1	1.0	1.50	—	—	1.50	1.50
Place side plate next to bulkhead	1	1.0	1.50	0.0	1.50	3.00	3.00
Screw into place	3	0.1	1.43	3.9	8.00	9.43	28.29
Attach top shell	1						
Place top shell on assy	1	1.0	1.50	—	—	1.50	1.50
Screw into place	4	0.1	1.43	3.9	8.00	9.43	37.72
Attach upper front shell	1						
Place assy bulkhead-down	1	1.0	1.50	—	—	1.50	1.50
Place upper front shell on assy	1	1.0	1.50	0.0	1.50	3.00	3.00
Screw into place	4	0.1	1.43	3.9	8.00	9.43	37.72
Attach lower front shell	1						
Place lower front shell on assy	1	1.0	1.50	—	—	1.50	1.50
Screw into place	4	0.1	1.43	3.9	8.00	9.43	37.72
Attach upper front shell	1						
Place assy bulkhead-down	1	1.0	1.50	—	—	1.50	1.50
Place upper front shell on assy	1	1.0	1.50	0.0	1.50	3.00	3.00
Screw into place	4	0.1	1.43	3.9	8.00	9.43	37.72
Front Module Total Assembly Time					**231.46**		

Table H.19: Boothroyd-Dewhurst analysis of Cyclone's Rear Module

		Manual Handling		Insertion		Operation Time	
Item	**QTY**	**Code**	**Time (s)**	**Code**	**Time (s)**	**Single (s)**	**Total (s)**
Attach sideplate to baseplate							
Place baseplate on side	1	1.0	1.50	—	—	1.50	1.50
Place screw 1 through baseplate	1	0.1	1.43	0.6	5.50	6.93	6.93
Bring sideplate to meet baseplate	1	1.0	1.50	0.0	1.50	3.00	3.00
screws 2 and 3 into place	2	0.1	1.43	3.9	8.00	9.43	18.86
Attach bullkhead							
Place assy upright on table	1	1.0	1.50	—	—	1.50	1.50
Place bulkhead next to assy	1	1.0	1.50	0.0	1.50	3.00	3.00
screw into place	8	0.1	1.43	3.9	8.00	9.43	75.44
Attach rear bumper							
Place rear bumper skin against assy	1	1.0	1.50	—	—	1.50	1.50
screw into place	4	0.1	1.43	3.9	8.00	9.43	37.72
Attach diagonal plate							
Place diagonal plate on assy	1	1.0	1.50	—	—	1.50	1.50
screw into place	4	0.1	1.43	3.9	8.00	9.43	37.72
Attach top plate							
place top plate on assy	1	1.0	1.50	—	—	1.50	1.50
screw into place	4	0.1	1.43	3.9	8.00	9.43	37.72
Front Module Total Assembly Time					**258.18**		

Table H.20: Boothroyd-Dewhurst analysis of Cyclone's Centre Module

		Manual Handling		Insertion		Operation Time	
Item	**QTY**	**Code**	**Time (s)**	**Code**	**Time (s)**	**Single (s)**	**Total (s)**
Attach Battery Sideplate to Bulkhead							
Place baseplate on side	1	1	1.50	—	—	1.50	1.50
Place screw 1 through baseplate	1	0.1	1.43	0.6	5.50	6.93	6.93
Bring sideplate to meet baseplate	1	1	1.50	0.0	1.50	3.00	3.00
screws 2, 3 and 4 into place	3	0.1	1.43	3.9	8.00	9.43	28.29
Attach Full Sideplate to Bulkhead							
Place baseplate on side	1	1	1.50	—	—	1.50	1.50
Place screw 1 through baseplate	1	0.1	1.43	0.6	5.50	6.93	6.93
Bring sideplate to meet baseplate	1	1	1.50	0.0	1.50	3.00	3.00
screws 2, 3, 4 and 5 into place	4	0.1	1.43	3.9	8.00	9.43	37.72
Attach Lid to assy							
place top plate on assy	1	1	1.50	—	—	1.50	1.50
screw into place	4	0.1	1.43	3.9	8.00	9.43	37.72
Centre Module Total Assembly Time					**128.09**		

Table H.21: Boothroyd-Dewhurst analysis of Cyclone's Centre Module

		Manual Handling		Insertion		Operation Time	
Item	**QTY**	**Code**	**Time (s)**	**Code**	**Time (s)**	**Single (s)**	**Total (s)**
Place and align bolt in MakerBeam	284	0.1	1.43	0.6	5.5	6.93	1968.12
Attach Connector Piece	45	1.0	1.5			1.5	67.5
Attach nut to bolt	260	0.1	1.43	3.9	8	9.43	2451.8
Place panel on assy	17	1.0	1.5	0.0	1.5	3	51
Attach MakerBeam Square	12	1.0	1.5			1.5	18
Align MakerBeam	59	1.0	1.5			1.5	73.5
Best Case Orion Assembly Time					**4629.92**		

H.3. Manufacturing Strategy

Table H.22: Manufacturing Priority List

Number	Priority	Component	Job Number
1	High	DT.MH.FL	3783
2	High	DT.MH.FR	3785
3	High	DT.MH.RL	3787
4	High	DT.MH.RR	3789
5	High	CH.9.CUT	3824
6	High	CH.8.AJ	3825
7	High	CH.6.AJ	3826
8	High	CH.9.AJ	3827
9	Mid	SUS.BAL	3602
10	Mid	SUS.BAR	3603
11	Mid	SUS.BB	3605
12	Mid	SUS.SA	3604
13	Mid	SUS.TS.01	3608
14	Mid	SUS.TS.02	3609
15	Mid	SUS.TUB	3607
16	Mid	SUS.SAB	3645
17	Mid	SUS.TB	3606
18	Mid	FM.A	3687
19	Mid	DT.DA.R	3782
20	Mid	FM.LB	3791
21	Mid	FM.DW	3686
22	Mid	DT.MH.FR.H	3786
23	Mid	DT.MH.FL.H	3784
24	Mid	DT.MH.RL.H	3788
25	Mid	DT.MH.RR.H	3790
26	Low	FM.SC	3688
27	Low	DT.MB.224	3797
28	Low	DT.RB.16	3798

Table H.22: Manufacturing Priority List

Number	Priority	Component	Job Number
29	Low	DT.DG.12	3846
30	Low	DT.AH.CP	3841
31	Low	DT.BH.C	3843
32	Low	CH.DM.BHL	3828
33	Low	CH.DM.RSPL	3829
34	Low	CH.DM.LSPL	3830
35	Low	CH.DM.BPL	3831
36	Low	CH.DM.CB	3832
37	Low	CH.FM.BHL	3833
38	Low	CH.FM.SPL	3835
39	Low	CH.CM.BPL	3836
40	Low	CH.CM.SPLB	3837
41	Low	CH.CM.SPLF	3838

H.4. Manufacturing Process

Table H.23: Processes Used During the Manufacture of Cyclone

Process
Milling
Turning
Drilling
Tapping
Broaching
Media Blasting
Sawing
Shearing
Bonding

I Build 1 System Testing

The following procedures should be conducted with methodology, and any failures which occur, recorded.

Parameters			
ID	**Requirement ID**	**Procedure**	**Pass**
S1	P2, P6, P9,	Deploy Robot	
S2	P3, P6, F8, F9, F13, F14, F16, F17	Drive and control Cyclone	
S3	F15, F16, S2	Drive Cyclone out of sight	
S4	P7, F10, F12,	Drive Cyclone up stairs	
S5	F23	Check the battery monitoring board periodically	
S6	F1	Drop Cyclone	